The potential of molten salts as heat transfer media in fast pyrolysis of wood

Saltsmelters potensiale som varmeoverføringsmedier i hurtigpyrolyse av tre

Philosophiae Doctor (PhD) Thesis

Ruth Heidi Samuelsen Nygård

Department of Mathematical Sciences and Technology
Faculty of Environmental Sciences and Technology
Norwegian University of Life Sciences

Ås 2014

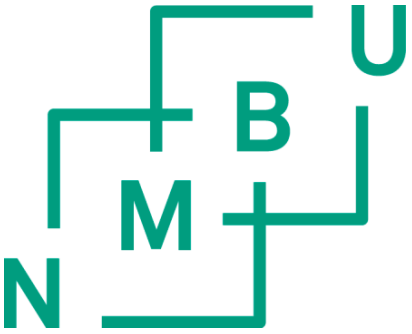

Thesis number 2015:1
ISSN 1894-6402
ISBN 978-82-575-1257-6

Summary

Growing energy consumption and greater environmental concerns have contributed to a need for more research on alternatives to fossil-derived products. Biomass such as wood is a potential source of renewable fuels and carbon-based chemicals. A method for conversion of biomass into a more useful form is fast pyrolysis, a process in which the feedstock is heated in the absence of oxygen, and converted into a mixture of gas, liquid (pyrolysis oil) and solid char. Important factors for maximizing the oil yield are rapid heating to moderate temperatures (~ 500 °C), short vapor residence times at elevated temperatures, followed by rapid quenching of the produced vapors.

The aim of this PhD study was to investigate the thermal behavior of wood particles during fast pyrolysis, as well as explore molten salts as potential heat transfer media in the process. Thermal processing of biomass in molten salts is a relatively small research area compared with more traditional conversion methods, and the work started with an extensive literature study (**Paper I**). Previous research showed that molten salts have good heat transfer characteristics, high thermal stability, and a catalytic effect in cracking and liquefaction of large molecules found in biomass. In addition, they could retain noxious compounds found in contaminated biomass. Most previous work was focused on gasification at higher temperatures or production of specific phenolic compounds from lignin, and there was a clearly need for more basic research on molten salt pyrolysis.

The experimental part behind this thesis started with a study of the effect of particle micro- and macrostructure and vapor outflow pattern on the char yield in a fluidized sand bed at 500 °C (**Paper II**). Artificial cylinders (L = 50 mm, d = 6 – 14 mm) were used as containers for milled beech wood (< 0.08 mm, 0.08 – 0.2 mm). The metal walls were solid (sw) or wire-mesh (wm), giving anisotropic and isotropic vapor outflow, respectively. The char yields from sw cylinders were comparable to those from natural wood cylinders of equal macrosize, both with an increasing trend with larger diameter. Hence, there was no notable effect of microstructure, and the char yield was predominantly determined by the outer cylinder diameter (i.e. macrostructure). The effect of outflow pattern was slightly more visible, with lower char yields from wm cylinders than sw cylinders. Although the observed effects were not very strong, it was suggested that vapors escaping in an isotropic manner have less contact with char, resulting in less polycondensations of vapors on char, and an overall lower yield.

The thermal behavior of single wood particles was studied further in molten salts (**Papers III** and **IV**). Temperature profiles were constructed by recording the center temperature of cylindrical wood particles during pyrolysis, and this was used to evaluate reaction temperatures, heating rates, and devolatilization times. In **Paper III**, experiments were carried out with beech and pine wood (L = 30 mm, d = 1 – 8 mm) in FLiNaK at 500 °C, and the results were compared to a similar study in a fluidized sand bed. In **Paper IV**, the behavior of beech wood (L = 30 mm, d = 3.5 mm) was investigated further in

several salt mixtures (FLiNaK, $(LiNaK)_2CO_3$, $ZnCl_2$-KCl, and KNO_3-$NaNO_3$) over a wider temperature range (400 – 600 °C). Finally, the whole pyrolysis process was studied in **Paper V**, including the construction and testing of an electrostatic precipitator (ESP) for collection of pyrolysis oil. Experiments were conducted with milled beech wood (0.5 – 2 mm) in FLiNaK and $(LiNaK)_2CO_3$ at temperatures between 450 and 600 °C. The yields of pyrolysis oil and char were determined, and the oils were analyzed with respect to water content.

The results contribute with basic knowledge about the heat transfer from molten salts to wood particles during pyrolysis. Hardwoods (represented by beech) have higher thermal conductivities than softwoods (represented by pine). This was reflected with higher heating rates at the particle center and faster devolatilization times for beech wood. An interesting observation was that the reaction temperatures for the two wood types were still comparable (**Paper III**). It was also found that the effective pyrolysis temperature, where most of the cellulose and hemicellulose decompose, depended strongly upon particle size (**Paper III**), but was almost unaffected by the reactor temperature and salt composition (**Paper IV**).

One of the most important findings during this work was that FLiNaK gives significantly higher heating rates compared with a fluidized sand bed for cylindrical beech wood particles with $d \leq 4$ mm. For smaller particles, the process was dominated by the heat transfer medium, while the wood properties limited the heat transfer for larger particles (**Paper III**). FLiNaK and $(LiNaK)_2CO_3$ showed better promise as effective heat transfer media than $ZnCl_2$-KCl, while KNO_3-$NaNO_3$ was found not suitable for thermal conversion of carbon containing materials due to exothermic reduction of nitrates to nitrites (**Paper IV**). The total devolatilization times were found to follow the empirical correlation $t_{dev} = Ad^n$. The corresponding activation energies indicated that the process was controlled by heat transfer rather than chemical kinetics.

In spite of the good heat transfer performance of FLiNaK and $(LiNaK)_2CO_3$ (**Papers III** and **IV**), the yields of pyrolysis oil were not comparable to other fast pyrolysis technologies, with a maximum of 34.2 wt % in FLiNaK at 500 °C (**Paper V**). The char yields were also higher than expected with regards to the high heating rates, and the oils were high in water content. A plausible explanation to these results are secondary reactions occurring because of mass transfer resistance in the melt leading to longer vapor residence times at elevated temperatures and prolonged contact with alkali elements (Na/K) found in the melts. However, the oil yields were generally higher than those previously reported for molten chloride pyrolysis of cellulose with cold trap condensers for oil collection.

Possible hydration reactions during thermal processing of biomass in FLiNaK were examined by simulations in HSC Chemistry software and FTIR measurements of the outlet gas, but the results did not imply any significant amounts of HF (**Paper V**).

Sammendrag

Økende energiforbruk og større miljøhensyn har bidratt til et behov for mer forskning på alternativer til fossilt fremstilte produkter. Biomasse som f.eks. trevirke er en potensiell kilde til fornybart brensel og karbon-baserte kjemikalier. En metode for å konvertere biomassen til en mer nyttig form er hurtigpyrolyse. Dette er en termokjemisk prosess der råvaren varmes opp uten tilgang til luft og omdannes til en blanding av gass, væske (pyrolyseolje) og fast stoff (kull). Viktige faktorer for å maksimere utbyttet av pyrolyseolje er rask oppvarming til moderate temperaturer (~ 500 °C), kort oppholdstid for de produserte gassene ved høye temperaturer og bråkjøling av de kondenserbare gassene.

Formålet med denne PhD-avhandlingen var å undersøke den termiske oppførselen til trepartikler i hurtigpyrolyse samt utforske saltsmelters potensiale som varmeoverførings-medier i prosessen. Termisk prosessering av biomasse i saltsmelter er et relativt lite forskningsområde sammenlignet med mer tradisjonelle konverteringsmetoder, og arbeidet startet derfor med et omfattende litteraturstudium (**Paper I**). Tidligere forskning viste at saltsmelter har gode varmeoverføringsegenskaper, høy termisk stabilitet og en katalytisk effekt i nedbrytning av store molekyler som finnes i biomasse. I tillegg vil skadelige forbindelser fra forurenset biomasse forbli i saltsmelten. Fokuset i de fleste tidligere arbeid var gassifisering ved høyere temperaturer eller produksjon av spesifikke fenolforbindelser fra lignin, og det var et klart behov for mer grunnleggende forskning innen saltsmelte-pyrolyse.

Den eksperimentelle delen bak denne oppgaven startet med å undersøke hvordan partiklers mikro- og makrostruktur, samt utstrømningsmønster av de dannede gassene (både kondenserbare og ikke-kondenserbare), påvirket utbyttet av fast stoff i en fluidisert sandreaktor ved 500 °C (**Paper II**). Kunstige sylindere (L = 50 mm, d = 6 – 14 mm) ble benyttet som beholdere for oppmalt bøk (< 0,08 mm, 0,08 – 0,2 mm). Sylinderne hadde vegger av metallfolie (sw [solid wall]) eller netting (wm [wire-mesh]), noe som gav henholdsvis anisotrop og isotrop utstrømning av de dannede gassene. Utbyttet av fast stoff fra sw-sylindere var sammenlignbart med det fra naturlige tresylindere av lik dimensjon, men begge gav økende utbytte for større diameter. Av dette kan det konkluderes med at mikrostruktur ikke gir noen merkbar effekt på utbyttet av fast stoff, men at det hovedsakelig påvirkes av sylindernes diameter (dvs makrostruktur). Effekten av utstrømningsmønster var noe mer synlig; utbyttet av fast stoff fra wm-sylindere var lavere enn fra sw-sylindere. Til tross for at de observerte effektene ikke var veldig tydelige, ble dette forklart ved at en isotrop utstrømning fører til mindre kontakt mellom de dannede gassene og fast stoff, noe som igjen resulterer i mindre polykondensasjon av gassene på fast stoff og et totalt lavere utbytte.

Den termiske oppførselen til trepartikler ble studert videre i saltsmelter (**Papers III** og **IV**). Temperaturprofiler ble konstruert ved å måle temperaturen i sentrum av sylindriske trepartikler under pyrolyse, og dette ble benyttet til å evaluere reaksjonstemperaturer,

oppvarmingsrater og reaksjonstider. Bøk og furu (L = 30 mm, d = 1 – 8 mm) ble pyrolysert i FLiNaK ved 500 °C (**Paper III)**, og resultatene ble sammenlignet med en lignende studie i en fluidisert sandreaktor. Den termiske oppførselen til bøk (L = 30 mm, d = 3,5 mm) ble videre undersøkt i flere saltblandinger (FLiNaK, $(LiNaK)_2CO_3$, $ZnCl_2$-KCl og KNO_3-$NaNO_3$) over et større temperaturområde (400 – 600 °C) (**Paper IV)**. Til slutt ble hele pyrolyseprosessen studert, inkludert konstruksjon og testing av et elektrostatisk filter (ESP) for kondensering av pyrolyseolje (**Paper V**). Forsøkene ble utført med oppmalt bøk (0,5 – 2 mm) i FLiNaK og $(LiNaK)_2CO_3$ ved temperaturer mellom 450 og 600 °C. Utbyttene av pyrolyseolje og fast stoff ble målt, og oljene ble analysert med hensyn til vanninnhold.

Resultatene gir grunnleggende kunnskap om varmeoverføring fra saltsmelter til trepartikler i pyrolyseprosessen. Løvtrær (representert ved bøk) har høyere termisk ledningsevne enn bartrær (representert ved furu). Dette ble gjenspeilet med høyere oppvarmingsrater og raskere reaksjonstider for bøk. En interessant observasjon er at på tross av dette, var reaksjonstemperaturene for de to tresortene fremdeles sammenlignbare (**Paper III**). Det ble også funnet at den effektive pyrolysetemperaturen der mesteparten av cellulosen og hemicellulosen dekomponerer, avhenger sterkt av partikkelstørrelse (**Paper III**), men er nesten upåvirket av reaktortemperatur og saltsammensetning (**Paper IV**).

Et av de viktigste funnene i dette arbeidet var at FLiNaK gir betydelig høyere oppvarmingsrater sammenlignet med fluidisert sand for sylindriske bøkepartikler med $d \leq 4$ mm. For mindre partikler domineres prosessen av varmeoverføringsmediet, mens treegenskapene begrenser varmeoverføringen for større partikler (**Paper III**). FLiNaK og $(LiNaK)_2CO_3$ gav mer effektiv varmeoverføring enn $ZnCl_2$-KCl, mens KNO_3-$NaNO_3$ ikke egnet seg for termisk konvertering av karbonholdige materialer på grunn av eksoterm reduksjon av nitrat til nitritt (**Paper IV**). Den totale reaksjonstiden ble funnet å følge den empiriske korrelasjonen $t_{dev} = Ad^n$. De beregnede aktiveringsenergiene indikerte at prosessen ble kontrollert av varmeoverføring heller enn kjemisk kinetikk.

Til tross for at FLiNaK og $(LiNaK)_2CO_3$ viste meget gode varmeoverføringsegenskaper (**Papers III** og **IV**), ble ikke utbyttet av pyrolyseolje sammenlignbart med andre hurtigpyrolyse-teknologier (**Paper V**). Det høyeste utbyttet ble målt til 34,2 vekt % i FLiNaK ved 500 °C. Utbyttet av fast stoff var også høyere enn forventet i forhold til de høye oppvarmingsratene, og vanninnholdet i oljene var høyt. En sannsynlig forklaring på disse resultatene er at de dannede gassene har fått massetransport-motstand i saltsmeltene, noe som igjen har ført til sekundære reaksjoner på grunn av lengre oppholdstider ved høye temperaturer og lengre kontakt med alkalielementer (Na / K) i saltsmeltene. Oljeutbyttene var imidlertid generelt høyere enn de som tidligere er rapportert for pyrolyse av cellulose i kloridsmelter der kjølefelle-kondensere ble benyttet.

Mulige hydrolysereaksjoner under termisk prosessering av biomasse i FLiNaK ble undersøkt ved simuleringer i HSC Chemistry og gassmålinger med FTIR-spektroskopi, men resultatene viste at det ikke ble dannet noen vesentlige mengder HF-gass (**Paper V**).

Acknowledgments

Many people have contributed directly or indirectly to this work. First of all, I would like to express my appreciation to my main supervisor Associate Professor Espen Olsen for his professional guidance and support. Our weekly meetings have been of great importance to the progression and completion of this thesis. I am very thankful for the good discussions and constructive feedback. I also appreciate the assistance of my co-supervisors. Dr. Arnstein Norheim came with valuable suggestions to the construction of the laboratory equipment during the first year of my studies, and also accompanied me to several conferences. Associate Professor Jorge Marchetti took over as co-supervisor during the last years, and his feedback and suggestions in the laboratory work, especially with regards to the water analyses, have been much appreciated.

The first part of my experimental work was carried out at the University of Twente (Netherlands). I am especially thankful to Associate Professor Wim Brilman who was my responsible supervisor and Roel Westerhof for the daily supervision during this visit. Thank you for including me in the TCCB research group, both professionally and socially. The collaboration was very useful, and gave me the knowledge and laboratory skills I needed to continue the research at NMBU.

Special thanks should be given to Arne Svendsen and Tom Ringstad for the all the support and discussions during the development of the experimental setup and the data collection system at NMBU, and for quick assistance in rebuilding the system when I had new ideas or accidently broke some parts of the existing setup. The experimental part of this thesis had not been possible without your technical support.

My gratitude also goes to fellow PhD candidates, post docs and other colleagues at NMBU. Regularly coffee breaks, floorball and running practice, and social events have given me necessary breaks and renewed motivation.

Finally, I would like to thank my family and friends for their support and encouragement throughout this study. To my husband Svend Are and our little boy Elias – you are the main energy source in my life and remind me of what is important when I've been buried in work for too long.

Ås, September 2014
Heidi S. Nygård

List of papers

Paper I

Nygård, Heidi S.; Olsen, Espen. Review of thermal processing of biomass and waste in molten salts for production of renewable fuels and chemicals. *International Journal of Low-Carbon Technologies* 2012, 7 (4), 318-324.

Paper II

Westerhof, R. J. M.; **Nygård, Heidi S.**; Swaaij, W. P. M. van; Kersten, S. R. A.; Brilman, D. W. F.. Effect of Particle Geometry and Microstructure on Fast Pyrolysis of Beech Wood. *Energy & Fuels* 2012; 26 (4), 2274-2280.

Paper III

Nygård, Heidi S.; Danielsen, Filip; Olsen, Espen. Thermal History of Wood Particles in Molten Salt Pyrolysis. *Energy & Fuels* 2012, 26 (10), 6419-6425.

Paper IV

Nygård, Heidi S.; Olsen, Espen. Effect of salt composition and temperature on the thermal behavior of beech wood particles in molten salt pyrolysis. *Energy Procedia* 2014, in press.

Paper V

Nygård, Heidi S.; Olsen, Espen. Use of electrostatic precipitator (ESP) for oil collection in molten salt pyrolysis of milled beech wood. Submitted to *Energy & Fuels*.

Additional scientific contributions

Oral presentations

Nygård, Heidi S.; Pyrolysis of biomass in molten salts. *CenBio Graduate School gathering,* Sarpsborg (Norway), January 13, 2010.

Nygård, Heidi S.; Olsen, Espen. Molten salt pyrolysis of biomass. *Renewable Energy Research Conference (RERC)*, Trondheim (Norway), June 7-8, 2010.

Nygård, Heidi S.; Olsen, Espen. Pyrolysis of biomass in FLiNaK. *Molten Salt Discussion Group (MSDG) Summer meeting*, Cambridge (UK), July 5-9, 2010.

Nygård, Heidi S.; Danielsen, Filip; Olsen, Espen. Thermal History of Wood Particles in Molten Salt Pyrolysis. *Renewable Energy Research Conference (RERC)*, Trondheim (Norway), April 16-18, 2012.

Nygård, Heidi S.; Olsen, Espen. Effect of Salt Composition and Temperature on Beech Wood in Molten Salt Pyrolysis. *Renewable Energy Research Conference (RERC)*, Oslo (Norway), June 16-18, 2014.

Poster presentations

Nygård, Heidi S.; Olsen, Espen. Pyrolysis of biomass in molten salts. *Molten Salt Discussion Group (MSDG) Christmas meeting*, London (UK), December 14, 2009.

Nygård, Heidi S.; Saltsmeltepyrolyse av biomasse. *Bioenergidagene*, Gardermoen (Norway), November 8-9, 2010.

Nygård, Heidi S.; Danielsen, Filip; Olsen, Espen. Thermal history of wood particles in FLiNaK pyrolysis. *Molten Salt Discussion Group (MSDG) Christmas meeting,* London (UK), December 17, 2012.

Abbreviations and symbols

CFB	Circulating fluid bed
CHP	Combined heat and power
DME	Dimethylether
DSC	Differential scanning calorimetry
ESP	Electrostatic precipitator
ETBE	Ethyl tertiary butyl ether
EU	European union
FAME	Fatty acid methyl ester
FB	Fluidized bed
FTIR	Fourier transform infrared
HHV	Higher heating value
HTU	Hydrothermal upgrading
IEA	International energy agency
KFT	Karl Fischer titration
OECD	Organization for economic cooperation and development
POM	Polyoxymethylene
RCR	Rotating cone reactor
RME	Rapeseed methyl ester
SEM	Scanning electron microscope
sw	Solid wall
TCCB	Thermochemical conversion of biomass
TGA	Thermogravimetric analyzer
toe	tonne of oil equivalent (1 toe = 11.63 MWh)
wm	Wire-mesh

d	Diameter
H	Height
h	Heating rate
I	Current
ID	Inner diameter
$k_{eff}(\parallel)$	Effective conductivity parallel to wood fibers
$k_{eff}(\perp)$	Effective conductivity perpendicular to wood fibers
L	Length
T	Temperature
t	Time
t_{dev}	Total devolatilization time
V	Voltage
ρ	Density

Table of Contents

1 Introduction

The world has experienced a significant increase in the total energy consumption the last four decades (Figure 1-1), and according to the International Energy Agency (IEA) it reached 8 918 Mtoe (103 716 TWh) in 2011.[1] Factors causing this increase include population growth, improving living standards in developing countries and an overall higher consumption in Western countries.

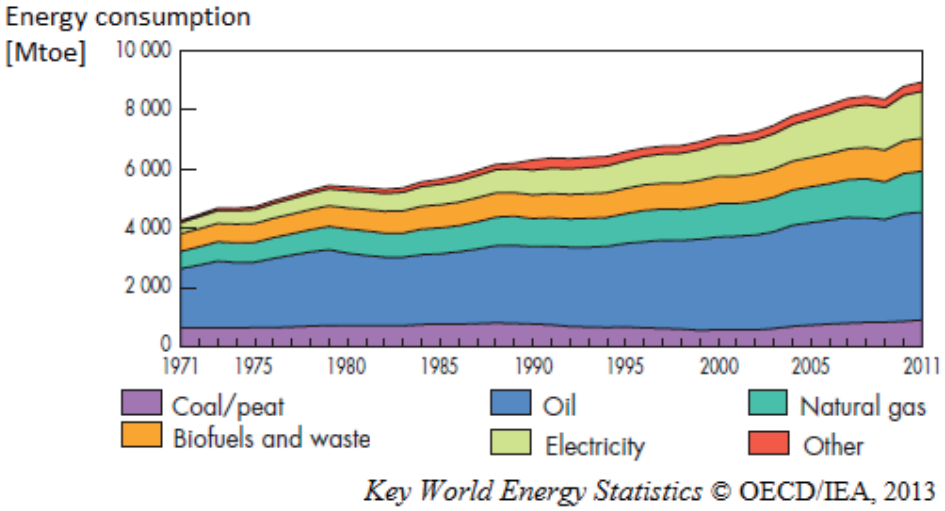

Figure 1-1. Evolution from 1971 to 2011 of world's total energy consumption by fuel (Mtoe). Data prior to 1994 for biofuels and waste have been estimated. Other includes geothermal, solar, wind, heat, etc.[1*]

In 2011, more than 80% of the world's energy consumption was based on fossil resources like coal, oil, and gas.[1] Fossil fuels are convenient energy sources that meet the energy demands of society very effectively today.[2] The resources are, however, limited, and we are nowadays experiencing decreasing oil reserves together with increasing oil prices.[3] Another issue is the increasing emissions of greenhouse gases such as CO_2 along with the increased use of fossil fuels. It is likely that there is a correlation between the emissions and climate change. In pace with growing energy consumption and greater environmental concerns, there has been a renewed interest in research on alternatives to fossil-derived products.[2]

Renewable energy is a basic ingredient for sustainable development. Renewable energy sources can supply the energy we need on a long-term basis, reduce local and global atmospheric emissions, and enhance diversity in energy supply markets.[4] Some of the main renewable resources available are wood and other forms of biomass including energy crops and agricultural and forestry wastes. There are many alternatives to renewable electricity, but biomass can provide the main source of renewable liquid,

[*] Figure reprinted with permission from OECD/IEA.

gaseous and solid fuels.[5] It is estimated that bioenergy contributes to 10 – 14% of the world's energy supply.[6]

When used as fuel, biomass releases the CO_2 it absorbed from the atmosphere in the recent past, not millions of years ago, as with fossil fuels. Because of the much shorter carbon cycle compared to fossil resources it contributes to less net CO_2 in the atmosphere.[2] Another advantage is that biomass is more evenly dispersed over the earth's surface and is thus suitable for distributed local energy production.[7]

A number of processes are available for conversion of biomass and residues to more valuable energy forms, including thermo-, bio-, and physiochemical processes. In thermochemical conversion, biomass can supply energy by direct combustion or via intermediates by gasification or pyrolysis.[8] Pyrolysis has been applied for thousands of years for charcoal production,[5] and in ancient Egyptian times tar from pyrolysis was used for caulking boats.[9] In the last 30 years, fast pyrolysis with pyrolysis oil as the main product has become of considerable interest. In this process, biomass is heated rapidly without any oxidizing agent to moderate temperatures of around 500 °C and short reaction times of up to a few seconds. When wood is used as feedstock in continuously operated laboratory reactors and pilot plants, the best reported oil yields are between 60 and 75 wt % on a dry-feed basis.[5] Pyrolysis oil is a renewable liquid fuel with significantly increased energy density compared with the feedstock. It can be easily stored and transported, and used for fuels, chemicals or as an energy carrier.[8]

1.1 Study aim and objectives

The aim of this work was to study the thermal behavior of wood particles during fast pyrolysis, as well as investigate molten salts as potential heat transfer media in the process. The work started with an extensive literature study. Thermal processing of biomass in molten salts is a relatively small research area, and only a few publications were found on the subject from every decade since the early 70s. No review was published before, and the literature study resulted in a review article of thermal processing of biomass and waste in molten salts for production of renewable fuels and chemicals (**Paper I)**. Most of the previous work focused on production of synthesis gas or specific chemical compounds. Very little work existed where the yields of pyrolysis oil were reported, and there was a need for more basic research on the subject.

At the start of this work, there was limited experience with thermochemical conversion of biomass at NMBU. In order to design and develop an experimental setup, it was necessary to visit a well-established laboratory. Collaboration with the TCCB research group (Thermochemical conversion of biomass) at the University of Twente (Netherland) was established, including a 3 months exchange stay. The purpose of the stay was mainly to learn about thermochemical conversion of biomass by performing experiments with existing, well-working equipment. A fluidized sand bed was used to study the effect of micro- and macrostructure and vapor outflow patterns in fast pyrolysis. This was done by

inserting milled beech wood into artificial cylindrical containers (L = 50 mm, d = 6 – 14 mm) and comparing the char yields with natural wood cylinders of equal macrostructure. The results were included in a joint paper (**Paper II)** on the effect of particle geometry, size and microstructure on fast pyrolysis of beech wood. Only the experimental part performed during the exchange stay is described in this thesis, but the results are discussed in the context of the whole article.

Based on the knowledge from the stay at Twente, a setup for molten salt pyrolysis was designed and constructed at NMBU. The study of the effect of particle size was continued, but in molten salt media. The focus in **Papers III** and **IV** was the thermal behavior of single wood particles in molten salts. The heat transfer characteristics of molten salts were studied by measuring the temperature at the center of cylindrical wood particles during heating. The temperature development was used to evaluate heating rates, reaction temperatures and devolatilization times. Beech and pine wood particles of various sizes (L = 30 mm, d = 1 – 8 mm) were studied in FLiNaK pyrolysis at 500 °C in **Paper III**. The samples were chosen as representatives for hardwood and softwood, respectively. The results were compared to a similar study in a fluidized sand bed. Beech wood (L = 30 mm, d = 3.5 mm) was studied further in **Paper IV**, where the effect of different salt mixtures (FLiNaK, $(LiNaK)_2CO_3$, $ZnCl_2$-KCl, and KNO_3-$NaNO_3$) was evaluated over a wider temperature range (400 – 600 °C).

The aim of **Paper V** was to study the whole pyrolysis process with emphasis on the yield of pyrolysis oil from milled beech wood (0.5 – 2 mm). An electrostatic precipitator (ESP) was constructed for condensing the pyrolysis oil. The salt mixtures that showed the most promising heat transfer performance in **Paper IV** were investigated systematically (FLiNaK and $(LiNaK)_2CO_3$), and the char yield, oil yield, and water content of the oil were measured.

2 Literature overview

2.1 Biomass as an energy resource

Biomass is defined as all organic material that is derived from living or recently living organisms.[10] A common way to categorize biomass into different groups is based on their origin:[3]

- Cellulose-rich plants – dry (forest fuels, energy forest, straw, hemp)
- Cellulose-rich plants – moist (forage, cornstalks, beet tops)
- Sugary / starchy plants (sugar beets, grain, potatoes)
- Oil rich plants (rapeseed, turnip-rape)
- Manure, garbage, sludge and other organic wastes

The energy in biomass is solar energy stored as chemical energy via photosynthesis reactions.[10] This energy can be recovered by burning biomass as a fuel, either directly or after conversion to intermediate liquid, solid or gaseous energy carriers. During combustion, previously absorbed heat and CO_2 are released, and the use of biomass is essentially the reversal of photosynthesis.[11] Biomass is considered a renewable energy source as long as it is based on sustainable utilization. If consumed at the same rate as new biomass is grown, there is no net atmospheric CO_2 emissions.[7]

Another advantage of bioenergy is that the geographic distribution is relatively even over the world,[12] making local production possible.[13] In this way, energy supply could be secured in regions without fossil fuel reserves.[14]

According to the International Energy Agency (IEA), about 12.5% of the world's energy consumption in 2011 came from biomass. The fraction in the EU-25 is lower (4.4%), but bioenergy is an important ingredient in the energy consumption in the Scandinavian countries (Figure 2-1).[1] Bioenergy has a significantly lower proportion of the energy mix in Norway compared with the neighboring countries.[3] Possible explanations to this are low electricity prices and few central heating facilities.[15] About half of the total consumption of bioenergy in Norway is linked to the use of wood stoves in private households.[16]

Many future energy scenarios predict large shares of bioenergy. The yearly global potential of bioenergy is believed to be between 788 and 27 100 Mtoe in 2050. The wide range of estimated numbers is due to insecurity about future demand for food,[13] productivity of forest and energy crops, and availability of land.[17]

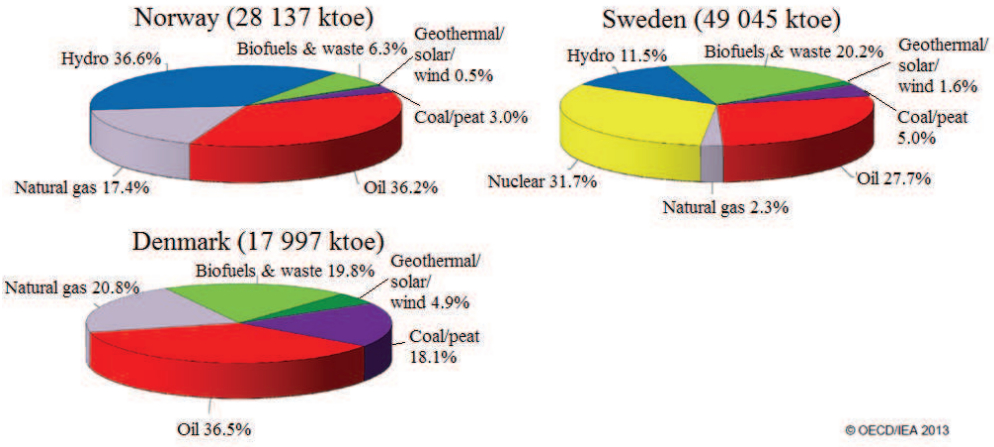

Figure 2-1. Primary energy consumption in the Scandinavian countries in 2011.[1*]

2.1.1 Overview of conversion technologies for energy purposes

There are many ways of processing biomass leading to a large variety of chemicals and materials, and of electricity and fuels.[18] The technologies for transforming biomass into more convenient energy carriers are mostly grouped as thermochemical (heat treatment), biochemical (microbiological), and physicochemical.[5] This is summarized in Figure 2-2.

Thermochemical conversion is primarily used on dry cellulose-rich plants such as wood.[3] There are three main processes available – combustion, gasification and pyrolysis.[19] Combustion is complete oxidation of the biomass material, and the final products are CO_2 and water / steam along with heat energy.[20] Direct combustion for heating and cooking is the oldest way of using biomass, and this is still responsible for more than 97% of the world's bioenergy production.[10] Combustion of biomass to produce electricity is applied commercially in many regions, and electrical efficiencies of 20 – 40% are possible at a scale of 20 – 100 MW. Often the electricity is produced along with heat or steam in combined heat and power plants (CHP).[12]

Gasification involves partial oxidation of the feedstock. Biomass gasification processes are generally designed to produce low- to medium-energy fuel gases or synthesis gases for the manufacture of chemicals such as methanol (CH_3OH) and other hydrocarbons.[20] It is very costly to store and transport the gases due to their low energy density, so they should be used immediately. In biomass gasification with turbine or engine to power production, efficiencies of 35 – 50% are achieved.[19] The gases may also be used (directly or upgraded to light hydrocarbons) in fuel cells for electricity production. Liquid hydrocarbons for use in vehicle motors could be produced from syngas by Fischer-Tropsch synthesis.[21]

[*] Figure reprinted with permission from OECD/IEA.

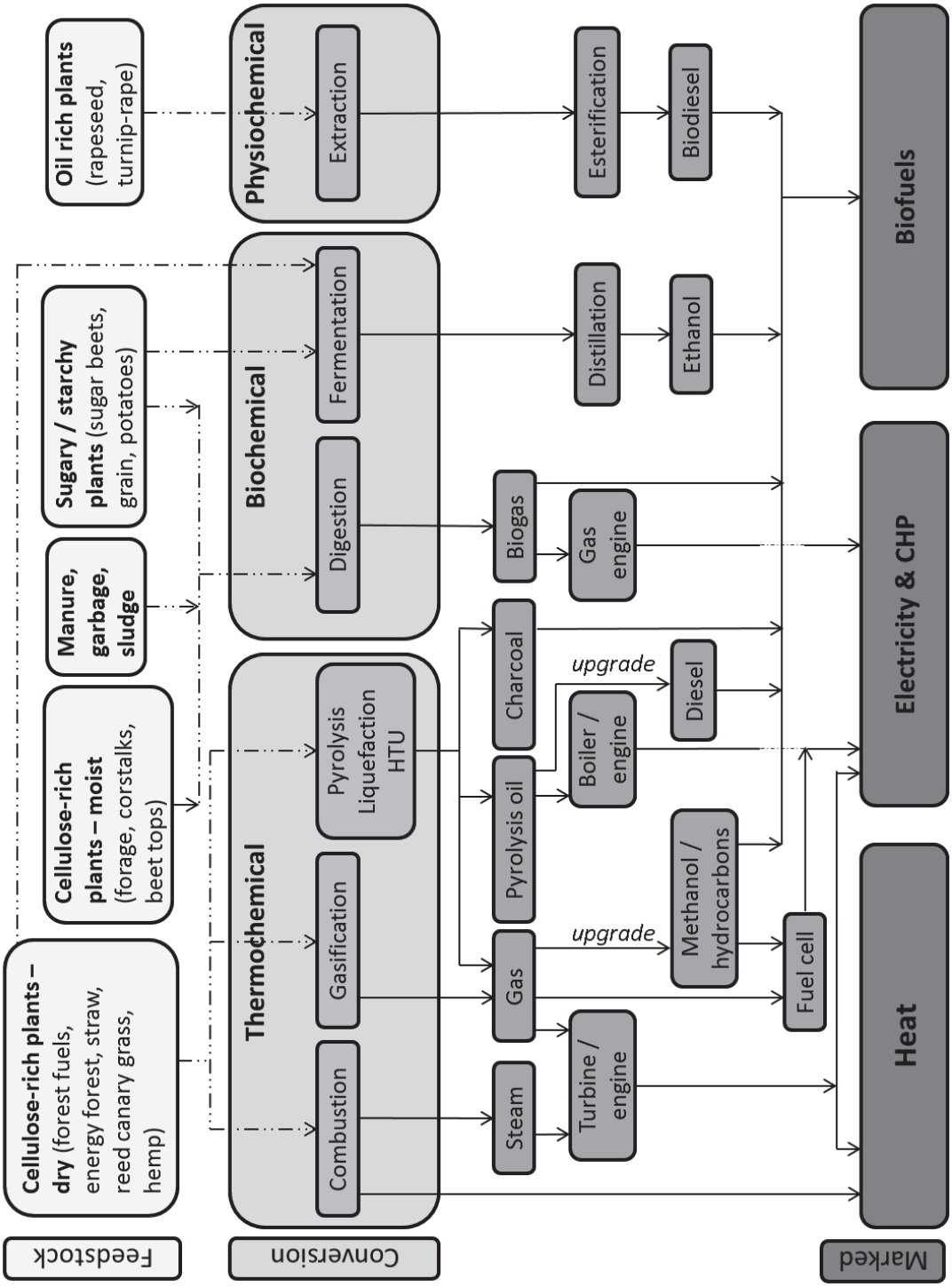

Figure 2-2. Main conversion routes for various biomass feedstock to secondary energy carriers (adapted from Kullander[3], Bridgwater[5] and Goldemberg[12]).

Biomass pyrolysis is thermal decomposition of the organic components without any oxidizing agent.[20] The material degrades to a mixture of gas, liquid (pyrolysis oil) and solid (charcoal), with relative yields depending on parameters such as temperature, heating rate, and vapor residence time.[22] Pyrolysis is also always the first step in combustion and gasification processes, followed by total or partial oxidation of the primary products.[19] The pyrolysis products can be combusted to produce heat and electricity, or upgraded to liquid fuels.[21] The pyrolysis process is described more extensively in Chapter 2.3.

Biochemical conversion includes digestion to produce biogas and fermentation to produce ethanol (CH_3CH_2OH). Typical raw materials for biogas production are moist cellulose-rich plants, manure, garbage, and sludge.[3] Anaerobic digestion of biomass for electricity production is commercially available, but the conversion efficiency is quite low (10 – 15%).[12] Sugary / starchy plants may also be used as feedstock for digestion, but these are more typical for ethanol production through fermentation.[3] Production of ethanol by fermenting sugars is a classic conversion route for sugar cane and corn on a large scale, especially in Brazil, France, and the United States.[12] Dry cellulose-rich plants such as wood or forestry residues could also be converted to ethanol through fermentation and hydrolysis, but these processes are usually more advanced.[21]

In physiochemical conversion, oil rich plants are pressed, extracted and the oil esterified (typically with methanol) to produce fatty acid methyl esters (FAME), popularly known as biodiesel.[3, 21]

2.1.2 Liquid biofuels

As described in Chapter 2.1.1, there are several process routes leading to liquid biofuels. The dramatic rise in oil prices seen in the last decade has enabled biofuels to become cost-competitive with petroleum-based transportation fuels, and this has led to a surge in research and production around the world.[21]

Biofuels are classified according to their source and type. Fuels derived from only parts of the plant are referred to as first generation.[23] The production technologies are well established and available on the market today, but they are in competition with the food / feed industry.[21] It is estimated that biofuels from primary agricultural products should not increase above 1% of all liquid motor fuels in order to secure food for people and animals.[3] Second generation biofuels are produced in a more sustainable way as they are derived from biomass that cannot be used in the food chain. The most typical feedstock is lignocellulosic material which makes up the majority of the cheap and abundant nonfood materials available from plants.[21] The processing leading to second generation biofuels are more advanced, and further research and development are required on feedstock pretreatment and conversion technologies before they become cost effective. Although the feedstock is not directly in competition with food industry, there is concern over competing land use or required land use changes. This has led to research on third

generation biofuels specifically derived from microbes and microalgae.[24] Third generation biofuels are not in the scope of this work, and will not be presented further.

The main types of liquid biofuels are ethanol and biodiesel, the equivalents of fossil gasoline and diesel, respectively. Ethanol has a high octane number (107) and an E10 blend (10% ethanol and 90% gasoline) could be used without modification of the gasoline engine. Higher concentrations such as E85 or E95 could be used with small modifications in so-called flexi-fuel vehicles. A major advantage of using ethanol is that NO_x and dust emissions are lower compared to gasoline use only.[25] Ethanol may also serve as feedstock for ethyl tertiary butyl ether (ETBE, $C_6H_{14}O$) which blends more easily with gasoline.[21] Worldwide, sugar cane and corn are the most important raw materials for first generation ethanol production,[3] while lignocellulosic biomass could be used for second generation ethanol. The latter is more complex and requires extensive pre-treatment to make the sugars available for fermentation.[21]

First generation biodiesel is produced from oil-containing seeds like rape seeds and soya beans. The oils may be used directly or modified through transesterification.[21] Biodiesel can be used as a substitute of diesel with minor engine modifications. Rapeseed methyl ester (RME) is most common in Europe and Canada, while soya oil is typical in the United States. Biodiesel could also be produced from residual oils and plants.[26] Addition of diesel oil is recommended when biodiesel is to be used at temperatures below −15 °C.

Thermal processes may be used to produce second generation biodiesel, either by gasification followed by upgrading to methanol, dimethylether (DME, $(CH_3)_2O$) or Fischer-Tropsch diesel, or by pyrolysis followed by upgrading of the pyrolysis oil.[21]

The types of liquid biofuels classified by generation are summarized in Figure 2-3.

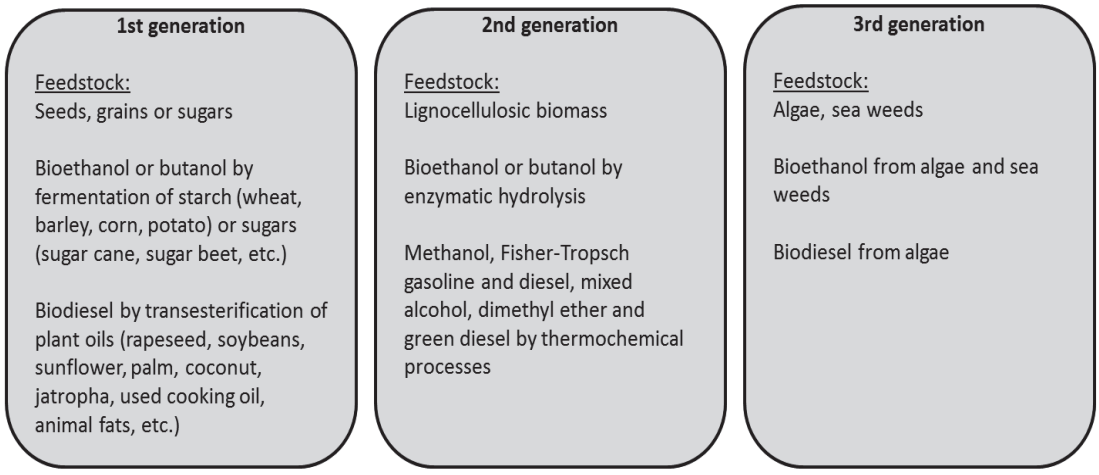

Figure 2-3. Classification of liquid biofuels according to the origin of the feedstock (adapted from Nigam[24]).

2.2 Wood structure and chemical composition

Lignocellulosic materials such as wood are potential feedstock for second generation biofuels.[3] About one third of the world's land surface is covered by forest.[27] Trees are seed-bearing plants which are divided into softwoods and hardwoods. Softwood belongs to the class of gymnospermeae trees, and many of these trees produce seed cones, pollen cones, or both. They have needlelike (e.g. pine, spruce) or scalelike (e.g. cedar) leaves which are retained for up to several years. Hardwood belongs to angiospermae trees. Hardwoods have leaves that are generally broad or bladelike and usually shed their leaves at the end of the tree's growing season once a year. Altogether 520 softwood and 30 000 hardwood tree species are known worldwide. In Europe, however, only 10 softwood and 51 hardwood species exist naturally.[28]

The structure of wood is important because it affects its decomposition behavior during thermal conversion. The elemental composition of wood is approximately 50 wt % carbon (C), 6 wt % hydrogen (H), and 44 wt % oxygen (O). The chemical substances are originally produced in living cells of a tree, but at the time of cutting, the major portion of the tree no longer contains living cells. Thus, there are essentially no proteins and other nitrogenous substances normally associated with living cells.[29]

Figure 2-4 shows the composition and structure of wood.[30] The dark-colored pith at the center of the tree trunk is the tissue formed during the first year of growth and is called heartwood. The stem has a concentric layered arrangement called growth rings (annual rings), with the light-colored sapwood found in the outer part. The cell division and radial growth of the tree takes place in a very thin layer consisting of living cells between the wood and the inner bark.[28]

The organic constituents of wood may be categorized as cell wall components or extraneous substances (extractives).[29] The structural cell wall components are mainly cellulose, hemicelluloses, and lignin, and these govern the physical properties of wood to a large extent. A simplified illustration is that cellulose forms a skeleton surrounded by other substances functioning as matrix (hemicellulose) and encrusting (lignin) materials.[28] The extractives are present in the cell wall, but they are often more prevalent in cell cavities or in specialized anatomical structures, such as resins and gum ducts.[29] In addition, wood materials also contain water and minor amounts of inorganic compounds known as "ash".[30]

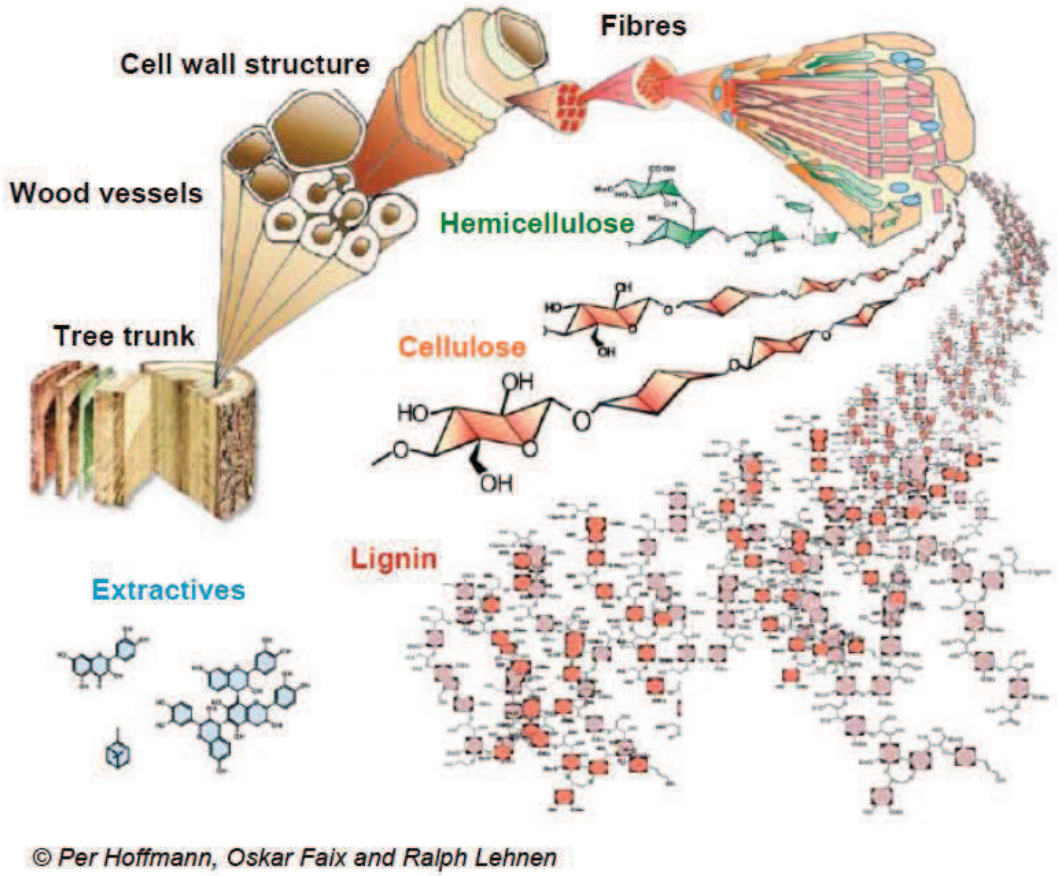

Figure 2-4. Wood structure. The macrostructure has a concentric layered arrangement with growth rings. The cell wall structure is fibrous and consists of cellulose, hemicellulose, and lignin, in addition to small amounts of extractives and ash.[*]

Cellulose is the main component of the cell wall (approximately 40 – 45% of the dry mass in most wood).[28] It is a homogeneous and linear polysaccharide with the elementary formula $(C_6H_{10}O_5)_n$.[31] The number of glucose monomers in a cellulose molecule ranges from a few to as many as 15 000, depending on its location within the cell wall.[29] Cellulose molecules aggregate together in the form of micro fibrils that are organized in fibrils through intra- and intermolecular hydrogen bonds. These are combined into cellulose fibers which are responsible for the fibrous nature of wood.[30] The spaces between the micro fibrils in the cell wall layers are available for deposition of different chemical substances[29] and for absorption of water through the numerous hydroxyl groups of cellulose.[31] Due to the fibrous structure and the strong hydrogen bonds, cellulose has a high tensile strength and is insoluble in most solvents,[28] including alkali and acids.[27]

Hemicellulose accounts for approximately 25 – 40% of the total mass of the cell wall.[29] It is also a polysaccharide, consisting of five- and six-carbon sugars.[27] The structure is heterogeneous and branched and with a degree of polymerization of only around 200. The

[*] Figure reprinted with permission from the authors on behalf of Oskar Faix.

main function of hemicellulose is as supporting material in the cell walls.[28] Together with lignin, hemicellulose forms the matrix in which the cellulose fibrils are embedded.[30] Hemicellulose is much more soluble and susceptible to chemical degradation than cellulose; it is mostly soluble in alkali, and it is relatively easily degraded by acid hydrolysis to simple sugars or sugar acids.[27]

Lignin is a complex three-dimensional polymer with apparently no ordered arrangement. The polymer is largely composed of three distinct phenyl propane monomer units with many different types of linkages between the building blocks. Lignin encrusts the intercellular space and any openings in the cell walls between the cellulose and hemicellulose molecules, and contributes to 20 – 30% of the mass of dry wood. The function is to bind the cells together and give rigidity to the cell wall. Lignin also protects the wood against microbial degradation and is totally insoluble in most solvents.[31]

The relative amounts of the components vary between different wood species, and data for some selected softwoods and hardwoods are given in Table 2-1.[27]

Table 2-1. Chemical composition (wt %) of some selected wood species (adapted from Wenzl[27]).

Species	Cellulose	Hemicellulose	Lignin	Extractives
Softwoods				
Scandinavian Spruce	43	27	29	1.8
Scandinavian Pine	44	26	29	5.3
Douglas Fir	39	23	29	5.3
Scots Pine	40	25	28	3.5
Hardwoods				
Scandinavian Birch	40	39	21	3.1
Silver Birch	41	30	22	3.2
American Beech	48	28	22	2.0

2.3 Pyrolysis

2.3.1 Characteristics of pyrolysis processes

Pyrolysis is thermal decomposition in the absence of an oxidizing agent in which large complex hydrocarbon molecules of biomass break down into relatively smaller and simpler molecules.[2] The process involves a complex set of parallel and serial chemical reactions influenced by heat and mass transfer. A common assumption is to lump the products into three main classes; gas, liquid (pyrolysis oil) and solid char. The gas is a mixture of the non-condensable vapors CO, CO_2, H_2, CH_4, and other small hydrocarbons, while pyrolysis oil is the fraction of the vapors that is liquid at room temperature. Char is defined as the solid residue left after devolatilization is complete.[32] Vapors are usually referring to both non-condensable and condensable gases, including aerosols that are

found in the pyrolysis oil. The three lumped product classes are always produced, but their relative yields can be varied over a wide range by adjustment of several process parameters including the heating rate, residence time, and final temperature.[2] The products may also partly shift towards each other during the conversion process.[32]

It is common to categorize pyrolysis processes into slow and fast pyrolysis according to the heating rate and residence time as shown in Table 2-2. In slow pyrolysis the heating rate is very low and the vapor residence time is on the order of minutes or longer, favoring the production of charcoal. Carbonization is the oldest form of slow pyrolysis, in use for thousands of years. This process leaves mostly charcoal as residue, while conventional pyrolysis involves nearly equal amounts of all three types of pyrolysis products.[2] Vapors do not escape as rapidly as they do in fast pyrolysis. Thus, components in the vapor phase continue to react with each other to form secondary products.[9] In fast pyrolysis, the heating rates are much higher and the vapor residence time is on the order of seconds or milliseconds. The primary goal for this type of pyrolysis is to maximize the production of pyrolysis oil.[2] When wood is used as a feedstock in continuously operated laboratory reactors and pilot plants for fast pyrolysis, oil yields could be as high as 75 wt % on a dry-feed basis,[8] but typical values are in the range 60 – 75 wt %.[5] Longer residence times on the order of 10 – 30 s will result in lower oil yield (50%) in 2 phases.[5] High temperatures and longer residence times will increase biomass conversion to gas.[2]

Table 2-2. Parameters and products (wt %) of some pyrolysis processes (adapted from Basu[2] and Bridgewater[5]).

Pyrolysis process	Residence time	Heating rate	Final temperature	Liquid	Solid	Gas
Carbonization (slow)	Days	Very low	400 °C	(Mostly charcoal)		
Conventional (slow)	5 – 30 min	Low	500 °C	30%	35%	35%
Intermediate	10 – 30 s	Intermediate	500 °C	50%	25%	25%
Fast	< 2 s	Very high	500 °C	75%	12%	13%

2.3.2 Reaction mechanisms

The reactions that occur during pyrolysis can be divided into primary or secondary reactions. The primary reactions are those in which the products are generated directly from the starting material. When the primary products are reacting to form other products, this is referred to as secondary reactions. An example of a primary reaction is wood devolatilizing to form pyrolysis oil, while a secondary reaction could be oil cracking further to gases.[32]

The reaction mechanisms of pyrolysis of wood and other biomass materials are chemically complex. The thermal decomposition proceeds through a complex series of chemical reactions, coupled with heat and mass transfer processes.[2] There are also great differences between the thermal behavior of cellulose, hemicellulose and lignin. Yang et al.[33] studied the pyrolysis characteristics of these three components using a thermogravimetric analyzer

(TGA) with differential scanning calorimetry (DSC) detector coupled with Fourier transform infrared (FTIR) spectroscopy. It was found that hemicellulose starts to decompose first, with the pyrolysis mainly between 220 and 315 °C. Cellulose pyrolysis occurs at higher temperatures (315 – 400 °C), while lignin decomposes slowly over a wider temperature range (150 – 900 °C).

Cellulose and hemicellulose are the main sources of volatiles. Of these, cellulose is a primary source of condensable vapors, while hemicellulose yields more non-condensable gases. Owing to its aromatic content, lignin degrades slowly, making a major contribution to the char yield.[2] Of the non-condensable gases released during pyrolysis, CO_2 originates mainly from primary pyrolysis, while CO and CH_4 are mainly secondary pyrolysis products. Cellulose generates the highest CO yield due to the thermal cracking of carbonyl and carboxyl. The highest yield of CO_2 originates from hemicellulose because of its higher carboxyl content. Pyrolysis of lignin releases more H_2 and CH_4 because of the presence of aromatic rings and methoxyl groups.[33]

Despite the different thermal behaviors, pyrolysis of the major constituent cellulose is often studied in detail in order to understand the mechanisms of wood pyrolysis. The Broido-Shafizadeh model (Figure 2-5) is the best-known model for cellulose pyrolysis. The model can be applied, at least qualitatively, to the pyrolysis of an entire biomass such as wood.[2]

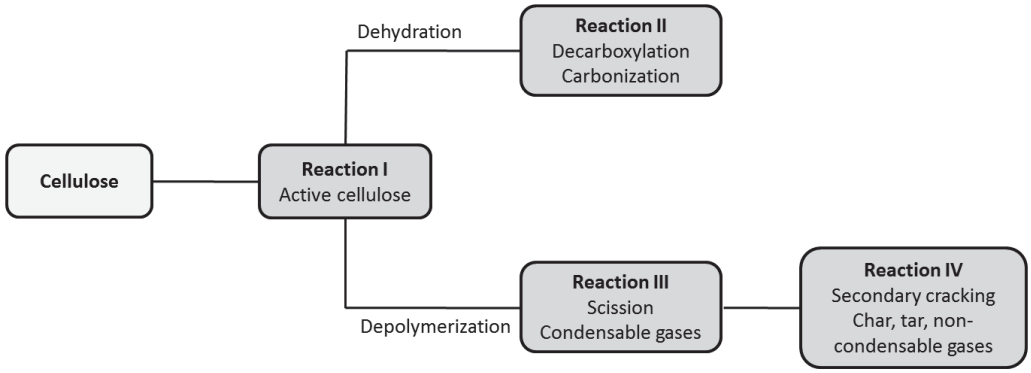

Figure 2-5. The Broido-Shafizadeh model for pyrolysis of cellulose (adapted from Basu[2]). The pyrolysis process involves an intermediate prereaction (I) followed by two competing first-order reactions (II and III). The products may further undergo secondary reactions (IV). The model could be reasonably applied to wood.

According to the Broido-Shafizadeh model, pyrolysis starts with an intermediate prereaction (I) in which active cellulose is formed. The active cellulose subsequently decomposes by two competing first-order reactions: dehydration (reaction II) and depolymerization (reaction III). Reaction II involves dehydration, decarboxylation, and carbonization through a sequence of steps producing primarily char, water and CO_2. Reaction III involves depolymerization and scission, forming vapors that may condense as pyrolysis oil. The activation energies for dehydration (reaction II) are lower than those of depolymerization (reaction III). Thus, a lower temperature (< 300 ^{o}C), slower heating rates

and a longer residence time favor dehydration reactions. Depolymerization is, on the other hand, favored at higher temperatures (> 300 ^{o}C), fast heating rates, and longer residence times due to the higher activation energies. The products can undergo secondary reactions (reaction IV), cracking further into secondary char, tar, and gases.[2] Intra-particle reactions can happen either homogeneously in the vapor phase or heterogeneously by reaction with the solid wood or char. The rate of volatiles mass transport within and away from the particle will influence the extent of these reactions.[32] However, secondary cracking inside the particles is relatively unimportant for small particles associated with fast pyrolysis.[8] But secondary reactions could also occur after escaping the particle, either homogeneously in the vapor phase or heterogeneously on the surface of other wood or char particles.[32] Secondary reactions may be avoided by moderate temperatures, short vapor residence times in the hot reactor zone followed by rapid quenching of the products.[2]

2.3.3 Reactor configurations for fast pyrolysis

An important part of fast pyrolysis processes is the reactor. It must be designed to meet the important criteria for achieving high yields of pyrolysis oil:[5]

- Rapid heat transfer and high heating rates in order to minimize carbonization
- Moderate reactor temperatures of around 500 °C
- Short vapor residence times and rapid quenching in order to minimize secondary reactions

The heat transfer can be divided into three parts:[7, 34]

1. To the reactor heat transfer medium
2. From the heat transfer medium to the biomass particle
3. Within the pyrolyzing biomass particle

The heat transfer medium (solid reactor walls, solid inert particles such as sand, fluids, gases) could be heated by burning the byproducts (char / gases). The mode of heat transfer from the heat transfer medium to the biomass particle in most configurations is mainly conduction, with smaller contributions from convection and radiation.[34] The heat transfer within the biomass particle is a combination of conduction in the cell wall substance and radiation and convection in the pore system.[7]

A number of laboratory reactor configurations for achieving the necessary heat transfer have been developed over the last 20 years. Several pilot plants have been constructed, in addition to a few demonstration installations. The principles of some selected reactor configurations are presented in Figure 2-6, followed by brief descriptions. For more details, the reader is referred to the review on fast pyrolysis technology development by Venderbosch.[8]

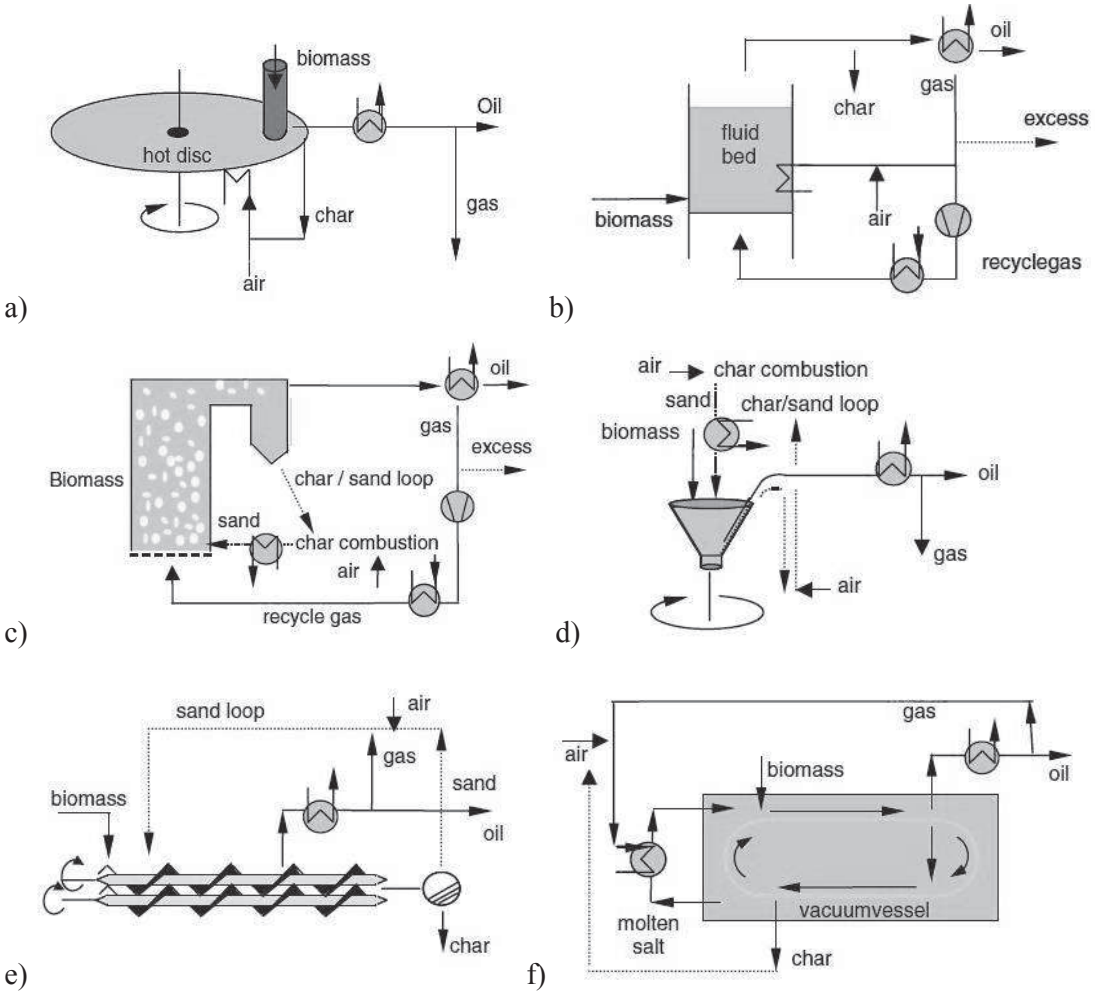

Figure 2-6. Principles of selected reactor configurations. a) ablative reactor, b) fluidized bed (FB) reactor, c) circulating fluid bed (CFB) reactor, d) rotating cone reactor (RCR), e) screw / auger reactor, f) vacuum reactor.[8*]

Ablative reactor

In an ablative reactor, biomass is pyrolyzed by being pressed onto a rotating hot disc (~ 600 °C). Due to the rotation, the biomass is mechanically moved away, leaving a residual oil film that both provides lubrication for successive biomass particles and also rapidly evaporates to give pyrolysis vapors.[35] It is possible to use larger particles, and there is no need for a carrier gas.[34] The disc surface is heated by a hot flue gas produced by combustion of pyrolysis gases and/or produced char.[8] The rate of reaction is strongly influenced by pressure, the relative velocity of biomass on the heat exchange surface, and the reactor surface temperature.[35] Oil samples have been produced in yields of up to 80 wt % (dry basis) in a small scale reactor of 2.5 kg/hr,[36] but the complexity of the system makes it less attractive for up-scaling.[8]

---

[*] Figure reprinted with permission from Robbie Venderbosch.

Fluidized bed (FB) reactor

FB reactors are popular due to their simple construction and operation.[37] The biomass is fed into the reactor and mixed with inert sand particles (~ 250 μm) that are fluidized by an inert gas. The residence time of the feedstock material is controlled by the fluidizing gas flow rate. The temperature control is good, and efficient heat transfer to biomass particles is achieved.[8] The heat is transferred from a heat source to the particles by a combination of convection and conduction. For efficient heat transfer throughout the sample, small particles of a few millimeters are required.[34] Pyrolysis oil yields from wood are up to 60 – 75 wt % on a dry feed basis.[5] The technology is well understood, but there are still technical problems such as char separation and bed material ending up in the liquid product. Another problem is the use of large quantities of inert gas for fluidization of the reactor bed. The inert gas is still mixed with the non-condensable gases after the pyrolysis oil is condensed. For continuous use, the inert gas must be separated and reheated. [8]

Circulating fluid bed reactor (CFB)

CFB reactors are based on the same heat transfer principles as FB reactors. The biomass is heated by mixing with inert sand particles in a fluidized bed. The same challenges with the large quantities of fluidization gas are experienced, but the main advantage of CFB is that sand is recirculated in the process. The sand and char are transported to a chamber where the char is combusted, resulting in reheating of the sand which may then be sent back to the reactor.[8] The technology is well understood, and yields above 70 wt % have been reported.[38] The operation, however, is somewhat problematic with substantial erosion problems and complications with the seals between various vessels.[8]

Rotating cone reactor (RCR)

In a RCR, biomass is fed near the bottom of a rotating cone together with excess flow of heat carrier material like sand.[39] The biomass and sand are driven up the wall of the cone due to fast rotation speeds (up to 600 rpm), and pyrolysis products exit from the top of the cone. The sand and char are further transported to a separate fluid bed where the combustion of char takes place. The produced vapors pass through a cyclone before entering the condenser, in which the vapors are quenched by re-circulated oil. No inert gas is needed in the system. Typical oil yields for a heated surface temperature of 600 °C are around 60 wt %.[37] It is demonstrated that it is possible to achieve auto thermal operation, but the technology is advanced and not that flexible for scale-up.[8]

Screw / auger reactor

The auger reactor is also based on mechanical mixing of biomass and a bulk solid heat transfer medium such as sand, but in contrary to RCR the mixing devices rotate inside a stationary horizontal reaction vessel. The vapors escape the system due to pressure differences, and there is no need for an inert carrier gas. The solid material (char and sand) leave at the end of the reactor into a combined heat exchanger and combustion reactor, in which the char is combusted and the sand is recirculated. The hot sand loop is maintained pneumatically or mechanically.[8] The main advantages of this system is the compact design.[40] Reported pyrolysis oil yields from wood are in the range of 40 – 50 wt %.[41]

Vacuum reactor

In the vacuum reactor, biomass is carried through hot horizontal plates, and the produced vapors are instantly removed via a vacuum pump. It is not a true fast pyrolysis technique as the heat transfer is much slower than that observed in other reactors. However, the vapor residence time is short, and secondary decomposition reactions are minimized due to the vacuum.[8] In the Pyrocycling process,[42] the biomass is heated indirectly by a mixture of potassium nitrate (KNO_3), sodium nitrite ($NaNO_2$), and sodium nitrate ($NaNO_3$). The salt itself is heated by burning the non-condensable gases from the process. It is possible to use larger particles, and there is no need for a carrier gas. Oil yields from wood is reported to be around 65 wt % at 15 kPa.[43] The process is mechanically complicated,[19] and the use of vacuum leads to larger equipment and higher cost.[34]

2.3.4 Properties and applications of pyrolysis oil

The liquid fraction of the pyrolysis products is mostly referred as pyrolysis oil, but it is also known under other names such as tar, bio-oil, bio-crude, and pyrolysis liquid. It is a dark brown, free-flowing liquid with a distinctive smoky odor.[44] The oil is a complex mixture of different size molecules derived from depolymerization and fragmentation of cellulose, hemicellulose and lignin.[45] More than 300 compounds have been identified,[46] with water being the single most abundant component.[47] However, complete chemical characterization is very difficult since the oil contains nearly all species of oxygenated organics, such as esters, ethers, aldehydes, ketones, phenols, carboxylic acids and alcohols.[48]

The composition and properties of pyrolysis oil is very different from petroleum-derived oils (Table 2-3),[49] with an elemental composition more like that of biomass.[44] The high water content of pyrolysis oil is due to original moisture in the feedstock and dehydration during decomposition. This lowers the heating value and flame temperature,[45] and at high concentrations the water causes the oil to separate in two phases.[49-50] The high oxygen content also lowers the heating value and makes it immiscible with hydrocarbon fuels. These properties make it difficult to use pyrolysis oil as a fuel directly in existing equipment constructed for petroleum-derived fuels. Also, the acidity makes the oil unstable and corrosive, resulting in more requirements on construction materials.[45]

Pyrolysis oil is a low-grade fuel compared to petroleum fuels,[51] but it has been successfully used as boiler fuel at commercial scale.[44] Combustion tests indicate that the oils burn effectively in standard or slightly modified boilers and engines.[49] It is also possible to use pyrolysis oils in gas turbines with some modifications of the equipment.[52, 53] However, the water content makes ignition a challenge, and the organic acids are highly corrosive to common construction materials.[49]

Table 2-3. Typical properties of pyrolysis oil (from wood) and heavy fuel oil (adapted from Oasmaa[49]).

Physical property	Pyrolysis oil	Heavy fuel oil
Water content (wt %)	15 – 30	0.1
pH	2.5	–
Spesific gravity	1.2	0.94
Elemental composition (wt %)		
C	54 – 58	85
H	5.5 – 7.0	11
O	35 – 40	1.0
N	0 – 0.2	0.3
Ash	0 – 0.2	0.1
HHV (MJ/kg)	16 –19	40
Viscosity (at 50 °C) (cP)	40 – 100	180
Solids (wt %)	0.2 – 1	1
Distillation residue (wt %)	up to 50	1

For the use as transportation fuels, it is possible to emulsify pyrolysis oil with diesel fuel with the aid of surfactants. A process for producing stable microemulsions with 5 – 30% pyrolysis oil in diesel has been developed,[54] but not commercialized due to high cost of surfactants and high amounts of energy required for emulsification. Another approach is deoxygenation of the oil, either by hydrotreating or catalytic vapor cracking. The processing costs are still very high, and the products are not competitive with fossil fuels.[44] However, this is a research of great interest in several institutes and universities around the world.[8]

Pyrolysis oil may also be the source of a range of chemicals. Some chemicals are already commercial, e.g. food flavoring (liquid smoke).[37] Other potential chemicals include replacement of formaldehyde-phenols in resins for particleboards,[55] biodegradable fertilizers, road de-icers, phenolic compounds, and sugars such as levoglucosan.[8, 44]

2.4 Thermal processing of biomass in molten salts

Thermal processing of biomass in molten salts is a relatively small research area compared to more conventional conversion methods. An overview is given here, and more details can be found in **Paper I**.

The idea behind thermal processing of biomass in molten salts is to perform the decomposition in a molten salt bath. The role of the molten salt in the process is as a heat carrier, catalyst, solvent, and as a fluid reaction bed. The salts are powders at room temperature, but become liquid when they are heated above the melting point. Once melted, they are very stable over a wide temperature range, from around 120 °C to well above 1000 °C depending on the type of salt and number of components in the salt

mixture. Due to their high heat capacity, they can store a great amount of energy over a long period of time.[56] Molten salts also have very good heat transfer characteristics. This has been studied for other purposes such as solar power towers and nuclear power plants.[57]

The thermal properties of molten salts make them potential as heat transfer media in pyrolysis or gasification. It has been shown that the heating rates for wood increase in chlorides and carbonates compared to in an inert atmosphere,[58] an important factor when it comes to maximizing the liquid fraction in fast pyrolysis.[8] Another advantage is the low viscosity of the salts leading to rapid enclosing and infiltration of the biomass particles. In this way, larger particle area will be exposed to heating by the salt.[56]

Some molten salts, especially halides, have a catalytic effect in the decomposition of larger molecules with respect to producing certain chemical compounds,[59] and may thus give a simpler product mix in the pyrolysis process. Zinc halides have been found to have a superior selectivity to produce single-ring aromatic compounds in hydrocracking of hydrocarbons.[60] This has been studied further for lignins, and it is reported that the yields of different phenolic compounds from pyrolysis of lignin in $ZnCl_2$-KCl are affected both by the ratio of the salt components[59] and salt-to-lignin ratio in the reactor.[61] The type of salt is also found to affect the water content of pyrolysis oil from cellulose and rice husk.[62]

Several researchers report higher concentrations of H_2 in the product gas for thermal processing of wood[63] and cellulose[64-65] in carbonates compared to inert atmospheres. For thermal treatment of municipal refuse, selected noxious contaminants are retained in the melt, and the H_2-rich product gas is essentially free of tars and oils. This means that the method is applicable for contaminated biomass and waste as well.[66] Na_2CO_3 gives rise in reaction rates for gasification of wastepaper,[67] while the carbon conversion is found to be most efficient with Li_2CO_3 present due to higher catalysis activity caused by the small Li-atoms.[68] Carbonates have also been used in gasification of organic waste.[69]

Chlorides have been used for recycling of plastics.[70-72] The yields of liquid hydrocarbons in $MgCl_2$ and KCl were poor, and HCl was observed in the product gas.[71] Switching to NaOH and Na_2CO_3 gave usable paraffins and waxes, and no HCl was produced. However, salt was consumed in the process.[72]

Molten salt gasification has been proposed in hybridization with solar energy, where a concentrating solar receiver could be used to heat and melt the salt. Due to the thermal stability and high heat capacities of molten salts, they could be used as a thermal storage for solar energy, making the gasification process stable under insolation fluctuations.[64] The process was originally considered for the gasification of coal and active carbon,[73-75] but the same principles may be applied for biomass.[64-65]

3 Experimental

This chapter describes the experimental work performed in **Papers II – V**. **Paper II** is a joint paper with the TCCB research group at the University of Twente (Netherland), and only the experimental part performed during the exchange stay is included in the following. There is no description of the first article (**Paper I**) since this is purely a literature study.

3.1 Preparation and characteristics of wood samples

Untreated wood was used as feedstock in all the experimental work in this thesis. Beech wood for **Paper II** was purchased as cylindrical wood sticks (d = 14 mm) from *Pijp-Lines Modelbouw & Hobby* (Enschede, Netherland). The wood sticks were milled and sieved in two fractions (< 0.08 mm, 0.08 – 0.2 mm). Wood for use as feedstock in **Papers III – V** was purchased from *Bauhaus* (Vestby, Norway). Beech (**Papers III** and **IV**) and pine (**Paper III**) wood cylinders (d = 1 – 8 mm) were prepared from cylindrical wood sticks with the length parallel to the fibers (Figure 3-1a). These were chosen as representatives for hardwood and softwood, respectively. Beech wood sawdust (0.5 – 2 mm) for **Paper V** was obtained by milling larger wood logs followed by sieving to the desired size fraction (Figure 3-1b). All wood samples were dried for 24 hours at 105 ^{o}C prior to the experiments in order to minimize the water content.

a)  b) 

Figure 3-1. Examples of feedstock used in the experimental work of this thesis. a) Beech wood cylinders prepared from cylindrical wood sticks. b) Beech wood sawdust prepared by milling larger wood logs.

The heat transfer within a wood particle is a combination of conduction in the cell walls and radiation and convection in the pore system. To account for these mechanisms, the term effective or equivalent conductivity (k_{eff}) is often introduced. Due to the anisotropic nature of wood, the heat transfer also depends on the direction of heat flow, and k_{eff} is often reported as either parallel (∥) or perpendicular (⊥) relative to the fibers. The effective conductivity parallel is usually between 1.5 to 2.7 times higher than that perpendicular to the fibers.[7] The properties and chemical composition of dry beech and pine wood are given in Table 3-1.

Table 3-1. Properties and chemical composition of dry beech and pine wood.[7]

	Beech (hardwood)	**Pine (softwood)**
Cellulose (wt %)	48	41
Hemicellulose (wt %)	28	26
Lignin (wt %)	22	28
Density, ρ (kg / m^3)	700	450
Effective conductivity (W / K·m)		
Parallell to fibers, k_{eff} (∥)	$3.490 \cdot 10^{-1}$	$2.593 \cdot 10^{-1}$
Perpendicular to fibers, k_{eff} (⊥)	$2.090 \cdot 10^{-1}$	$9.769 \cdot 10^{-2}$

The wood cylinders (**Papers III** and **IV**) with a diameter of 2 – 8 mm had a constant length of L = 30 mm, while the smallest cylinders (d = 1 mm) had a shorter length (L = 15 mm). All the cylinders had an aspect ratio (L/d) larger than 3, which makes the particles one-dimensional with respect to internal heat transfer,[76] and the conductivity perpendicular to the fibers, k_{eff} (⊥), is of importance. A hole was drilled from top to the center of the cylinders where a type K thermocouple was placed for measuring the particle center temperature. A 0.5 mm thermocouple was used for cylinders with d ≤ 3 mm, while a 1 mm thermocouple was used for the larger cylinders. It was confirmed experimentally that the two thermocouples gave similar results for cylinders with d ≥ 3.5 mm, and the largest was chosen for practical reasons.

3.2 Preparation and characteristics of artificial cylinders

In the study reported in **Paper II**, the effects of wood micro- and macrostructure and vapor outflow patterns (isotropic / anisotropic) on the char yield were studied in a fluidized sand bed. This was done by constructing two types of artificial cylindrical containers for milled wood as shown in Figure 3-2. The first type was made completely out of wire-mesh material, and the second type consisted of a solid wall covered with wire-mesh at the top and bottom, giving isotropic and anisotropic vapor outflow, respectively. The mesh used as wall in wire-mesh cylinders and bottom / top in both cylinder types was 9 μm. This pore size was chosen in order to let the produced vapors flow freely out, and at the same time char particles were retained inside the cylinders. The solid cylindrical wall was made of a double layer of 0.025 mm thick metal foil. The artificial cylinders were welded and filled with milled beech wood, with an overall density (mass wood / internal volume artificial cylinder) of 660 kg/m^3; identical to the natural wood cylinders for comparison purposes. The largest cylinders were also filled with natural wood cylinders of 14 mm to study the effect of the artificial walls. The macrostructure was varied by using cylinders of different sizes (L = 50 mm, d = 6, 10, and 14 mm), and the microstructure was varied by using different fractions of milled wood (< 0.08 mm, 0.08 – 0.2 mm).

a)  b) 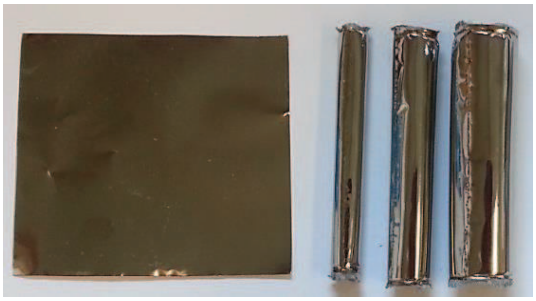

Figure 3-2. Artificial cylinders for the study of effects of wood microstructure and vapor outflow patterns in Paper II. a) Complete wire-mesh cylinders (9 µm) giving isotropic vapor outflow. b) Solid wall cylinders covered with wire-mesh at the top and bottom giving anisotropic vapor outflow.

3.3 Salts and inert gases

The salts used for the experiments in **Papers III – V** were purchased separately in their simplest form from *Sigma-Aldrich* (> 98.5% purity). The salts were mixed mechanically to obtain the eutectic compositions as listed in Table 3-2.

Table 3-2. Composition of salts used for the experiments in Papers III – V.

Molten salts composition (wt %)	Melting point	Paper
LiF-NaF-KF (29.2 – 11.7 – 59.1)	454 °C[77]	**III**, **IV** and **V**
Li_2CO_3-Na_2CO_3-K_2CO_3 (31.7 – 33.7 – 34.7)	397 °C[65]	**IV** and **V**
$ZnCl_2$-KCl (68.0 – 32.0)	181 °C[62]	**IV**
$NaNO_3$-KNO_3 (60.0 – 40.0)	220 °C[78]	**IV**

The salts are powders at room temperature, but become free flowing fluids when heated above the melting point (Figure 3-3).

a)  b) 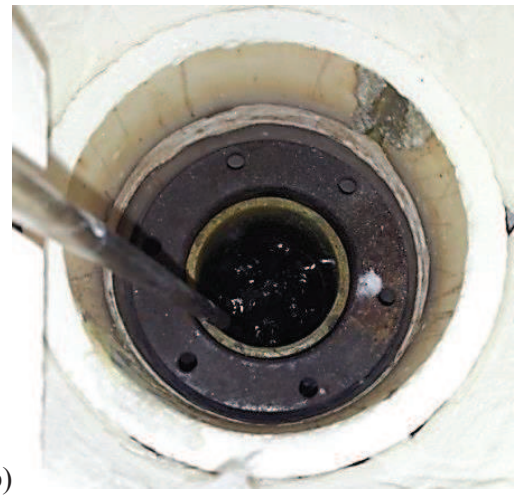

Figure 3-3. a) FLiNaK powder before melting (T ~ 25 °C). b) Molten FLiNaK with inert gas bubbling (T ~ 500 C).

The salts used for the experiments in **Papers III** and **IV** were dried for at least 24 h at 200 °C. For the experiments in **Paper V**, it was essential that the salts were completely moisture free before the crucibles were placed in the reactor since the char yield was determined by weighing the reactor before and after experiments. The salts were therefore pre-melted at 500 °C and kept in a drying cabinet at 200 °C until used (> 24 h).

AGA provided the inert gases (Ar and N_2) used in all the experimental work. The concentrations and most important impurities of the gases are listed in Table 3-3.

Table 3-3. Concentration and most important impurities of the inert gases used in the experimental work.

	Argon (Ar)	Nitrogen (N_2)
Concentration	99.99%	99.999%
Impurities		
H_2O	≤ 20 ppm	≤ 3 ppm
O_2	≤ 20 ppm	≤ 3 ppm
C_nH_m	n.a.	≤ 1 ppm

3.4 Experimental setup and procedure

Two types of experimental setups were used during this study. The experimental work in **Paper II** was performed in an existing fluidized sand bed reactor at the University of Twente. For the experimental work in **Papers III – V**, a molten salt reactor was developed at NMBU. The two setups are described separately, with most emphasis on the molten salt reactor, as the development of this reactor was a part of the PhD study.

3.4.1 Fluidized sand bed reactor

The experimental work in **Paper II** was performed in a fluidized sand bed reactor (Figure 4, **Paper II**). For the experiments with the artificial cylinders, only the first part of the pyrolysis system was used. The reactor was constructed of stainless steel (H = 200 mm, ID = 90 mm) and placed in an electric furnace for independent temperature control. The reactor temperature was kept at 500 ^oC for all experiments, continuously controlled by a submerged K type thermocouple. The incoming fluidization gas (N_2, 12 L/min) was preheated to 500 ^oC and led to the bottom part of the reactor. After entering the reactor, the hot gas was led through a gas diffuser with pores of 30 μm in order to distribute the gas evenly into the fluidized bed. 1 kg silica sand (particle size 212 – 300 μm) was used as bed material.

The artificial cylinders with milled wood were fed to the reactor by a batch-wise feeding system consisting of two ball valves. The lower valve was closed, and three identically prepared cylinders were placed in the space between the valves. The upper valve was then closed, and the lower valve was opened so that the samples would fall into the reactor. A small N_2 flow was introduced along with the samples. After the pyrolysis reactions were

completed, the power was turned off, and the reactor was left under N_2 flow until ambient temperature was reached. The artificial cylinders were recovered from the sand bed, and the char yield was determined by weighing each cylinder separately before and after experiments. Due to the small number of cylinders fed to the reactor in each experiment, it was not possible to determine accurate oil and gas yields.

3.4.2 Molten salt reactor

The general experimental equipment used in molten salt pyrolysis (**Papers III – V**) is shown in Figure 3-4. Schematic representations may also be found in the respective papers (Figure 1 in **Paper III** / **IV**, Figure 3 in **Paper V**).

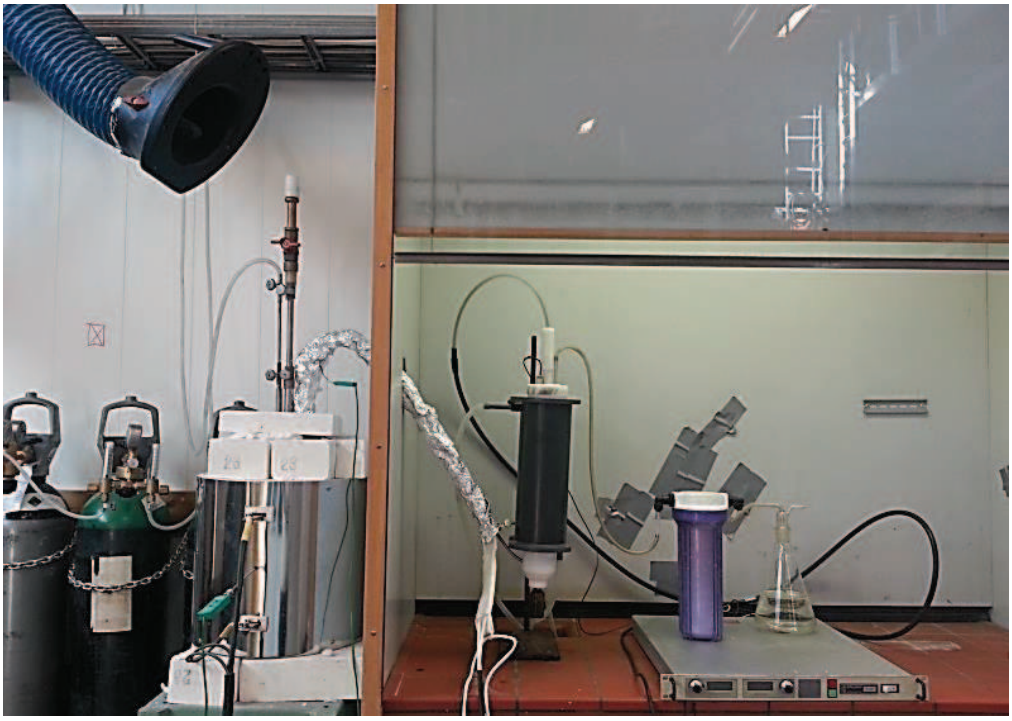

Figure 3-4. General experimental setup for molten salt pyrolysis.

The salt mixture (200 g [**Papers III** and **IV**] or 300 g [**Paper V**]) was filled in a nickel crucible (H = 190 mm, ID = 52 mm), giving molten bed heights ranging from 45 to 70 mm depending on the type of salt and final reactor temperature. The parts in contact with the molten salt were constructed out of nickel because this material is more resistant to the corrosive environment associated with molten salts at high temperatures.[57] The crucible was placed inside a stainless steel reactor (H = 200 mm, ID = 62 mm) that was sealed at both ends by bolt type flanges with mineral wool (Superwool 607 Paper, 2 mm) as gasket material (Figure 3-5a). The tubes for inert gas, feeding of wood samples, temperature measurements, and outlet of vapors were welded on the top of the sealed reactor and connected to other parts of the system by tube fittings (Swagelock-316).

a)  b) 

Figure 3-5. Experimental equipment for molten salt pyrolysis. a) Nickel crucible (left) and stainless steel reactor (right). b) Ball valve based feeding system.

The reactor was placed in an open ceramic tube furnace (< 1250 °C) having a base of insulating ceramic blocks. The heating was controlled by a programmable temperature regulator (Eurotherm 3200). Ceramic blocks and mineral wool (Superwool 607 Blanket, 38 mm) were used as isolation around the reactor at the top of the furnace. Preliminary experiments showed a uniform temperature throughout the furnace. The reactor temperatures for the different experiments are given in the respective papers.

The inert gas (Ar / N_2) was flowed into the reactor through a 4 mm nickel tube with a flow rate of 2 L/min (**Papers III** and **IV)** or 0.6 L/min (**Paper V**). The tube was kept above the salt during the heating, but immersed to a depth of 1 cm from the bottom of the crucible after the salt was completely melted. The turbulent bubbling of inert gas ensured an oxygen free atmosphere, enhanced the heat transfer from the salt to the wood during the pyrolysis process, and led the produced vapors (both condensable and non-condensable) out of the reactor.

The samples were introduced to the reactor manually through a ball valve based feeding system similar to the one described for the fluidized sand bed reactor (Chapter 3.4.1), but with a plug at the top (Figure 3-5b). It was designed so that tubes / rods could slide through the plug without any gases entering or leaving the system. For the temperature measurement experiments (**Papers III** and **IV**), the samples were attached to a long thermocouple (L = 1000 mm), placed inside a steel tube for mechanical support. In this way, the samples could be pushed down, and it was made sure that they were completely submerged in the molten salt bath during the experiments (Figure 1, **Paper III** / **IV**). The thermocouple was connected to a logging system (HIOKI 8430-20 Memory Hilogger), and the temperature was measured at a frequency of 2 (**Paper III**) or 5 (**Paper IV**) times per second. The data was further processed in Wolfram Mathematica (version 8).

The milled wood particles (**Paper V**) were fed in batches of 0.3 – 0.5 gram (ca 20 – 25 grams in total). The feeding tube was kept 1 – 2 cm above the molten salt bath, and the particles were forced into the reactor with the aid of a push rod. The mixing of small particles in a fluid bed was checked visually in a cold-flow glass model with a water-sugar solution to obtain similar characteristics as molten salts, and a quick mixing was observed due to the turbulent bubbling of the inert gas.

A 9 μm wire-mesh filter was placed at the exit of the reactor for in situ filtration of char and ash from the hot pyrolysis vapors. This type of filtration prior to condensation has been shown to give yields comparable to those obtained when cyclones are used, but with less solids, alkali metals, and ash in the liquid product.[79] In the experiments during this study, there was much less clogging of the outlet tube when this filter was used. Also, it keeps unreacted wood particles inside the hot reactor. The vapors were led out of the reactor through a 4 mm transfer line heated externally to 450 °C by a heating wire (SAN Electro Heat, 316W). An electrostatic precipitator (ESP) was constructed for collection of pyrolysis oil (Figure 1, **Paper V**). The ESP consisted of a grounded cylinder made of stainless steel (H = 150 mm, ID = 50 mm) placed inside an outer cylinder made of the isolating material polyoxymethylene (POM). POM was chosen due to its low coefficient of friction, good dielectric properties, and good resistance to oils, greases, and solvents.[80] A stainless steel wire (1 mm) co-axial with the grounded cylinder was connected to a high voltage source (Spellman, SL300) and used as discharge electrode (positive potential, 0 – 20 kV). The ESP was cooled externally with tap water (~ 20 °C). Initial tests were carried out to choose the proper settings of the ESP giving stable operation without spark-overs and complete separation of the condensable vapors from the remaining gas stream. A bubble flask with water was attached at the exhaust, and it could be easily observed if the outlet gas contained any uncondensed pyrolysis vapors, as these would fill the empty part of the flask with white "smoke" as shown in Figure 3-6.

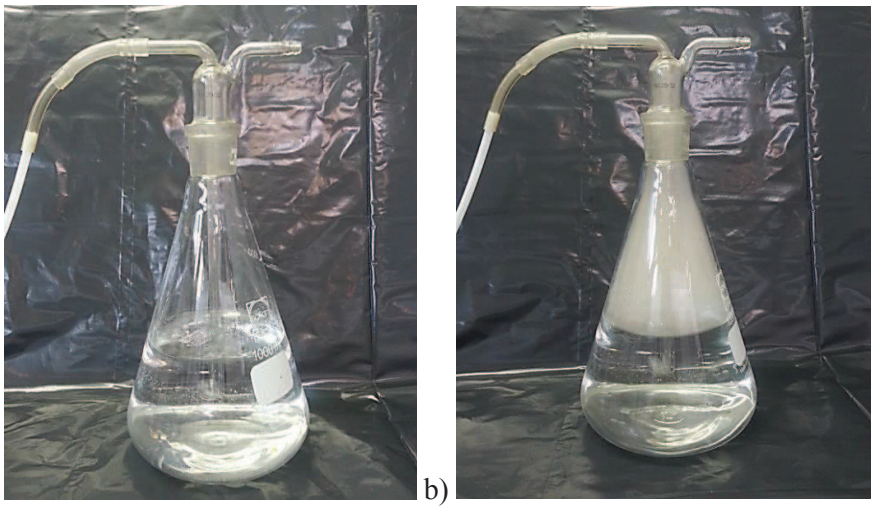

Figure 3-6. For the testing of the electrostatic precipitator (ESP), a bubble flask with water was attached at the exhaust of the ESP. a) Normal operation of the ESP. No uncondensed vapors are observed. b) Failure of the ESP (too low voltage or spark-overs). The pyrolysis vapors are clearly visible.

A tubular cotton gas filter (filtration level 10 μm) was used for capturing the remaining vapors, and the non-condensable gases were vented off. After the experiments were completed, the power was turned off, and the system was left under inert atmosphere until ambient temperature was reached.

For the temperature history studies (**Papers III** and **IV)**, only the first part of the system was used, since the small amounts of feedstock did not provide enough oil for accurate yield measurements. The char product was covered and infiltrated with salt (Figure 4-5, p. 33), making accurate char yield measurements difficult as well.

In **Paper V**, the char yield was determined by weighing the reactor filled with salt and char before and after the experiment. The pyrolysis oil yield was determined gravimetrically by reweighing the entire ESP and cotton filter. The water content of the oil recovered from the ESP was determined by Karl Fischer titration (KFT) (Metrohm 870 KF Titrino plus). The used titer was Hydranal Composite 5. The outlet gas was analyzed to detect possible produced HF gas from FLiNaK pyrolysis with a FTIR gas analytical cell (Thermo Scientific, Nicolet 6700 FTIR spectrometer).

4 General results and discussion

In this chapter, the most important outcomes from the experimental work (**Papers II – V**) are presented and discussed. A summary of the literature study (**Paper I**) was given in the theoretical part of the thesis (Chapter 2.4). For **Paper II**, the main focus is on the experiments performed during the exchange stay at the University of Twente, but the results are discussed in the context of the whole paper. In the last subchapter, challenges with molten salts in thermal processing of biomass are discussed.

4.1 Effect of particle structure and vapor outflow pattern in a fluidized sand bed

In order to achieve rapid heating associated with fast pyrolysis, biomass particles are traditionally kept smaller than 2 – 3 mm.[34] However, later research by Wang et al.[76, 81] has shown that the biomass particle size of wood cylinders (d = 0.7 – 14 mm) only has a minor effect on the lumped product yields in both theoretical simulations and experimental work. Salehi et al.[82] reported a rapid decrease in oil yield for sawdust particles as the size was raised from < 0.59 mm to 1 mm, while the decrease in oil yield leveled off for larger particles. The effect of smaller biomass particles (0.18 – 5.6 mm) was also studied by Shen et al.[83] It was found that the yield of pyrolysis oil decreased rapidly with particle size up to 1.5 mm, but no significant effects on the yields were discovered for larger particles. For both studies, the very high oil yields for the smallest particles were accompanied by low char yields. Shen et al.[83] suggested that changes in biomass cell structure during grinding could make the components more available for decomposition and give the high oil yields and low char yields observed for the smallest particles.

The aim of **Paper II** was to study this hypothesis further. Artificial wood containers were constructed (L = 50 mm, d = 6, 10, and 14 mm) and filled with milled beech wood particles (< 0.08 mm, 0.08 – 0.2 mm). These were used to evaluate the effect of wood micro- and macrostructure and vapor outflow patterns on the char yield in a fluidized sand bed at 500 °C. Figure 4-1 describes the outflow pattern of the wood particles and the artificial containers. Natural wood cylinders have channels in the longitudinal direction, and the vapor outflow is anisotropic. This channel structure is destructed when the wood goes through extensive milling, and the particles consist only out of cell wall material. Scanning electron microscope (SEM) was used to confirm this destruction (Figure 4-2). The microstructure of the extensively milled particles was very different than for larger particles. Particles of 1 mm still had the channel structure intact (Figure 4-2a), while the small particles used in this study consisted only of cell wall material (Figure 4-2b). This means that the vapors produced during pyrolysis can flow freely out in all directions. In addition, the particles in the artificial cylinders are randomly packed, in contrast to the highly structured longitudinal channels found in natural wood cylinders. Artificial solid wall cylinders give anisotropic outflow, while wire-mesh cylinders give isotropic outflow.

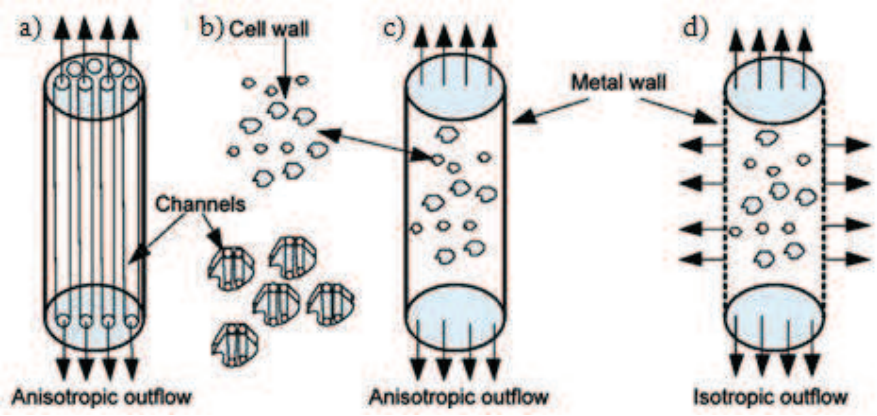

Figure 4-1. Wood particles and artificial containers. Arrows out of the cylinders indicate the direction of the outflow of produced vapors. (a) Natural wood cylinders with channels in longitudinal direction, giving anisotropic outflow. (b) Milled wood where the channel structure has been destructed. (c) Milled wood in solid wall cylinders giving anisotropic outflow. (d) Milled wood in wire-mesh wall cylinders giving isotropic outflow.

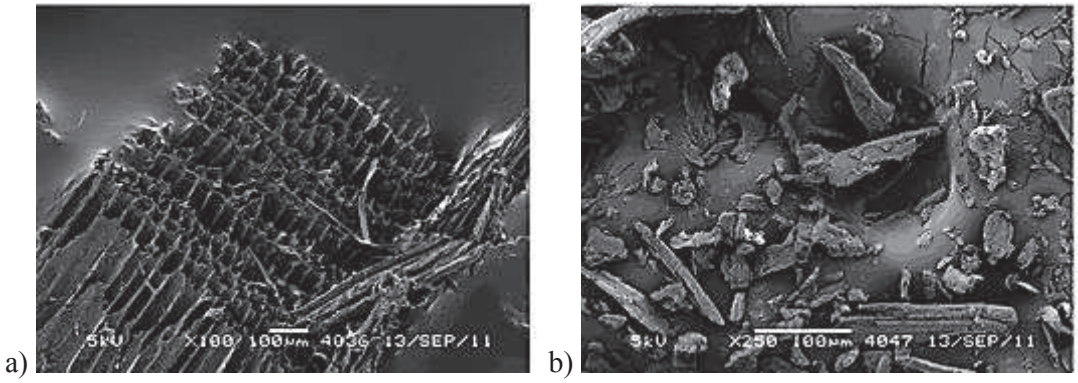

Figure 4-2. Scanning electron microscope (SEM) of milled beech wood particles. (a) 1 mm particles with the wood channels still intact. b) Particles smaller than 0.08 mm with the wood structure completely destructed. The same destruction was also observed for the fraction 0.08 – 0.2 mm (not shown).

By inserting the extensively milled particles (< 0.08 mm) in artificial cylinders of different sizes and comparing the results with natural wood cylinders, it was possible to evaluate whether internal microstructure or macrostructure is dominant with respect to the char yield. Due to too high char loss (1 – 3 wt %) for the artificial wire-mesh cylinders with the smallest particles, these experiments could only be performed with solid wall cylinders. The effect of outflow pattern was examined by inserting the other particle fraction (0.08 – 0.2 mm) in the wire-mesh cylinders. Although the particles were slightly larger, the channel structure was still destructed for this particle fraction. Hence, the microstructure was the same, but the vapors formed in the solid wall cylinders could only flow out in the longitudinal direction of the cylinder, while they were allowed to flow out in all directions in the wire-mesh cylinders.

In order to ensure that the metal walls did not influence the heating rate nor give any catalytic effects, natural wood cylinders of 14 mm were inserted in the artificial cylinders. The char yield of the wood cylinders enclosed by the solid wall and wire-mesh wall

cylinders were identical to the char yield of separately pyrolyzed wood cylinders (23.0, 23.1, and 23.0 wt %, respectively). Hence, no heat transfer limitations or catalytic effects of the materials in the artificial cylinders were discovered. It was also confirmed in separate experiments that the artificial wood cylinders experienced equal heating rates as the natural wood cylinders of equal size, and that no significant amounts of sand entered the artificial cylinders during sand fluidization. The char loss was found to be less than 0.4% of the initial char for all cases except for the already mentioned case with the smallest particles (< 0.08 mm) in wire-mesh cylinders.

Three cylinders were used in each experiment. The cylinders were weighed separately to ensure reproducibility, and the standard deviation between the char yields of experiments of identical artificial cylinders was always smaller than 0.3%. Table 4-1 shows the data for a typical experimental run, and Figure 4-3 shows an example of a wire-mesh cylinder (d = 14 mm) filled with milled beech wood before and after an experiment. A few experiments had to be repeated because of too high deviation in the results. It was assumed that sand had entered the cylinders or char was lost due to poor welding or other experimental errors. In most of these cases, rupture of the artificial cylinders could be observed.

Table 4-1. Data for a typical experiment with artificial cylinders (Paper II).

Information			
Experiment number	14		
Date	4/29/2011		
Wood particle size (mm)	0.08 – 0.2		
Cylinder diameter (mm)	14		
Cylinder wall material	Wire-mesh		
Results			
Cylinder	i	ii	iii
Wood input (g)	5.558	5.458	5.242
Char yield (g)	1.080	1.068	1.012
Char yield (wt %)	19.4	19.6	19.3
Average (wt %)	19.4		
Standard deviation	0.13		

Figure 4-3. Artificial wire-mesh cylinder (d = 14 mm) before (left) and after (right) pyrolysis in a fluidized sand bed (500 °C)

Figure 4-4 shows the average char yield of the artificial cylinders as function of cylinder size, expressed as percent of the initial dry wood mass. Data for loose particles and natural wood cylinders are included for comparison. It was clear that the char yield increased as the particle size was increased. A discontinuity was observed between loose milled particles and wood cylinders. The same discontinuity was also observed for the oil and gas yields (Figure 5, **Paper II**): the milled particles had higher oil and lower gas yields. The loose particles have a shorter particle length, and will thus experience faster heating rates

in all directions. The vapors will also have a shorter escape route, minimizing the probability of secondary reactions within the particles.

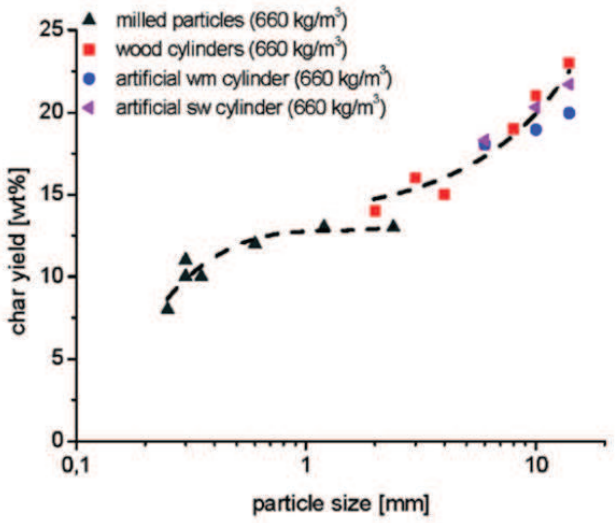

Figure 4-4. Char yields as function of particle size in a fluidized sand bed at 500 °C. The char yield of the natural wood cylinders, and the artificial solid wall (sw) and wire-mesh (wm) cylinders are plotted as function of cylinder size.

The char yields of artificial solid wall cylinders and natural wood cylinders of equal size were comparable within the accuracy of the data. Although the microstructure was very different, it appeared that this had no notable effect on the char yield of large cylinders (6 – 14 mm). The yields of artificial cylinders were nowhere near the yields of the loose milled particles in spite of the same microstructure. Instead, the char yield was predominantly determined by the outer cylinder diameter. This could be because the larger particles have a lower heating rate due to the poor conductivity of wood. This will give a lower average temperature at which the pyrolysis reactions occur, leading to more char.

The effect of outflow pattern was slightly more visible, with lower char yields for wire-mesh cylinders compared to solid wall cylinders. The hypothesis was that when the vapors escape from artificial cylinders in an isotropic manner, there is less contact of formed vapors with char due to shorter outflow distances. This results in no further polycondensations of the vapors on char, and an overall lower char yield. The hypothesis was not contradicted by the experiments, but the observed effects were not very strong.

Although only the char yield was measured in the experiments with the artificial cylinders in **Paper II**, this was an indication on the mechanisms occurring during the pyrolysis process. During pyrolysis of only cell wall material, resulting droplets can vaporize much faster than inside a channel of a large particle. Slower vaporization processes of droplets under high temperature pyrolysis conditions result in the formation of more char by cross-linking reactions instead of the outflow of produced vapors from the reacting particle(s).

4.2 Temperature history of wood particles in molten salt pyrolysis

In **Papers III** and **IV**, the aim was to investigate the thermal behavior of wood particles, as well as gain a better understanding of molten salts as heat transfer media during fast pyrolysis. The temperature at the center of cylindrical wood particles was recorded during molten salt pyrolysis, and this was used to evaluate heating rates, reaction temperatures and devolatilization times. The experiments were performed in triplicate to ensure acceptable reproducibility. Figure 4-5 shows a pine wood cylinder (d = 6 mm) before and after pyrolysis in FLiNaK at 500 °C. The charred particles were in most cases still left on the thermocouple after the experiment, but they were very brittle. It could be observed that the samples were covered and infiltrated with salt.

a) 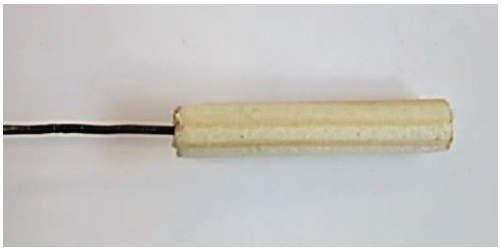 b) 

Figure 4-5. Pine wood cylinder (L = 30 mm, d = 6 mm) before (a) and after (b) pyrolysis in FLiNaK at 500 °C. The solid residue was covered and infiltrated with salt.

4.2.1 Definitions of characteristic points during wood pyrolysis

The temperature at the particle center was measured, and the heating rate was calculated using three point estimation according to Eq. 4-1.

$$h_i = \frac{T_{i+1} - T_{i-1}}{t_{i+1} - t_{i-1}} \qquad (4\text{-}1)$$

Figure 4-6 shows the recorded temperature and the calculated heating rate for pyrolysis of beech wood (d = 6 mm) in FLiNaK at 500 °C. The shape of the temperature profiles and the heating rate curves are qualitatively the same for all the experiments performed in **Papers III** and **IV** (except for pyrolysis in nitrates, these results are treated separately). The temperature rises rapidly until the main degradation of cellulose and hemicellulose occur at a nearly constant temperature plateau. The temperature at this point could be regarded as representative of the effective pyrolysis temperature.[84] After the endothermic degradation of cellulose and hemicellulose is nearly completed, the slower, high-temperature exothermic degradation of lignin dominates.[85] The temperature rises rapidly before the particle temperature reaches and stabilizes at the reactor temperature. In some cases a maximum temperature higher than the bed temperature is observed. This was more prominent for the thickest particles used in **Paper III** due to the higher mass of lignin and the longer time for the gases to escape from the particle.

Several characteristic points stand out clearly during the wood pyrolysis process. We have chosen to follow the same definitions of these as given by Di Blasi and Branca in their

study of pyrolysis of cylindrical beech wood particles (L = 20 mm, d = 2 – 10 mm) in a hot sand bed (T = 534 °C) fluidized by nitrogen.[86] Brief descriptions of the points are given in Table 4-2, and more thorough descriptions may be found in the result part of **Paper III**.

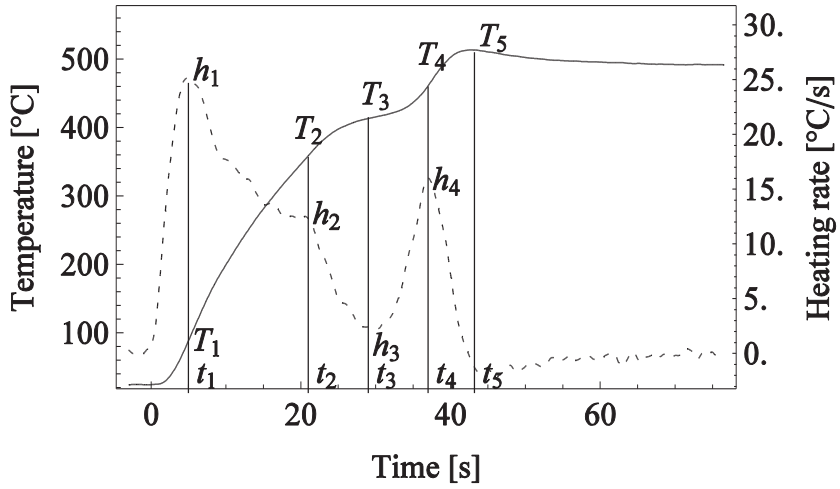

Figure 4-6. Temperature profile and calculated heating rate at center of cylindrical beech wood (L = 30 mm, d = 6 mm) in FLiNaK pyrolysis at reactor temperature T = 500 °C. Several characteristic points stand out clearly, and these are described in Table 4-2.

Table 4-2. Description of characteristic points during pyrolysis of wood particles.

Characteristic points	Description
h_1 / t_1 /T_1	Maximum heating rate. This is measured right before any reactions occur. After this point, degradation starts in the outer part of the cylinder and inward heat transfer is hindered.
h_2 / t_2 /T_2	Point of high variation. This indicates the beginning of the endothermic degradation of cellulose and hemicellulose at the particle center.
h_3 / t_3 / T_3	Local minimum of heating rate. This point represents the main occurrence of degradation of cellulose and hemicellulose, and T_3 may be regarded as the effective pyrolysis temperature.
h_4 / t_4 / T_4	Local maximum of heating rate. The exothermic degradation of lignin – which happens over a wider temperature range – starts to slow down. At this point, the conversion is about 95%.
t_5 / T_5	Maximum temperature. The conversion process is practically terminated, and t_5 may be regarded as the total devolatilization time.

4.2.2 Effect of wood type and particle size

In **Paper III**, the focus was to evaluate the effect of wood type and particle size in FLiNaK at 500 °C. In general, molten fluoride salts are known to have high thermal conductivities, high specific heats, low viscosities, and high boiling points.[57] FLiNaK has in particular shown good heat transfer performance in previous research of heat transfer media for solar power towers and nuclear power plants.[77] Two types of wood were chosen for **Paper III**, namely beech and pine wood. These were chosen as representatives for hardwood and softwood, respectively. Beech wood has a higher thermal conductivity than pine wood (Table 3-1, p. 22), and this was reflected as beech wood particles reached the different pyrolysis stages faster than pine wood with the same dimensions (Figure 4-7).

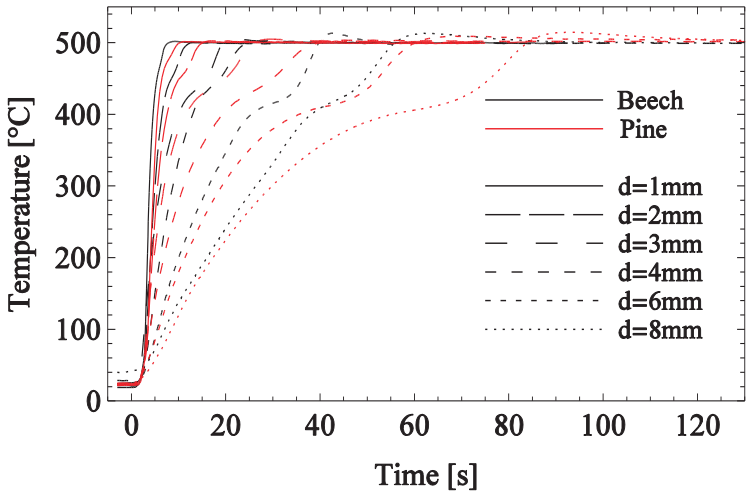

Figure 4-7. Temperature profiles at the center of cylindrical beech (black) and pine (red) wood particles in FLiNaK at 500 °C.

In spite of the time difference during heating, the characteristic temperatures were comparable for the two wood types (Figure 4-8). This indicated that the thermal properties of the wood sample play a less important role for the reaction temperatures during pyrolysis. The high scatter in T_1 was ascribed to the associated high heating rates (Figure 4-9), making precise evaluation of the corresponding temperatures difficult. T_2 and T_4 were practically independent of the particle size, while the effective pyrolysis temperature (T_3) decreased from 469 ± 4.5 °C for d = 1 mm to 412 ± 6.5 °C for d = 8 mm. This particle dependence was in accordance with both simulations and experimental work for wood pyrolysis in a fluidized sand bed reactor at 500 °C by Wang et al.[76,81]

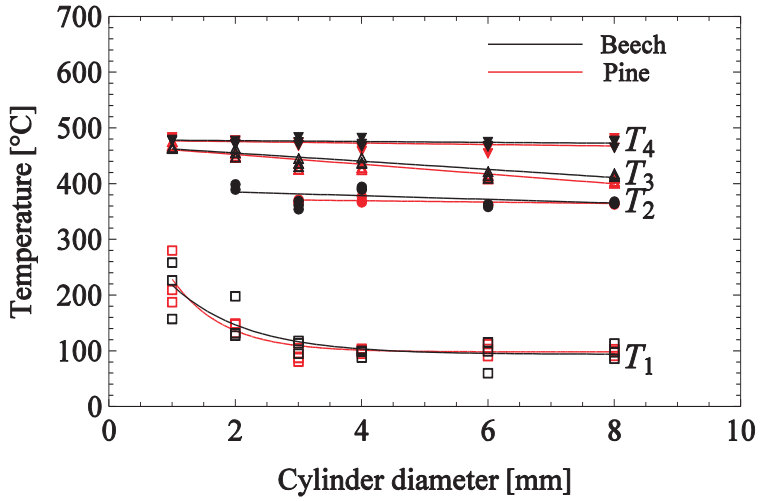

Figure 4-8. Characteristic temperatures as a function of cylinder diameter at the center of cylindrical beech (black) and pine (red) wood particles in FLiNaK at 500 °C.

Figures 4-9 – 4-12 show the characteristic heating rates (h_1 – h_4) as a function of cylinder diameter. Beech and pine wood cylinders are represented by black and red lines, respectively. Results for fluidized sand bed estimated from Di Blasi and Branca[86] (green lines) are included for comparison. All the heating rates decreased with increasing particle size because of increasing internal heat transfer resistance inside the particles. For molten salt pyrolysis, the values were always slightly higher for beech wood than pine wood for otherwise identical conditions. This was ascribed to the higher thermal conductivity of hardwoods (Table 3-1, p. 22).

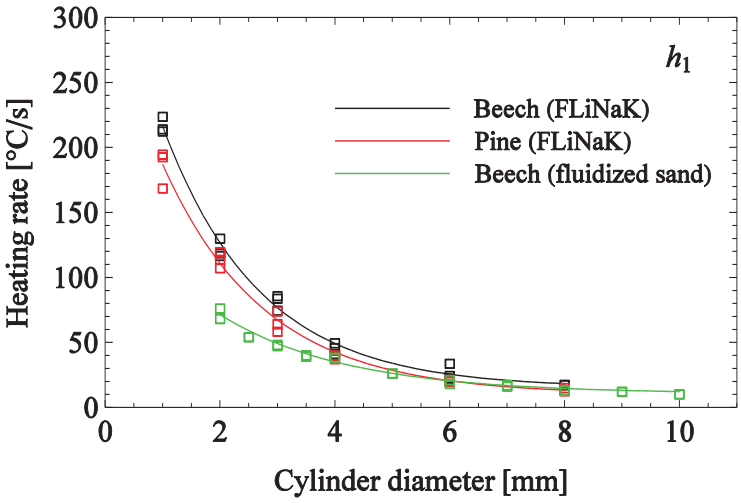

Figure 4-9. Maximum heating rate h_1 at the center of cylindrical beech (black) and pine (red) wood particles in FLiNaK at 500 °C. Reference values (green) are estimated for beech wood in a fluidized sand bed at 534 °C.[86]

One of the most important findings in **Paper III** was that the maximum heating rate (h_1) was significantly higher in FLiNaK than in fluidized sand for beech wood cylinders with $d \leq 4$ mm (Figure 4-9). h_1 is of special interest because it is measured before the thermal decomposition starts, and differences between the heating media appear. Heating rates as high as 218 ± 6 and 186 ± 15 °C/s were observed for beech and pine wood, respectively, but with an exponential decrease with increasing particle size. For particles with $d > 4$ mm, there were practically no effects of wood type or heating media.

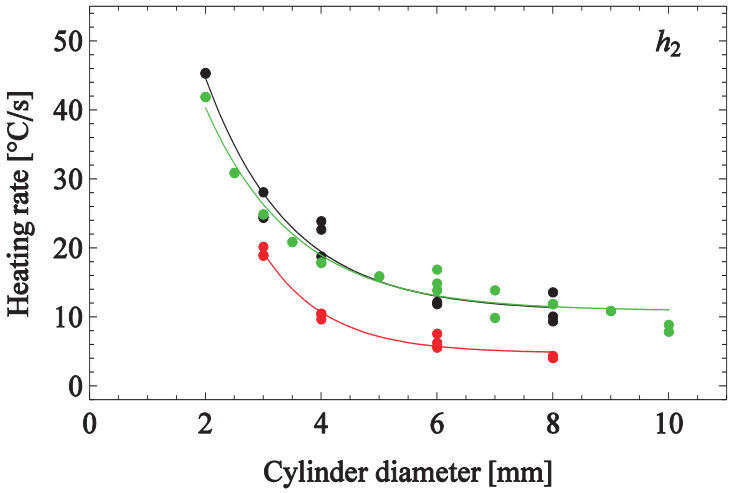

Figure 4-10. Point of high variation of the heating rate h_2 at the center of cylindrical beech (black) and pine (red) wood particles in FLiNaK at 500 °C. Reference values (green) are estimated for beech wood in a fluidized sand bed at 534 °C.[86]

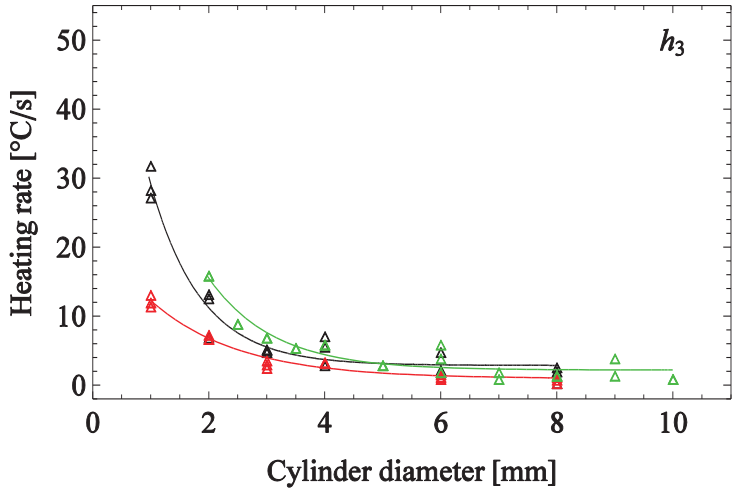

Figure 4-11. Local minimum heating rate h_3 at the center of cylindrical beech (black) and pine (red) wood particles in FLiNaK at 500 °C. Reference values (green) are estimated for beech wood in a fluidized sand bed at 534 °C.[86]

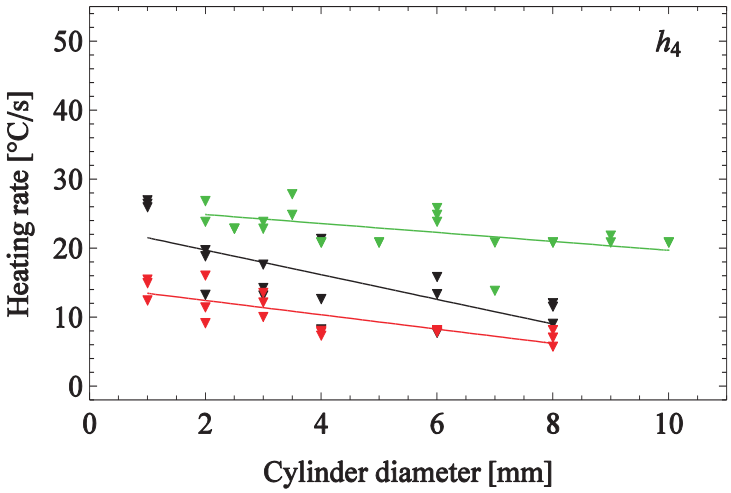

Figure 4-12. Local maximum heating rate h_4 at the center of cylindrical beech (black) and pine (red) wood particles in FLiNaK at 500 °C. Reference values (green) are estimated for beech wood in a fluidized sand bed at 534 °C.[86]

Cellulose and hemicellulose degrade over a very narrow range of temperatures,[87] and the heating rates associated with this (h_2 / h_3) were not much affected by the heating media (Figures 4-10 and 4-11). They were, however, strongly dependent on the wood type and particle size. An exponential decrease with increasing particle size was observed, but not as prominently as for the maximum heating rate. The decrease was explained by a combination of heat transfer limitations and an increased cooling effect due to higher amounts of endothermic reacting cellulose and hemicellulose. Lignin decomposes over a wider temperature range.[85] This was reflected in h_4 with a stronger dependence on the heating media, as well as wood type (Figure 4-12). Differences in reactor temperature in FLiNaK and fluidized sand bed (500 °C and 534 °C, respectively) could also be a reason for the differences observed for h_4.

4.2.3 Effect of salt composition and reactor temperature

Paper III showed that the maximum heating rates for beech wood in FLiNaK were significantly higher than in fluidized sand for particles with $d \leq 4$ mm. In **Paper IV**, the aim was to investigate the effect of different salt compositions and reactor temperatures. The constant particle size (L = 30 mm, d = 3.5 mm) was a compromise between small enough particles in order to discover differences between heating media and large enough particles to facilitate sample preparation and execution of the experiments.

Four different salt mixtures were chosen; FLiNaK, $(LiNaK)_2CO_3$, $ZnCl_2$-KCl, and KNO_3-$NaNO_3$. FLiNaK had already shown promise as an effective heat transfer medium in wood pyrolysis (**Paper III**). The choice of the other salt mixtures was based on previously reported results (**Paper I**). Several researchers have demonstrated a strong influence by molten carbonates on thermal processing of coal[73-75] and cellulose.[64,65]

Adinberg et al.[64] reported an increase of 20% in the reaction rate of cellulose in a eutectic mixture of K_2CO_3 and Na_2CO_3 compared to in an inert gas atmosphere at 850 °C. Hathaway et al.[65] added Li_2CO_3 to the carbonate mixture and measured an increase in the pyrolysis rate by 74% compared to in an inert gas atmosphere. This was explained by enhanced heat transfer within the salt. $ZnCl_2$-KCl has been used in pyrolysis of lignin. Sada et al.[59, 61, 88] focused on the yield of phenolic compounds from kraft and solvolysis lignins heated in mixtures of molten $ZnCl_2$ and KCl. It was found that the yields of different phenolic compounds depend on both the molar ratio of the two salts[59] and the salt-to-lignin ratio in the reactor.[61] In the Pyrocycling process, a mixture of KNO_3, $NaNO_2$ and $NaNO_3$ was used as an indirect heat transfer medium in vacuum pyrolysis.[42] The heat transfer characteristics for nitrates were also investigated for the purpose of storing thermal solar energy. "Solar salt" (KNO_3-$NaNO_3$) was found to be a better candidate than "Hitec" ($NaNO_3$-KNO_3-$NaNO_2$) due to higher heat transfer efficiency during heat storage and discharge stages.[78]

The experiments in **Paper V** were performed in the temperature range of 400 – 600 °C, with some differences due to respective melting and decomposition temperatures of the salt mixtures (Table 3-2, p. 23). The characteristic points during the pyrolysis process were defined in the same way as for **Paper III** (Figure 4-6, p.34). Figure 4-13 shows the recorded temperature at the center of cylindrical beech wood particles (d = 3.5 mm) at reactor temperature 500 °C, where one representative curve is chosen for each salt mixture.

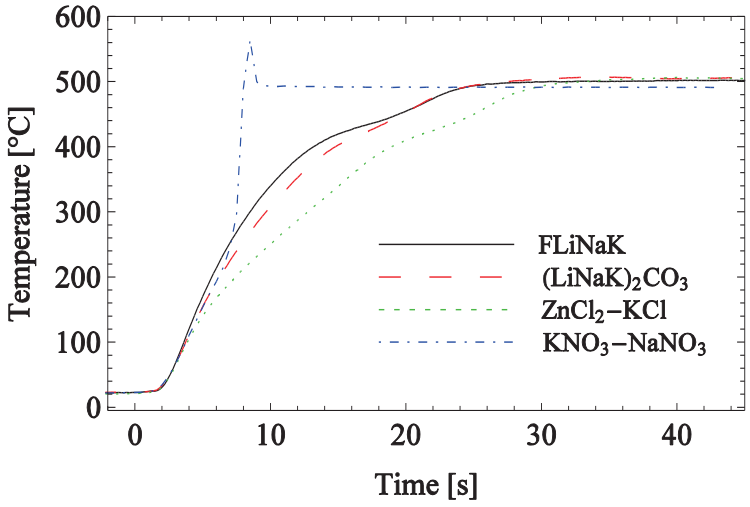

Figure 4-13. Temperature profiles at the center of beech wood particles (L = 30 mm, d = 3.5 mm) at reactor temperature T = 500 °C in FLiNaK (black), $(LiNaK)_2CO_3$ (red), $ZnCl_2$-KCl (green), and KNO_3-$NaNO_3$ (blue).

The temperature profile for pyrolysis of beech wood in nitrates differed greatly from the other salt mixtures. After a few seconds, a sudden increase in temperature was observed. This was followed by a maximum much higher than the reactor temperature, indicating that an exothermic reaction occurred. Simulations performed in HSC Chemistry software[59]

(Eqs. 4-2 and 4-3) showed that nitrates are reduced by carbon to nitrites. Since carbon is one of the products formed during pyrolysis, this is a plausible explanation to the strange observation. The same behavior was observed for the other reactor temperatures, and the results for nitrates were excluded from further analyses.

$$2KNO_3(l) + C \leftrightarrow CO_2(g) + 2KNO_2(l), \quad \Delta G_{500\,°C} = -311.86\ kJ/mol \qquad (4\text{-}2)$$

$$2NaNO_3(l) + C \leftrightarrow CO_2(g) + 2NaNO_2(l), \quad \Delta G_{500\,°C} = -562.09\ kJ/mol \qquad (4\text{-}3)$$

It was very clear that the composition of the molten salt affected the thermal behavior of the wood particles (Figure 4-13), but the reaction temperatures were not affected to a great extent (Figure 4-14). For T_1 there was a relatively high scatter in the observations, but the variation within one salt was greater than the variation between the salts, and it was therefore not possible to say if there were differences between the salt mixtures. The scatter was large for T_1 in **Paper III** as well (Figure 4-8, p.36), and this was ascribed to the high heating rates observed at the first characteristic point (h_1), making it difficult to evaluate the corresponding temperatures accurately. In **Paper III**, the sampling rate was 2 times per second, while it was increased to 5 times per second in **Paper IV**. The scatter was reduced, but it is not clear whether it was an effect of higher sampling frequency.

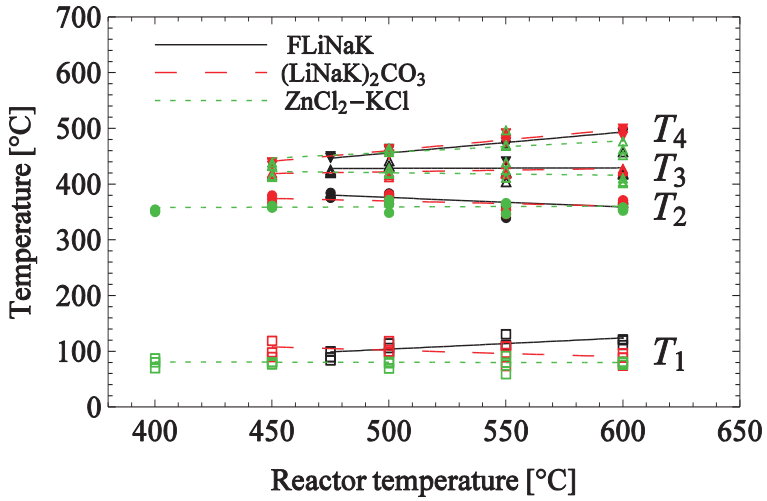

Figure 4-14. Characteristic temperatures at the particle center for beech wood cylinders (L = 30 mm, d = 3.5 mm) as functions of the reactor temperature in FLiNaK (black), $(LiNaK)_2CO_3$ (red), and $ZnCl_2$-KCl (green).

The other characteristic temperatures were slightly, but not significantly, lower for $ZnCl_2$-KCl. The values for all the salt mixtures were comparable to a corresponding study in a fluidized sand bed by Di Blasi and Branca.[86] These findings from **Paper IV** showed that the heat transfer medium is of less importance to the reaction temperatures during pyrolysis.

For T_2 and T_3 there was only a weak dependence on reactor temperature. As also stated in **Paper III**, these temperatures are associated with the degradation of cellulose and

hemicellulose, reactions that are known to occur at a narrow temperature range,[87] and these results were as expected. Values for the effective pyrolysis temperature (T_3) were in the range of 404 to 438 °C. T_3 was much more affected by the particle size (**Paper III**), indicating that the properties of the wood dominate the process to a larger extent than the heating media and reactor temperature. The reactor temperature had a stronger effect on T_4 because this is related to the degradation of lignin, reactions that may happen over a wider temperature range.[85]

All the characteristic heating rates (h_1–h_4) showed an increasing trend with increasing reactor temperature (Figures 4-15 – 4-18).

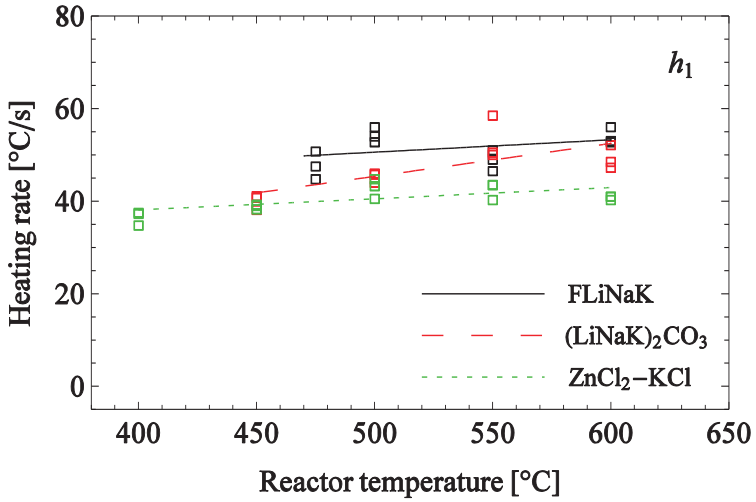

Figure 4-15. Maximum heating rate h_1 at the particle center of beech wood cylinders (L = 30 mm, d = 3.5 mm) as functions of the reactor temperature in FLiNaK (black), (LiNaK)2CO3 (red), and ZnCl2-KCl (green).

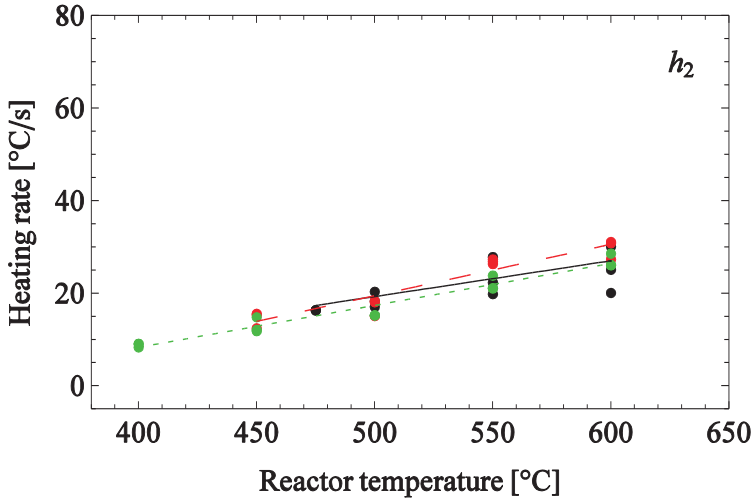

Figure 4-16. Point of high variation of the heating rate h_2 at the particle center of beech wood cylinders (L = 30 mm, d = 3.5 mm) as functions of the reactor temperature in FLiNaK (black), (LiNaK)2CO3 (red), and ZnCl2-KCl (green).

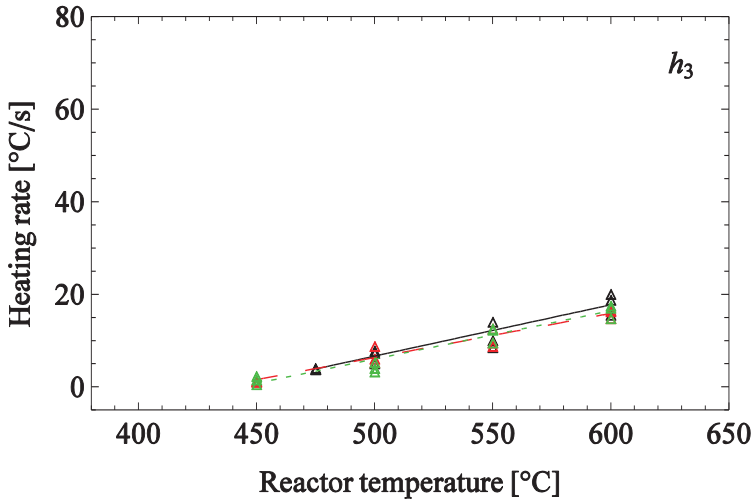

Figure 4-17. Local minimum of heating rate h_3 at the particle center of beech wood cylinders (L = 30 mm, d = 3.5 mm) as functions of the reactor temperature in FLiNaK (black), (LiNaK)2CO3 (red), and ZnCl2-KCl (green).

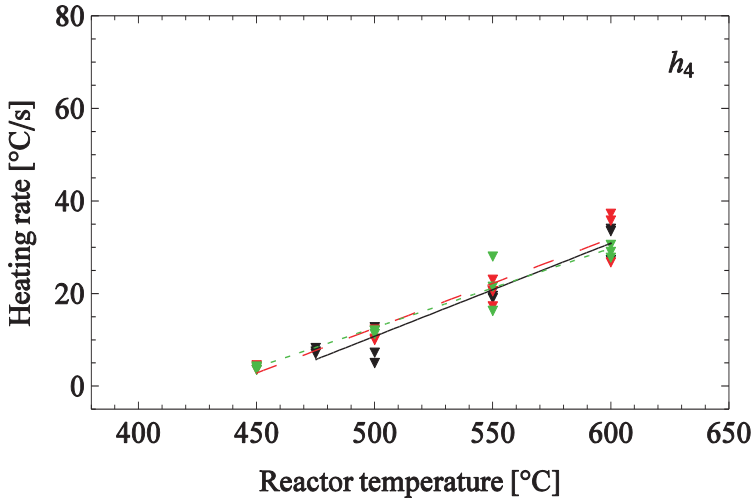

Figure 4-18. Local maximum of heating rate h_4 at the particle center of beech wood cylinders (L = 30 mm, d = 3.5 mm) as functions of the reactor temperature in FLiNaK (black), (LiNaK)2CO3 (red), and ZnCl2-KCl (green).

As pointed out both in **Paper III** and **IV**, the maximum heating rate (h_1) is of special interest because it is measured before any reactions occur, and this is where variations between heat transfer media are shown. Although there was some scatter in the observations, it was clear that the highest heating rates were obtained in FLiNaK (46 – 56 °C/s), followed by $(LiNaK)_2CO_3$ (38 – 52 °C/s) and then $ZnCl_2$-KCl (35 – 43 °C/s). The other characteristic heating rates showed a strong dependence on reactor temperature, but the differences between the salts were negligible.

4.2.4 Prediction of devolatilization times

Prediction of the total devolatilization time in pyrolysis is important for reactor design. A typical empirical correlation for the effect of particle size is the power-law relation given by Eq. 4-4:[89]

$$t_{dev} = Ad^n \tag{4-4}$$

where A and n are fitted to match the experimental data. According to Kanury,[90] n should be either 1 or 2, depending on external or internal heat and mass transfer control, respectively. If the value is between 1 and 2, the particles that the experiments are based on cover both regimes. The correlation was originally proposed for coal,[89] but has later been shown to be applicable for wood particles as well.[86,91,92]

Several definitions for total devolatilization time are used in literature; measurements of gas evolution,[91] rate of weight loss,[93] or temperature history.[84] In **Paper III**, the total devolatilization time was defined as the time when the particle center attained the maximum temperature (t_5). This is the time when the reactions are practically terminated.[86] In **Paper IV**, it was not possible to distinguish the maximum temperature T_5 from small temperature oscillations associated with structural changes or measurement errors in all the experiments (possibly due to higher sampling frequency), and t_4 was used instead. This corresponds to the second local maximum in the heating rate at the particle center, and the conversion is about 95%.[84]

For pyrolysis of beech and pine wood cylinders in FLiNaK at 500 °C (**Paper III**), it was found that the total devolatilization time followed the empirical correlation:

$$t_{dev} = \rho\left(0.146e^{-k_{eff}} - 1.09\right)d^{1.05} \tag{4-5}$$

with the values for ρ and k_{eff} (⊥) as given in Table 3-1 (p. 22). There was a good agreement between the experimental data and the empirical correlations (Figure 4-19). According to Eq. 4-5, the devolatilization time should increase with increasing density, but this effect vanished on the expense of the exponential decrease with higher conductivity, and beech wood was found to decompose faster than pine wood for all the examined particle sizes. The correlations were in accordance with previous model predictions performed by Di Blasi,[94] stating that density and thermal conductivity are the most important physical properties affecting the conversion time in biomass pyrolysis.

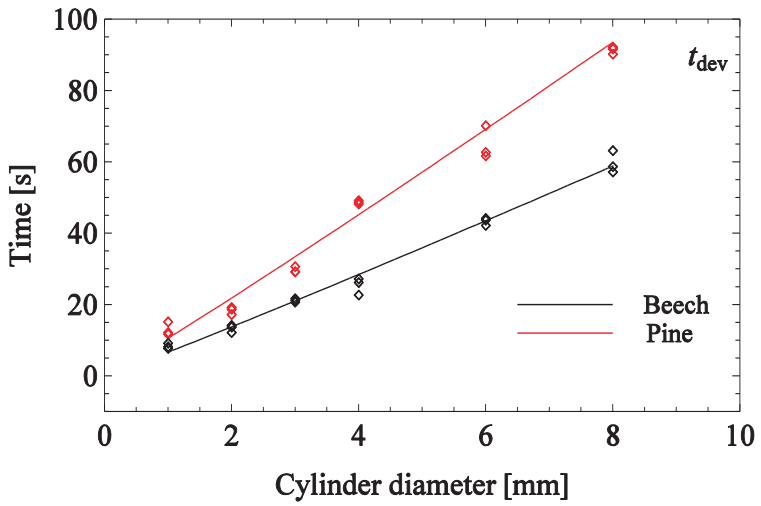

Figure 4-19. Total devolatilization times (expressed as $t_5 = t_{dev}$) for beech (black) and pine (red) cylinders as functions of the cylinder diameter in FLiNaK at 500 °C. Symbols are for the experiments and solid lines for the empirical correlation given by Eq. 4-5.

In **Paper IV**, the focus was the temperature dependence of the parameter A. Since only one wood type was used, the dependence on the physical properties was disregarded. However, the value n = 1.05 was retained, since the particle size (d = 3.5) was within the particle range used in **Paper III** (d = 1 – 8 mm). The devolatilization times in FLiNaK and $(LiNaK)_2CO_3$ were comparable within the accuracy of the data for all reactor temperatures, while the decomposition took longer time in $ZnCl_2$-KCl for the lowest temperatures (Figure 4-20). The differences diminished with increasing reactor temperature, and for T = 600 °C the devolatilization times were practically the same in all the melts.

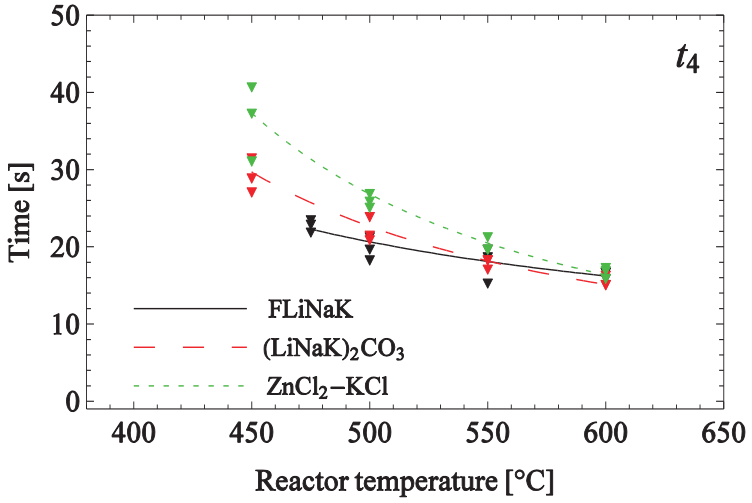

Figure 4-20. Effect of reactor temperature on the devolatilization times (expressed as t_4 [~ 95% conversion] for beech wood particles (L = 30 mm, d = 3.5 mm) in FLiNaK (black), $(LiNaK)_2CO_3$ (red), and $ZnCl_2$-KCl (green).

An Arrhenius plot was constructed (Figure 4-21) to show that A depended exponentially on reactor temperature with the relations given in Table 4-3. This was in close agreement with the results reported by other researchers for both coal[89] and wood.[86, 92] The corresponding activation energies (Table 4-3) were in the same range as found by other researchers,[86, 89] and their low values indicated that the process was controlled by heat transfer rather than chemical kinetics.[95]

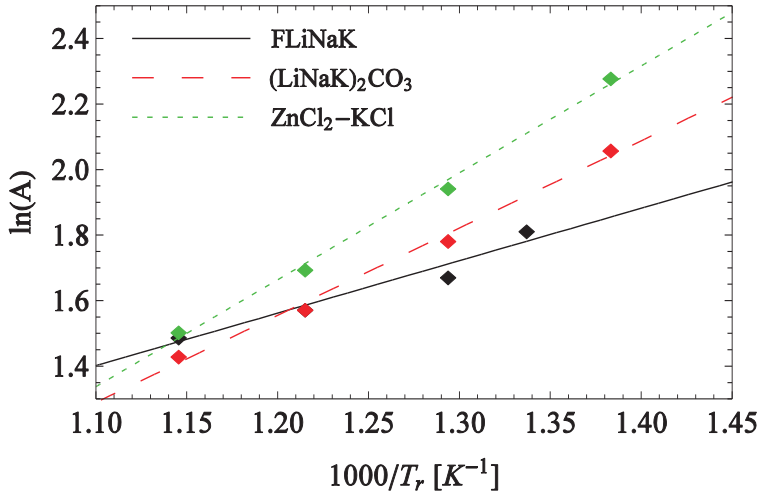

Figure 4-21. Effect of reactor temperature on the correlation parameter A (Eq. 4-5) for the devolatilization times for beech wood particles (L = 30 mm, d = 3.5 mm) in FLiNaK (black), $(LiNaK)_2CO_3$ (red), and $ZnCl_2$-KCl (green).

Table 4-3. Correlation parameter A, R^2 values, and activation energies for beech wood cylinders (L = 30 mm, d = 3.5 mm) in molten salt pyrolysis.

Molten salt	A	R^2	Corresponding activation energy
FLiNaK	$0.698e^{1600/T}$	95.98	13.3 kJ/mol
$(LiNaK)_2CO_3$	$0.194e^{2662/T}$	99.28	22.1 kJ/mol
$ZnCl_2$-KCl	$0.105e^{3264/T}$	99.51	27.4 kJ/mol

4.3 Construction of an electrostatic precipitator (ESP)

As described in Chapter 2.3.3, a large volume of inert gas is needed in most types of pyrolysis reactors.[8] In molten salt pyrolysis, inert gas is used for turbulent mixing of the biomass and the melt, and for transportation of the produced vapors out of the reactor. The vapors are mostly in the form of aerosols, and contribute to less than 5 vol % of the total gas stream. This makes separation a difficult task.[37, 96] In early pyrolysis configurations, quenching and solvent methods were widely used.[5] Later research has found electrostatic precipitation (ESP) to be more effective,[97] and this is currently the preferred method.[5]

One of the objectives in **Paper V** was the design and testing of a tubular ESP for oil collection in molten salt pyrolysis. Earlier attempts showed that external cooling both with tap water (~ 20 °C) and ice (~ 0 °C) was not sufficient, as it could be observed that uncondensed vapors were flowing out of the condensers. Solvent methods were not considered because the subsequent separation would complicate and add cost to the process,[97] as well as give less accurate mass balances in laboratory scale experiments.

In an ESP, the vapors are charged by a corona discharge and separated from the remaining gas stream by an electric field. The charged droplets are attracted to a grounded wall where they are neutralized and collected.[98] No additional solvent has to be introduced to the system. The design of the ESP used in **Paper V** was adopted from Bedmutha et al.[98] (Figure 1, **Paper V**).

A challenge when using an ESP is spark-overs, a phenomenon occurring when electrons find a conducting path and reach the grounded wall without being captured by molecules or particles. Spark-overs can happen when the voltage is too high or the inert gas breaks down.[99] A lot of experimental effort was put in finding the settings that would give a stable operation during pyrolysis without experiencing any spark-overs. The ESP was operated by setting the central electrode at a positive potential ranging from 0 to 20 kV, and the V-I characteristics were determined by increasing the voltage slowly until spark-over occurred. This was repeated several times to assure reproducibility. The values of the output voltage and current were read directly from the power supply, with the results shown graphically in Figure 4-22. Initial tests were performed with pure inert gases (Ar and N_2) and during pyrolysis experiments with milled beech wood particles (0.5 – 2 mm) in a FLiNaK melt at 500 °C.

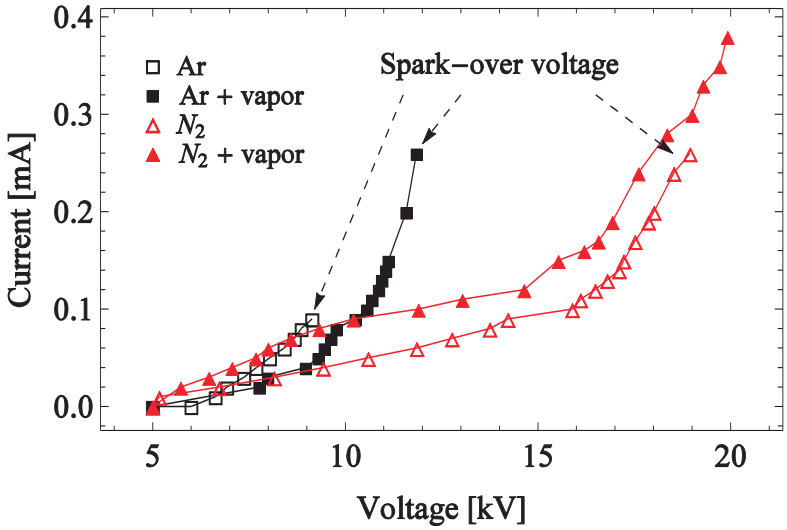

Figure 4-22. Current vs voltage characteristics for the electrostatic precipitator (ESP).

The ESP showed most stable operation when N_2 was used as inert gas. The increase in current with applied voltage was slower, indicating poor conductivity of the gas. In

addition, spark-over occurred at a higher voltage. The different behavior was ascribed to lower break down voltages for Ar[100] and differences of impurities of the inert gases (Table 3-3, p.24), the latter an effect also reported by Bedmutha et al.[98] When pyrolysis vapors were included in the gas stream, the point for spark-over was raised. This was most likely because the vapors absorbed the electrons formed at the cathode, and thus reduced the possibility for the electrons to reach the grounded wall and cause sparking.

By observing the outlet gas from the ESP through a bubble flask (Figure 3-6, p. 27), it was revealed that a minimum of 12 kV was required for separation of condensable pyrolysis vapors from the remaining gas stream. Since it was not possible to achieve stable operation with Ar at such high voltages, N_2 was chosen as inert gas for the rest of the experimental work in **Paper V**.

4.4 Molten salt pyrolysis of milled beech wood

There is limited work within molten salt pyrolysis where the yields of pyrolysis oil have been reported. The only study with published results was performed by Jiang et al.[62] Pyrolysis experiments were carried out in molten chlorides with cold trap condensers for collection of pyrolysis oil. The highest oil yield from cellulose was 35.0 wt % in a $ZnCl_2$ melt at 450 °C, while the use of other chloride mixtures ($ZnCl_2$-KCl, KCl-CuCl, $ZnCl_2$-KCl-CuCl, ZnCl-KCl-$FeCl_2$) only gave yields up to 15.0 wt %.

In **Papers III** and **IV**, the melts FLiNaK and $(LiNaK)_2CO_3$ showed most promise as heat transfer media in pyrolysis. These salts were therefore selected for the pyrolysis experiments in **Paper V**, where the aim was to produce and collect pyrolysis oil. It was chosen to use milled beech wood particles (0.5 – 2 mm) in order to ensure rapid heat transfer throughout the samples.

The feeding of the milled wood was a challenge. Several feeding methods were tested, but problems with clogging of the feeding tube occurred repeatedly. It was attempted to add the particles directly below the melt surface, but the feeding tube was clogged after a few batches, even when inert gas was introduced along with the samples. In the end, a ball valve based feeding system with a push rod was chosen (described in Chapter 3.4.2). It was important to add the particles in small batches and wait for complete mixing with the melt before adding a new batch. Due to the difficulties with the feeding, it was decided to perform three identical experiments with beech wood in FLiNaK at 500 °C to assure reproducibility of the experimental method. The rest of the experiments were performed once. Data for a typical experiment is shown in Table 4-4. Figure 4-23 shows an example of the pyrolysis oil collected from the ESP.

Table 4-4. Data for a typical experiment with milled beech wood (Paper V).

Information	
Experiment number	7
Date	5/19/2014
Wood particle size (mm)	0.5 – 2
Salt	$(LiNaK)_2CO_3$
Reactor temperature	550 °C
Results	
Wood input (g)	23.1
Char yield (g)	5.0
Char yield (wt %)	21.6
Total pyrolysis oil yield (g)	5.2
ESP (g)	5.0
Cotton filter (g)	0.2
Total pyrolysis oil yield (wt %)	22.5
Water content of pyrolysis oil (wt %)	59.0

Figure 4-23. Pyrolysis oil collected from the ESP during pyrolysis of milled beech wood in molten salts.

Figure 4-24 and 4-25 show the influence of reactor temperature and salt composition on the yields of pyrolysis oil and char. The water content of the pyrolysis oil is depicted in Figure 4-26. Only the oil collected from the ESP (92 – 97 wt % of total oil yield) was analyzed with respect to water content.

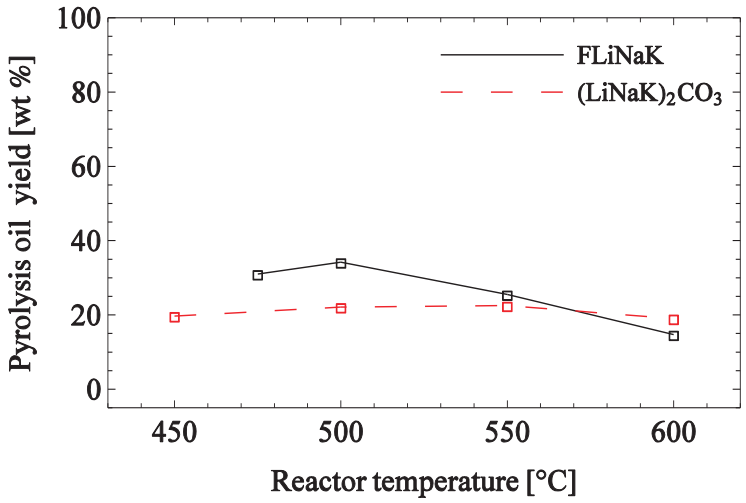

Figure 4-24. Pyrolysis oil yield (collected in ESP and cotton filter) as a function of the reactor temperature in FLiNaK (black) and $(LiNaK)_2CO_3$ (red).

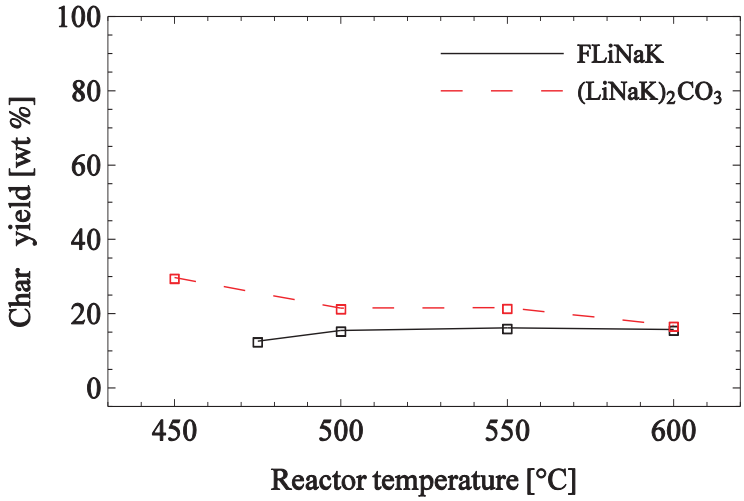

Figure 4-25. Char yield as a function of the reactor temperature in FLiNaK (black) and $(LiNaK)_2CO_3$ (red).

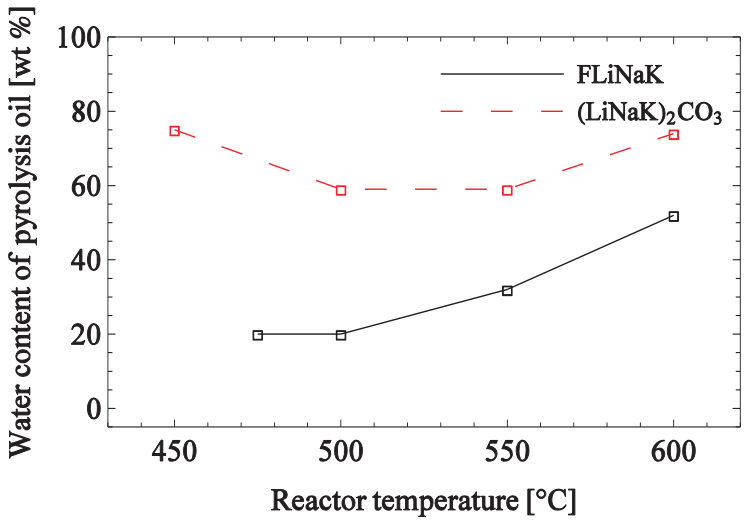

Figure 4-26. Water content of pyrolysis oil collected from the ESP as a function of the reactor temperature in FLiNaK (black) and $(LiNaK)_2CO_3$ (red).

The highest pyrolysis oil yield was achieved in FLiNaK, with a maximum of 34.2 wt % at 500 °C, followed by a decrease with increasing reactor temperature. The pyrolysis oil yield in $(LiNaK)_2CO_3$ was nearly constant with temperature (19.0 – 22.5 wt %). Only minor temperature dependence on the char yield was observed in both salt mixtures for reactor temperatures above 500 °C. The water content varied greatly between pyrolysis in FLiNaK and $(LiNaK)_2CO_3$, but the same trend with lower water content for higher oil yields were observed.

The oil yields were lower and the char yields higher compared with other fast pyrolysis technologies. For example, the yields for milled beech wood of equal particle size in a

fluidized sand bed at 500 °C (**Paper II**) were ~ 60 wt % pyrolysis oil and ~ 12 wt % char. In addition, very high water contents of the pyrolysis oil were observed in molten salt pyrolysis. This was somewhat unexpected, given the good heat transfer characteristics of the employed salts revealed in **Papers III** and **IV**. These findings from **Paper V** demonstrated that rapid heating of wood was not sufficient for maximizing the yields of pyrolysis oil, even if the reaction temperatures were comparable with other fast pyrolysis technologies (**Papers III** and **IV**). The results were explained by secondary reactions occurring. Early research has stated that longer vapor residence times were a major factor for secondary reactions, while later research has shown that the product yields are not as dependent on the residence time as originally assumed.[81, 101] However, minerals containing the alkali elements Na and K are known to promote the formation of gaseous species and char on the expense of pyrolysis oil.[102] Hence, the poor pyrolysis oil yields are most likely caused by a combination of mass transfer resistance in the melt leading to longed vapor residence times at elevated temperatures and at the same time giving prolonged contact with alkali elements found in the melts catalyzing further cracking. The oil yields were, however, generally higher than those previously reported for molten chloride pyrolysis of cellulose with cold trap condensers.[62]

4.5 Challenges with molten salts in thermal processing of biomass

Hydration of metal halides can result in formation of HX, where X represents a halide ion.[103] In wood pyrolysis, water is one of the major products.[47] Given the hygroscopic nature of FLiNaK, formation of HF gases according to Eqs. 4-6 – 4-11 is a concern. The HF gas could contaminate the pyrolysis products and also lead to extensive corrosion of metal elements found in process equipment.[103]

$$2LiF(l) + H_2O(g) \leftrightarrow Li_2O(l) + 2HF(g) \quad (4\text{-}6)$$
$$2NaF(l) + H_2O(g) \leftrightarrow Na_2O(l) + 2HF(g) \quad (4\text{-}7)$$
$$2KF(l) + H_2O(g) \leftrightarrow K_2O(l) + 2HF(g) \quad (4\text{-}8)$$
$$LiF(l) + H_2O(g) \leftrightarrow LiOH(l) + HF(g) \quad (4\text{-}9)$$
$$NaF(l) + H_2O(g) \leftrightarrow NaOH(l) + HF(g) \quad (4\text{-}10)$$
$$KF(l) + H_2O(g) \leftrightarrow KOH(l) + HF(g) \quad (4\text{-}11)$$

The possible hydration reactions were simulated in HSC Chemistry software,[59] with the results shown graphically in Figure 4-27. According to the simulations, hydration will not occur in the experimental temperatures ranges used in **Papers III** – **V**. It should be noted that the Gibbs free energies are well above zero for temperatures relevant for gasification processes as well.

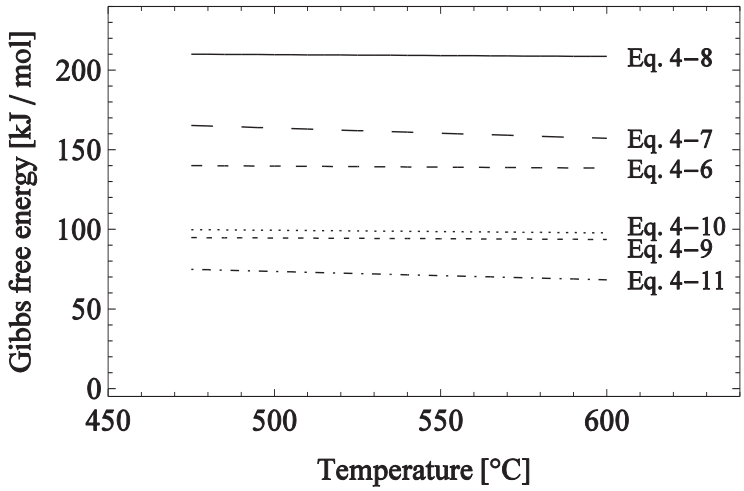

Figure 4-27. Gibbs free energy as a function of temperature for the possible hydration reactions in FLiNaK.

The concentration of HF in the outlet gas was also examined during pyrolysis of milled beech wood in FLiNaK at 600 °C by means of a FTIR gas analyzer (**Paper V**), but no significant amounts were detected.

Using molten salts in thermal processing of biomass and waste has several technical challenges compared with more traditional methods. The choice of reactor materials is limited due to the corrosive nature of most molten salts. The challenge is greatest with halides, while oxygenated melts such as nitrates and carbonates actually passivate metals at moderate temperatures.[66] The corrosion problem could be solved by using ceramic-lined vessels and pipes instead of metals.

Because the melts solidify at ambient temperatures, a form of storage and dump tank is needed for the startup and shutdown of continuous systems. Once melted, the salts may be easily circulated and pumped centrifugally or with gear pumps, or by simple gas-lift pumps.[56]

Another possible obstacle is the separation of char and salt. It has been proposed to drain out the char residue due to density differences[64] or burn out the char from the salt mixture.[66] The latter would produce sufficient energy to make the process auto thermal. Because of the very low vapor pressure and high boiling point, the salts will not decompose in the process. Another possibility is to gasify the remaining char in a separate reactor, and produce valuable syngas at the same time. The remaining ash in the salt may be removed electrolytically or as slag at higher temperatures, and the salt could be reused.[56]

5 Conclusion

The aim of this PhD work was divided in two main parts; the study of the thermal behavior of single wood particles of various sizes in fast pyrolysis and the investigation of molten salts as heat transfer media in the process. The literature research (**Paper I**) revealed that molten salts had previously been found to have good heat transfer characteristics, an important factor for achieving the rapid heating associated with fast pyrolysis. Molten salts also have very high thermal stability, a catalytic effect in cracking and liquefaction of large hydrocarbons, and selected noxious compounds could be retained in the melt after processing contaminated biomass. The focus in most of the reviewed work was gasification at higher temperatures or production of specific phenolic compounds from lignin, and it was clearly a need for more basic research on molten salt pyrolysis.

The experimental work started with investigations of the effect of particle micro- and macrostructure and vapor outflow pattern in fast pyrolysis (**Paper II**). It was found that artificial solid wall cylinders (L = 50 mm, d = 6 – 14 mm) filled with milled beech wood (< 0.08 mm) and natural beech wood cylinders of equal macrosize gave comparable char yields in a fluidized sand bed reactor at 500 °C, meaning that no significant effect of microstructure was observed. At the same time, they both showed increasing char yields for larger cylinder diameters. In other words, the char yield was predominantly determined by the macrostructure. The outflow pattern showed a slightly more noticeable effect. Lower char yields were obtained for artificial wire-mesh cylinders (isotropic outflow) compared to solid wall cylinders (anisotropic outflow) filled with milled beech wood particles (0.08 – 0.2 mm). Although the observed effects were not very strong, it was claimed that the lower char yields were a result of less polycondensations of the vapors on char due to the fact that the vapors having an isotropic outflow have less contact with char.

The study of thermal behavior of single wood particles was continued in molten salt media (**Papers III** and **IV**), and the discoveries provided basic knowledge on the heat transfer from molten salts to wood particles during pyrolysis. Beech wood cylinders (L = 30 mm, d = 1 – 8 mm) showed higher heating rates at the particle center and faster devolatilization times than pine wood cylinders of equal size in FLiNaK pyrolysis at 500 °C. This was ascribed to the higher thermal conductivity of the former. Yet, the all the reaction temperatures were still comparable for the two wood types (**Paper III**).

One of the most important outcomes from the experimental work in this thesis was that the maximum heating rates were significantly higher in FLiNaK than in a fluidized sand bed for cylindrical beech wood particles with $d \leq 4$ mm (**Paper III**). For smaller particles, the type of heat transfer medium was dominating, while the wood properties limited the process for larger particles. Comparison of several salt mixtures concluded that FLiNaK and $(LiNaK)_2CO_3$ showed better promise as heat transfer media than $ZnCl_2$-KCl.

KNO_3-$NaNO_3$ was on the other hand not suitable for pyrolysis based on the observation of exothermic reactions between the salt and the formed carbon (**Paper IV**).

The experimental results also showed that the effective pyrolysis temperature (T_3), in which most of the cellulose and hemicellulose decompose, decreased rapidly with increasing particle size (**Paper III**). However, T_3 was almost unaffected by reactor temperature (400 – 600 °C) and heating media (**Paper IV**).

The total devolatilization times for cylindrical wood particles were found to follow the empirical correlation $t_{dev} = Ad^n$ (**Papers III** and **IV**). In **Paper III**, beech and pine wood cylinders were compared, and the parameter A was found to depend on the physical properties (density and thermal conductivity) of the wood. Based on the value of the exponent of the diameter (n = 1.05), it was claimed that the studied particle range covered both internal and external heat and mass transfer control. The parameter A also showed an exponential dependence upon reactor temperature (**Paper IV**) for beech wood (d = 3.5 mm). The corresponding activation energies were rather low (13.3 – 27.4 kJ/mol), indicating that pyrolysis of beech wood was controlled by heat transfer rather than chemical kinetics.

Paper V dealt with the whole pyrolysis process with focus on collection of the produced pyrolysis oil. A tubular electrostatic precipitator (ESP) was designed and tested, and it was established that N_2 as inert gas gave the most stable operation. A minimum of 12 kV was required for separation of the condensable pyrolysis vapors from the remaining gas stream. Pyrolysis experiments were conducted with milled beech wood (0.5 – 2 mm) in FLiNaK and $(LiNaK)_2CO_3$ at reactor temperatures between 450 and 600 °C. In spite of the good heat transfer performance of the employed salts (**Papers III** and **IV**), the oil yields were not comparable to other fast pyrolysis technologies, with a maximum of 34.2 wt % in FLiNaK at 500 °C (**Paper V**). The char yields and water contents of the oils were also higher than anticipated, and it was concluded that high heating rates were not sufficient for maximizing the oil yields, even if the reaction temperatures were proven to be comparable to other fast pyrolysis technologies (**Papers III** and **IV**). It is likely that mass transfer resistance in the melts have led to longer vapor residence times and more contact with alkali elements (Na/K) found in the melts, causing secondary reactions. However, the oil yields were for most parts higher than those reported for molten chloride pyrolysis of cellulose where cold trap condensers were utilized for oil collection.

A possible concern when using FLiNaK as a reaction medium in thermochemical conversion of biomass is the reaction between the salt and produced water to form HF gas. According to both simulations and FTIR measurements of the outlet gas (**Paper V**), no significant amounts of HF are produced during beech wood pyrolysis in FLiNaK.

6 Future perspectives

The focus in this work has mainly been on the heat transfer characteristics of molten salts during fast pyrolysis. Several salts showed good promise as heat transfer media, but the yields of pyrolysis oil were not as good as expected. It was suggested that prolonged vapor residence time and / or contact with alkali elements (Na / K) found in the melts were the cause of this. There are several ways in which this could be explored further:

- The flow rate of inert gas stream affects the vapor residence time. The effect of the flow rate of the inert gas on the yields of pyrolysis oil should be investigated in more detail.

- The residence time is also affected by the void space above the melt. The salts densify drastically after melting. In this study, the crucibles were filled completely with salt powders, yet the salt height was less than half the crucible height after melting. More salt could be added through several premelting steps, giving less empty space in the reactor and a shorter vapor residence time.

- The alkali elements Na and K are known to catalyze gasification on the expense of oil production if the produced vapors are kept in contact with them for longer times at elevated temperatures. It would be an idea to investigate other salt types that do not involve these elements.

In this study, complete mass balances were not conducted due to lack of equipment for gas analyses. It was assumed that all the condensable gases were captured in the ESP and the cotton filter (based on visual observations), but there could also be losses that were not detected. By including a gas meter to measure the total gas flow and a micro-GC for quantifying the non-condensable gases, the produced gas fraction could be calculated, and potential losses in the system would be revealed. In addition, quantification of the non-condensable gases could imply if secondary reactions are occurring, since it is known that CO_2 originates mainly from primary pyrolysis, while CO and CH_4 are mainly secondary pyrolysis products.

The feeding system of milled wood could be improved. Continuously feeding of biomass by e.g. a mechanical screw would give both smoother feeding and pyrolysis reactions. In this way, even smaller particles could be added without experiencing clogging of the feeding tube, possibly leading to increased oil yields. The feeding tube could also be cooled to avoid decomposition of the feedstock before reaching the melt. Better mixing of biomass particles and melt could be achieved with mechanical stirring in addition to inert gas bubbling. However, these improvements require a redesign of the whole reactor setup.

In this work, the obtained pyrolysis oil was only analyzed with respect to water content. An important next step is to characterize the oils further in order to explore the possible applications of the oil obtained from molten salt pyrolysis.

Another approach that would be interesting to pursue is gasification of biomass in FLiNaK and $(LiNaK)_2CO_3$. Pyrolysis is always the first step in gasification, and rapid heat transfer and reaction rates are important for gasification processes as well. Gasification has been the focus in previous research within thermal processing of biomass in molten salts, and perhaps this is a more promising way to utilize the good transfer characteristics of the salts. $(LiNaK)_2CO_3$ has been studied previously, but there are no published data on the use of FLiNaK in biomass gasification.

7 References

1. *Key World Energy Statistics © OECD/IEA*; 2013.

2. Basu, P., *Biomass Gasification and Pyrolysis: Practical Design and Theory*. Elsevier Science: 2010.

3. Kullander, S., Energy from biomass. *Eur. Phys. J. Spec. Top.* **2009,** *176* (1), 115-125.

4. Goldemberg, J.; Teixeira Coelho, S., Renewable energy—traditional biomass vs. modern biomass. *Energy Policy* **2004,** *32* (6), 711-714.

5. Bridgwater, A. V., Review of fast pyrolysis of biomass and product upgrading. *Biomass and Bioenergy* **2012,** *38* (0), 68-94.

6. McKendry, P., Energy production from biomass (part 1): overview of biomass. *Bioresource Technology* **2002,** *83* (1), 37-46.

7. Grønli, M. G. A Theoretical and Experimental Study of the Thermal Degradation of Biomass. Norwegian University of Science and Technology, 1996.

8. Venderbosch, R. H.; Prins, W., Fast pyrolysis technology development. *Biofuels, Bioproducts and Biorefining* **2010,** *4* (2), 178-208.

9. Mohan, D.; Pittman, C. U.; Steele, P. H., Pyrolysis of wood/biomass for bio-oil: a critical review. *Energy & Fuels* **2006,** *20* (3), 848-889.

10. Demirbas, A., Potential applications of renewable energy sources, biomass combustion problems in boiler power systems and combustion related environmental issues. *Progress in Energy and Combustion Science* **2005,** *31* (2), 171-192.

11. Demirbaş, A., Biomass resource facilities and biomass conversion processing for fuels and chemicals. *Energy Conversion and Management* **2001,** *42* (11), 1357-1378.

12. Goldemberg, J.; Programme, U. N. D.; Economic, U. N. D. o.; Affairs, S.; Council, W. E., *World energy assessment: energy and the challenge of sustainability*. United Nations Development Programme: 2000.

13. Hoogwijk, M.; Faaij, A.; van den Broek, R.; Berndes, G.; Gielen, D.; Turkenburg, W., Exploration of the ranges of the global potential of biomass for energy. *Biomass and Bioenergy* **2003,** *25* (2), 119-133.

14. Field, C. B.; Campbell, J. E.; Lobell, D. B., Biomass energy: the scale of the potential resource. *Trends in Ecology & Evolution* **2008,** *23* (2), 65-72.

15. Trømborg, E.; Bolkesjø, T. F.; Solberg, B., Biomass market and trade in Norway: Status and future prospects. *Biomass and Bioenergy* **2008,** *32* (8), 660-671.

16. Langerud, B.; Størdal, S.; Wiig, H.; Ørbeck, M. *Bioenergi i Norge – potensialer, markeder og virkemidler*; 2007.

17. Berndes, G.; Hoogwijk, M.; van den Broek, R., The contribution of biomass in the future global energy supply: a review of 17 studies. *Biomass and Bioenergy* **2003,** *25* (1), 1-28.

18. Chum, H. L.; Overend, R. P., Biomass and renewable fuels. *Fuel Processing Technology* **2001,** *71* (1–3), 187-195.

19. Bridgwater, A. V., Renewable fuels and chemicals by thermal processing of biomass. *Chemical Engineering Journal* **2003,** *91* (2–3), 87-102.

20. Klass, D. L., *Biomass for Renewable Energy, Fuels, and Chemicals*. Elsevier Science: 1998.

21. Naik, S.; Goud, V. V.; Rout, P. K.; Dalai, A. K., Production of first and second generation biofuels: a comprehensive review. *Renewable and Sustainable Energy Reviews* **2010,** *14* (2), 578-597.

22. Bridgwater, A., Production of high grade fuels and chemicals from catalytic pyrolysis of biomass. *Catalysis today* **1996,** *29* (1), 285-295.

23. Koh, L. P.; Ghazoul, J., Biofuels, biodiversity, and people: understanding the conflicts and finding opportunities. *Biological conservation* **2008,** *141* (10), 2450-2460.

24. Nigam, P. S.; Singh, A., Production of liquid biofuels from renewable resources. *Progress in Energy and Combustion Science* **2011,** *37* (1), 52-68.

25. Balat, M.; Balat, H.; Öz, C., Progress in bioethanol processing. *Progress in Energy and Combustion Science* **2008,** *34* (5), 551-573.

26. Hall, D., Biomass energy in industrialised countries—a view of the future. *Forest ecology and management* **1997,** *91* (1), 17-45.

27. Wenzl, H. F. J., *The chemical technology of wood*. Academic Press: 1970.

28. Sjöström, E., *Wood chemistry: fundamentals and applications*. Academic Press: 1993.

29. Bodig, J.; Jayne, B. A., *Mechanics of wood and wood composites*. Van Nostrand Reinhold: 1982.

30. de Wild, P.; Reith, H.; Heeres, E., Biomass pyrolysis for chemicals. *Biofuels* **2011,** *2* (2), 185-208.

31. Siau, J. F., *Transport processes in wood*. Springer-Verlag: 1984.

32. Boroson, M. L., *Secondary Reactions of Tars from Pyrolysis of Sweet Gum Hardwood*. Massachusetts Institute of Technology, Department of Chemical Engineering: 1987.

33. Yang, H.; Yan, R.; Chen, H.; Lee, D. H.; Zheng, C., Characteristics of hemicellulose, cellulose and lignin pyrolysis. *Fuel* **2007,** *86* (12), 1781-1788.

34. Bridgwater, A. V.; Meier, D.; Radlein, D., An overview of fast pyrolysis of biomass. *Organic Geochemistry* **1999,** *30* (12), 1479-1493.

35. Bridgwater, A. V., Principles and practice of biomass fast pyrolysis processes for liquids. *Journal of Analytical and Applied Pyrolysis* **1999,** *51* (1–2), 3-22.

36. Peacocke, G. V. C.; Bridgwater, A. V., Ablative plate pyrolysis of biomass for liquids. *Biomass and Bioenergy* **1994,** *7* (1–6), 147-154.

37. Bridgwater, A. V.; Peacocke, G. V. C., Fast pyrolysis processes for biomass. *Renewable and Sustainable Energy Reviews* **2000,** *4* (1), 1-73.

38. Lappas, A. A.; Samolada, M. C.; Iatridis, D. K.; Voutetakis, S. S.; Vasalos, I. A., Biomass pyrolysis in a circulating fluid bed reactor for the production of fuels and chemicals. *Fuel* **2002,** *81* (16), 2087-2095.

39. Wagenaar, B. M.; Prins, W.; van Swaaij, W. P. M., Pyrolysis of biomass in the rotating cone reactor: modelling and experimental justification. *Chemical Engineering Science* **1994,** *49* (24, Part 2), 5109-5126.

40. Mohan, D.; Pittman, C. U.; Steele, P. H., Pyrolysis of Wood/Biomass for Bio-oil: A Critical Review. *Energy & Fuels* **2006,** *20* (3), 848-889.

41. Thangalazhy-Gopakumar, S.; Adhikari, S.; Ravindran, H.; Gupta, R. B.; Fasina, O.; Tu, M.; Fernando, S. D., Physiochemical properties of bio-oil produced at various temperatures from pine wood using an auger reactor. *Bioresource Technology* **2010,** *101* (21), 8389-8395.

42. Roy, C.; Morin, D.; Dubé, F., The biomass Pyrocycling™ process. In *Biomass Gasification and Pyrolysis: State of the Art and Future Prospects*, Kaltschmidt, M.; Bridgwater, A. V., Eds. CPL Scientific Ltd, Newbury, Berkshire, UK, 1997; pp 307-315.

43. Roy, C.; Blanchette, D.; De Caumia, B.; Labrecque, B., Conceptual design and evaluation of a biomass vacuum pyrolysis plant. In *Advances in Thermochemical Biomass Conversion*, Springer: 1993; pp 1165-1186.

44. Czernik, S.; Bridgwater, A., Overview of applications of biomass fast pyrolysis oil. *Energy & Fuels* **2004,** *18* (2), 590-598.

45. Zhang, Q.; Chang, J.; Wang, T.; Xu, Y., Review of biomass pyrolysis oil properties and upgrading research. *Energy Conversion and Management* **2007,** *48* (1), 87-92.

46. Oasmaa, A.; Kuoppala, E.; Solantausta, Y., Fast pyrolysis of forestry residue. 2. Physicochemical composition of product liquid. *Energy & Fuels* **2003,** *17* (2), 433-443.

47. Westerhof, R. J. M.; Kuipers, N. J. M.; Kersten, S. R. A.; van Swaaij, W. P. M., Controlling the Water Content of Biomass Fast Pyrolysis Oil. *Industrial & Engineering Chemistry Research* **2007,** *46* (26), 9238-9247.

48. Yan, G.; Yao, W.; Fei, W.; Yong, J., Research Progress in Biomass Flash Pyrolysis Technology for Liquids Production. *Chemical Industry and Engineering Progress* **2001,** *20* (8), 13-17.

49. Oasmaa, A.; Czernik, S., Fuel oil quality of biomass pyrolysis oils state of the art for the end users. *Energy & Fuels* **1999,** *13* (4), 914-921.

50. Czernik, S.; Johnson, D. K.; Black, S., Stability of wood fast pyrolysis oil. *Biomass and Bioenergy* **1994,** *7* (1–6), 187-192.

51. Lu, Q.; Li, W.-Z.; Zhu, X.-F., Overview of fuel properties of biomass fast pyrolysis oils. *Energy Conversion and Management* **2009,** *50* (5), 1376-1383.

52. Gupta, K. K.; Rehman, A.; Sarviya, R. M., Bio-fuels for the gas turbine: A review. *Renewable and Sustainable Energy Reviews* **2010,** *14* (9), 2946-2955.

53. Chiaramonti, D.; Oasmaa, A.; Solantausta, Y., Power generation using fast pyrolysis liquids from biomass. *Renewable and sustainable energy reviews* **2007,** *11* (6), 1056-1086.

54. Ikura, M.; Mirmiran, S.; Sawatzky, H.; Stanciulescu, M., Pyrolysis liquid-in-diesel oil microemulsions. Google Patents: 1998.

55. Effendi, A.; Gerhauser, H.; Bridgwater, A. V., Production of renewable phenolic resins by thermochemical conversion of biomass: A review. *Renewable and Sustainable Energy Reviews* **2008,** *12* (8), 2092-2116.

56. Lovering, D. G., *Molten salt technology*. Plenum Press: 1982.

57. Olson, L. C.; Ambrosek, J. W.; Sridharan, K.; Anderson, M. H.; Allen, T. R., Materials corrosion in molten LiF–NaF–KF salt. *Journal of Fluorine Chemistry* **2009,** *130* (1), 67-73.

58. Yasunishi, A.; Tada, Y., WOOD PYROLYSIS IN MOLTEN-SALT. *Kagaku Kogaku Ronbunshu* **1985,** *11* (3), 346-349.

59. Sada, E.; Kumazawa, H.; Kudsy, M., Pyrolysis of lignins in molten salt media. *Industrial & Engineering Chemistry Research* **1992,** *31* (2), 612-616.

60. Scarrah, W. P., Molten Salt Hydrocracking of Lignite. Screening of Viscosity Reducers and Hydrogen Sources. *Industrial & Engineering Chemistry Product Research and Development* **1980,** *19* (3), 442-446.

61. Kudsy, M.; Kumazawa, H., Pyrolysis of kraft lignin in the presence of molten ZnCl2-KCl mixture. *The Canadian Journal of Chemical Engineering* **1999,** *77* (6), 1176-1184.

62. Jiang, H.; Ai, N.; Wang, M.; Ji, D.; Ji, J., Experimental Study on THermal Pyrolysis of Biomass in Molten Salt Media. *Electrochemistry* **2009,** *77* (8), 730-735.

63. Tada, Y.; Yasunishi, A., WOOD PYROLYSIS WITH MOLTEN-SALT AS HEATING MEDIUM. *Kagaku Kogaku Ronbunshu* **1987,** *13* (3), 376-379.

64. Adinberg, R.; Epstein, M.; Karni, J., Solar Gasification of Biomass: A Molten Salt Pyrolysis Study. *Journal of Solar Energy Engineering* **2004,** *126* (3), 850-857.

65. Hathaway, B. J.; Davidson, J. H.; Kittelson, D. B., Solar Gasification of Biomass: Kinetics of Pyrolysis and Steam Gasification in Molten Salt. *Journal of Solar Energy Engineering* **2011,** *133* (2), 021011.

66. Hammond, V. L.; Mudge, L. K. *Feasibility study of use of molten salt technology for pyrolysis of solid waste. Final report*; Battele Pacific Northwest Labs., Tichland, Wash., 1975.

67. Jin, G.; Iwaki, H.; Arai, N.; Kitagawa, K., Study on the gasification of wastepaper/carbon dioxide catalyzed by molten carbonate salts. *Energy* **2005,** *30* (7), 1192-1203.

68. Iwaki, H.; Ye, S.; Katagiri, H.; Kitagawa, K., Wastepaper gasification with CO2 or steam using catalysts of molten carbonates. *Applied Catalysis A: General* **2004,** *270* (1-2), 237-243.

69. Sugiura, K.; Minami, K.; Yamauchi, M.; Morimitsu, S.; Tanimoto, K., Gasification characteristics of organic waste by molten salt. *Journal of Power Sources* **2007,** *171* (1), 228-236.

70. Chambers, C.; Larsen, J. W.; Li, W.; Wiesen, B., Polymer waste reclamation by pyrolysis in molten salts. *Industrial & Engineering Chemistry Process Design and Development* **1984,** *23* (4), 648-654.

71. Menzel, J.; Perkow, H.; Sinn, H., RECYCLING PLASTICS. *Chemistry & Industry* **1973,** (12), 570-573.

72. Bertolini, G. E.; Fontaine, J., Value recovery from plastics waste by pyrolysis in molten salts. *Conservation & Recycling* **1987,** *10* (4), 331-343.

73. Yoshida, S.; Matsunami, J.; Hosokawa, Y.; Yokota, O.; Tamaura, Y.; Kitamura, M., Coal/CO2 gasification system using molten carbonate salt for solar/fossil energy hybridization. *Energy & fuels* **1999,** *13* (5), 961-964.

74. Matsunami, J.; Yoshida, S.; Oku, Y.; Yokota, O.; Tamaura, Y.; Kitamura, M., Coal gasification by CO2 gas bubbling in molten salt for solar/fossil energy hybridization. *Solar Energy* **2000,** *68* (3), 257-261.

75. Matsunami, J.; Yoshida, S.; Oku, Y.; Yokota, O.; Tamaura, Y.; Kitamura, M., Coal gasification with CO2 in molten salt for solar thermal/chemical energy conversion. *Energy* **2000,** *25* (1), 71-79.

76. Kersten, S. R. A.; Wang, X.; Prins, W.; van Swaaij, W. P. M., Biomass Pyrolysis in a Fluidized Bed Reactor. Part 1: Literature Review and Model Simulations. *Industrial & Engineering Chemistry Research* **2005,** *44* (23), 8773-8785.

77. Williams, D., Assessment of candidate molten salt coolants for the NGNP/NHI Heat-Transfer Loop. *ORNL/TM-2006/69, Oak Ridge National Laboratory, Oak Ridge, Tennessee* **2006**.

78. Mao, A.; Park, J. H.; Han, G. Y.; Seo, T.; Kang, Y., Heat transfer characteristics of high temperature molten salt for storage of thermal energy. *Korean Journal of Chemical Engineering* **2010,** *27* (5), 1452-1457.

79. Hoekstra, E.; Hogendoorn, K. J. A.; Wang, X.; Westerhof, R. J. M.; Kersten, S. R. A.; van Swaaij, W. P. M.; Groeneveld, M. J., Fast Pyrolysis of Biomass in a Fluidized Bed Reactor: In Situ Filtering of the Vapors. *Industrial & Engineering Chemistry Research* **2009,** *48* (10), 4744-4756.

80. Lüftl, S.; M, V. P.; Chandran, S., *Polyoxymethylene Handbook: Structure, Properties, Applications and their Nanocomposites*. Wiley: 2014.

81. Wang, X.; Kersten, S. R. A.; Prins, W.; van Swaaij, W. P. M., Biomass Pyrolysis in a Fluidized Bed Reactor. Part 2: Experimental Validation of Model Results. *Industrial & Engineering Chemistry Research* **2005,** *44* (23), 8786-8795.

82. Salehi, E.; Abedi, J.; Harding, T., Bio-oil from Sawdust: Effect of Operating Parameters on the Yield and Quality of Pyrolysis Products. *Energy & Fuels* **2011,** *25* (9), 4145-4154.

83. Shen, J.; Wang, X.-S.; Garcia-Perez, M.; Mourant, D.; Rhodes, M. J.; Li, C.-Z., Effects of particle size on the fast pyrolysis of oil mallee woody biomass. *Fuel* **2009,** *88* (10), 1810-1817.

84. Di Blasi, C.; Branca, C.; Santoro, A.; Gonzalez Hernandez, E., Pyrolytic behavior and products of some wood varieties. *Combustion and Flame* **2001,** *124* (1–2), 165-177.

85. Antal, M. J., Jr.; Varhegyi, G., Cellulose Pyrolysis Kinetics: The Current State of Knowledge. *Industrial & Engineering Chemistry Research* **1995,** *34* (3), 703-717.

86. Di Blasi, C.; Branca, C., Temperatures of Wood Particles in a Hot Sand Bed Fluidized by Nitrogen. *Energy & Fuels* **2003,** *17* (1), 247-254.

87. Di Blasi, C.; Branca, C., Kinetics of Primary Product Formation from Wood Pyrolysis. *Industrial & Engineering Chemistry Research* **2001,** *40* (23), 5547-5556.

88. Kudsy, M.; Kumazawa, H.; Sada, E., Pyrolysis of kraft lignin in molten ZNCL2-KCL media with tetralin vapor addition. *The Canadian Journal of Chemical Engineering* **1995,** *73* (3), 411-415.

89. Ross, D. P.; Heidenreich, C. A.; Zhang, D. K., Devolatilisation times of coal particles in a fluidised-bed. *Fuel* **2000,** *79* (8), 873-883.

90. Kanury, A., Combustion characteristics of biomass fuels. *Combustion Science and Technology* **1994,** *97* (4-6), 469-491.

91. de Diego, L. F.; García-Labiano, F.; Abad, A.; Gayán, P.; Adánez, J., Modeling of the Devolatilization of Nonspherical Wet Pine Wood Particles in Fluidized Beds. *Industrial & Engineering Chemistry Research* **2002,** *41* (15), 3642-3650.

92. Gaston, K. R.; Jarvis, M. W.; Pepiot, P.; Smith, K. M.; Frederick, W. J.; Nimlos, M. R., Biomass Pyrolysis and Gasification of Varying Particle Sizes in a Fluidized-Bed Reactor. *Energy & Fuels* **2011,** *25* (8), 3747-3757.

93. Di Blasi, C.; Hernandez, E. G.; Santoro, A., Radiative Pyrolysis of Single Moist Wood Particles. *Industrial & Engineering Chemistry Research* **2000,** *39* (4), 873-882.

94. Di Blasi, C., Influences of physical properties on biomass devolatilization characteristics. *Fuel* **1997,** *76* (10), 957-964.

95. Jia, L.; Becker, H. A.; Code, R. K., Devolatilization and char burning of coal particles in a fluidized bed combustor. *The Canadian Journal of Chemical Engineering* **1993,** *71* (1), 10-19.

96. Oasmaa, A.; Peacocke, C., Properties and fuel use of biomass-derived fast pyrolysis liquids. *VTT PUBLICATIONS 731* **2010,** (731).

97. Mochizuki, T.; Toba, M.; Yoshimura, Y., Effect of Electrostatic Precipitator on COllection Efficiency of Bio-oil in Fast Pyrolysis of Biomass. *Journal of the Japan Petroleum Institute* **2013,** *56* (6), 401-405.

98. Bedmutha, R. J.; Ferrante, L.; Briens, C.; Berruti, F.; Inculet, I., Single and two-stage electrostatic demisters for biomass pyrolysis application. *Chemical Engineering and Processing: Process Intensification* **2009,** *48* (6), 1112-1120.

99. Lucas, J. R., High voltage engineering. *Colombo, Open University of Sri. Lanka* **2001**, 64-89.

100. Klas, M.; Radmilović-Radjenović, M.; Radjenović, B.; Stano, M.; Matejčik, Š., Transport parameters and breakdown voltage characteristics of the dry air and its constituents. *Nuclear Instruments and Methods in Physics Research Section B: Beam Interactions with Materials and Atoms* **2012,** *279* (0), 96-99.

101. Scott, D. S.; Majerski, P.; Piskorz, J.; Radlein, D., A second look at fast pyrolysis of biomass—the RTI process. *Journal of Analytical and Applied Pyrolysis* **1999,** *51* (1–2), 23-37.

102. Hoekstra, E.; Westerhof, R. J. M.; Brilman, W.; Van Swaaij, W. P. M.; Kersten, S. R. A.; Hogendoorn, K. J. A.; Windt, M., Heterogeneous and homogeneous reactions of pyrolysis vapors from pine wood. *AIChE Journal* **2012,** *58* (9), 2830-2842.

103. Ouyang, F.-Y.; Chang, C.-H.; Kai, J.-J., Long-term corrosion behaviors of Hastelloy-N and Hastelloy-B3 in moisture-containing molten FLiNaK salt environments. *Journal of Nuclear Materials* **2014,** *446* (1–3), 81-89.

Papers

Paper I

Nygård, Heidi S.; Olsen, Espen. Review of thermal processing of biomass and waste in molten salts for production of renewable fuels and chemicals. *International Journal of Low-Carbon Technologies* 2012, 7 (4), 318-324.

International Journal of Low-Carbon Technologies Advance Access published January 22, 2012

Review of thermal processing of biomass and waste in molten salts for production of renewable fuels and chemicals

Heidi S. Nygård* **and Espen Olsen**

Department of Mathematical Sciences and Technology, Norwegian University of Life Sciences, 1432 Ås, Norway

Abstract

Renewable energy has gained great attention and interest in recent years due to growing energy consumption and greater environmental concerns. Biomass is regarded as a promising candidate for replacing fossil-derived products, through either thermal, biological, or physical processes. This review focuses on thermal processing of biomass in molten salts for production of renewable fuels and chemicals, concepts based on dispersion of biomass or waste particles in a molten salt bath. Inorganic salts have very high heat capacities and good thermal stability at high temperatures. Some molten salts have catalytic properties, and in thermal processing of biomass, the product yields and compound compositions of products can be adjusted by varying compositions and amount of molten salts. In addition, molten salts will retain noxious contaminants, and it is thus possible to use difficult convertible- and/or contaminated biomass as feedstock.

Keywords: pyrolysis; gasification; biofuels; molten salts; renewable energy

*Corresponding author:
heidi.nygard@umb.no

Received 28 September 2011; revised 18 November 2011; accepted 5 December 2011

1 INTRODUCTION

The world energy consumption has increased significantly the last four decades. This increase is in pace with population growth, improving living standards in developing countries and an overall higher consumption in Western countries [1]. Due to the use of fossil fuels, the emissions of greenhouse gases such as CO_2 have increased. With growing energy consumption and greater environmental concerns, there is a need for more research on alternatives to fossil-derived products [2]. There are many alternatives to renewable electricity, but biomass such as wood, energy crops and agricultural and forestry wastes can provide the main source of renewable liquid, gaseous and solid fuels [3]. When used as fuel, biomass releases the CO_2 it absorbed from the atmosphere in the recent past, not millions of years ago as with fossil fuel. Because of the much shorter carbon cycle than fossil fuels, it contributes to less net CO_2 in the atmosphere [2]. There are a number of processes for the conversion of biomass and residues to more valuable energy forms. These include thermal, biological, mechanical or physical process. In thermochemical conversion, biomass can supply energy by direct combustion or via intermediates by gasification or pyrolysis [4].

A common biomass material in thermochemical conversion is wood [5]. Wood is an organic material that consists of ~50% carbon, 6% hydrogen and 44% oxygen. The chemical substances are originally produced in living cells of a tree, but at the time of cutting, the major portion of the tree no longer contains living cells. Thus, there are essentially no proteins and other nitrogenous substances normally associated with living cells [6]. The chemical structure of wood consists mainly of cellulose (40–45%), hemicellulose (25–30%) and lignin (15–35%). A simplified illustration is that cellulose forms a skeleton surrounded by other substances functioning as matrix (hemicellulose) and encrusting (lignin) materials [5].

This review focuses on pyrolysis and gasification of biomass and waste in molten salts with renewable fuels and chemicals as the main products. The research reviewed includes many investigations that have not so far progressed beyond the laboratory scale. Thermal processing in molten salts is a relatively small research area compared with "traditional" conversion methods. There have been only a few publications within the

International Journal of Low-Carbon Technologies 2012, 0, 1–7

doi:10.1093/ijlct/ctr045

subject every decade since the early 70s, and no review has been published before.

2 PRINCIPLES OF THERMOCHEMICAL CONVERSION PROCESSES

In thermochemical conversion, heat is supplied and the biomass decomposes to a mixture of liquids (tars/oils), non-condensable gases and solid chars. Char is the solid residue left after devolatilization is complete. Tars/oils are defined as the volatile products that are liquid at room temperature. The remaining products are non-condensable gases such as CO, CO_2, H_2, CH_4 and other small hydrocarbons. The relative yields depend on the amount of the oxidizing agent, process temperature, pressure, heating rates and reaction time. The choice of conversion technologies depends on properties and quantity of the feedstock as well as on the desired main product [3].

2.1 Pyrolysis

In pyrolysis, the decomposition of biomass occurs without any oxidizing agent. The relative yields of the products depend mostly on the rate of heating and the final temperature. The production of charcoal is favored in slow pyrolysis—slowly heating at low temperatures and long vapor residence times. Higher yields of gas are achieved with higher temperatures and longer residence times. Fast pyrolysis is applied when the aim is to maximize the liquid fraction (bio-oil/pyrolysis oil) [4]. In fast pyrolysis, biomass is heated rapidly to moderate temperatures of around 500°C and short reaction times of up to 2 s. When wood is used as a feedstock material in continuously operated laboratory reactors and pilot plants, typical oil yields are between 60 and 70 wt% on a dry-feed basis. This has been shown in a number of laboratory reactor configurations developed over the last 20 years, including bubbling fluid beds, circulating and transported beds, cyclonic reactors and ablative reactors. Several pilot plants have been constructed, in addition to a few demonstration installations. A detailed description of the reactor configurations may be found in the review of fast pyrolysis technology development by Venderbosch and Prins [3].

Pyrolysis oil is a dark brown, free-flowing liquid. The oil is a complex mixture of components from depolymerization of cellulose, hemicellulose and lignin [7]. Several hundred components have so far been identified, with water being the single most abundant component [3]. Other major groups of compounds identified are hydroxyaldehydes, hydroxylketones, sugars, carboxylic acids and phenolic compounds. The elemental composition resembles that of biomass rather than that of fossil fuel oil, and the properties of pyrolysis oils are therefore somewhat different from that of heavy fossil fuel oil [7].

The heating value of pyrolysis oil is ~50% that of heavy fossil fuel oils due to the high moisture and oxygen contents. However, the moisture content also reduces the viscosity and enhances fluidity, which is beneficial for combustion in an engine. Much of the oxygen is distributed in carboxylic acids, which makes the pyrolysis oil unstable and corrosive and thus imposes requirements on construction materials in boilers and engines if it is to be used directly. The viscosity of the pyrolysis oil decreases rapidly at higher temperatures, but increases during storage [7].

2.2 Gasification

Gasification is thermal decomposition by partial oxidation. The first step in biomass gasification is evaporation of the moisture. This is followed by pyrolysis, in which the biomass decomposes to give a mixture of gas, vaporized tars or oils and a solid char residue [4]. Using cellulose as representative feedstock composition under idealized conditions, the pyrolysis reaction is given by [5]:

$$C_6H_{10}O_5 \rightarrow 5CO + 5H_2 + C \quad (1)$$

The pyrolysis products will further react with a gasifying agent to give permanent gases of CO, CO_2, H_2 and small quantities of hydrocarbon gases [4]. This could be represented by carbon gasification. Two general routes are gasification with CO_2 (Boudouard reaction) or steam (water gas shift reaction), respectively [8]:

$$C + CO_2 \rightarrow 2CO \quad (2)$$
$$C + H_2O \rightarrow CO + H_2 \quad (3)$$

The carbon reduces the gasifying agent and the main product is synthesis gas, a mixture of H_2 and CO. The synthesis gas could be used directly as a low-to-medium energy fuel gas or further upgraded to liquid fuels, synthetic natural gas or other hydrocarbons [5].

Due to reactor and chemical reaction limitations, it is not possible to achieve a complete reaction of all the pyrolysis products. Hence, the final product gas is contaminated with tars to a certain extent. Tar formation is the most significant technical barrier, and much research is focused on thermal and/or catalytic tar cracking [4].

A number of reactor configurations have been developed and tested for biomass gasification; mainly downdraft (co-current) fixed bed gasifiers, but also fluid bed reactors are available. Several technologies have been successfully demonstrated at a large scale, but the process is still expensive compared with fossil-based energy. The available reactor configurations for biomass gasification have been reviewed by Bridgwater [4].

3 THERMAL PROCESSING IN MOLTEN SALTS

In molten salt pyrolysis and gasification, the thermal decomposition of biomass is performed in a molten salt bath. During

the process, the molten salt is simultaneously used as the heat carrier, catalyst and solvent.

Inorganic molten salts, ranging from zinc chloride and alkali metal halides to alkali metal carbonates and nitrates, have very good heat transfer characteristics [9]. They have large heat capacities and are very stable at high temperatures and may be used over a wide range of temperature, from around 120°C to well over 1000°C. These properties make molten salts suitable for rapid heat supply in thermal processing of biomass [10]. It has been shown that thermal processing in molten salts give higher heating rates than without molten salts [11], an important factor in fast pyrolysis in order to maximize the liquid fraction [3].

Some molten salts, especially halides, have a catalytic effect in the decomposition of larger molecules with respect to producing certain chemicals [12] and may thus give a simpler product mix in the pyrolysis process. The catalytic effect makes it possible to adjust the product yields and compound compositions of products by varying the composition and amount of molten salts [9, 12–14].

In the gasification process, carbonates are known to catalyze the carbon gasification reactions with CO_2 and steam [10], according to the following mechanisms [15]:

Carbon gasification by CO_2:

$$M_2CO_3 + 2C \rightarrow 2M + 3CO \quad (4)$$

$$2M + CO_2 \rightarrow M_2O + CO \quad (5)$$

$$M_2O + CO_2 \rightarrow M_2CO_3 \quad (6)$$

Carbon gasification by H_2O:

$$M_2CO_3 + 2C \rightarrow 2M + 3CO \quad (7)$$

$$2M + 2H_2O \rightarrow 2MOH + H_2 \quad (8)$$

$$2MOH + CO \rightarrow M_2CO_3 + H_2 \quad (9)$$

M is an alkali metal. The total reactions are the Boudouard reaction [Equation (2)] and water gas shift reaction [Equation (3)], respectively, and no salt is consumed in the process.

Another advantage in thermal processing of biomass in molten salts is that selected noxious contaminants are retained in the melt [16], which makes it possible to apply the method on contaminated biomass and waste.

The use of molten salts in thermochemical processing of biomass has several technical challenges compared with conventional methods. The choice of reactor vessel and other process materials is limited by the high corrosiveness of the melts. Halides are the most troublesome, and in some cases, ceramic-lined vessels and pipes have to be used instead of metals. Oxygenated melts such as nitrates and carbonates may on the other hand passivate metals at moderate temperatures. The startup and shutdown in an industrial scale is more of a problem than in conventional processes due to the fact that melts solidify at ambient temperatures. Some form of storage and dump tank is required where the salt could be melted prior to being pumped to the reactor system. The melt can be circulated and pumped centrifugally or with gear pumps or by simple gas-lift pumps [10].

3.1 Wood pyrolysis

Yasunishi and Tada [11, 17] studied wood pyrolysis in molten salts. Sapwood of sugi (*Cryptomeria japonica*) and konara (*Quercus serrata*) were in both studies pyrolyzed at 600–900°C in different mixtures of carbonates and chlorides. In the first study [11], molten salt was found to give heating rates of sample wood 4–10 times that in an inert atmosphere, with the highest heating rate being 12 500°C/min in a mixture of sodium chloride (NaCl) and potassium chloride (KCl) at 900°C. It was also found that molten salt gave increased yields of wood gas and char. The focus in the second study [17] was the composition of the yields. Carbonates or mixtures of zinc chloride ($ZnCl_2$) and KCl were found to give highest concentrations of hydrogen in the gas, while the mixture of NaCl and KCl gave the highest concentration of methane and ethylene.

A more recent experimental study of pyrolysis of biomass in molten salt media was conducted by Jiang *et al.* [13]. Samples of cellulose and rice stalk were pyrolyzed in molten mixtures of metal chlorides and nitrates at temperatures between 400 and 600°C. The yields of bio-oil increased and then decreased with increasing temperature, with an optimal temperature at ~530°C. This was explained by the fact that increasing temperature also causes secondary cracking reactions and thus higher yields of gaseous products at the sacrifice of liquid products. Both liquid yield and water content of bio-oil were found to be strongly dependent on the molten salt composition. $ZnCl_2$ have the highest yield of bio-oil (35 wt%), but with a water content of 46 wt%. A mixture of KCl and CuCl gave a much lower water content (21 wt%), and the yield of bio-oil was also significantly lower (11.8 wt%).

3.2 Pyrolysis of lignin for production of phenolic compounds

A few studies on the pyrolysis of lignin in molten salts for the production of chemicals have been reported [12, 14, 18]. Lignin is a major constituent of wood and other biomass materials. It is constructed from aromatic subunits, and it is suggested that valuable chemicals such as phenolic compounds can be derived from lignin [12]. In order to achieve high yields of phenolic compounds, there is need for a method that promotes the production of aromatic compounds. Previous research on the hydrocracking of coal have shown that zinc halides have a superior selectivity to produce single-ring aromatic compounds due to a low hydrocracking activity on single-ring coal derivatives [19].

Sada *et al.* [12] studied the conversion of kraft and solvolysis lignin into phenolic compounds by molten salt pyrolysis. The pyrolysis was performed in mixtures of molten $ZnCl_2$ and KCl with molar ratios of 3/7 and 7/6 over the temperature range of 500–800°C. KCl was added to $ZnCl_2$ as a viscosity reducer to promote phase separation, in addition to reducing

the melting point of the salt. The yields of phenolic compounds were influenced by both the temperature and the molten salt composition. At low temperatures, the major products were cresols, while higher temperatures also gave phenols. Further, it was shown that a molar ratio of 7/6 had a high selectivity to cresols, giving a maximum yield of 4.6 wt% from solvolysis lignin at 600°C. For kraft lignin, a maximum yield of cresols of 1.8 wt% was found under the same conditions.

In order to improve the liquid yields in the molten salt pyrolysis of lignin, Kudsy *et al.* [14] continued the studies by adding tetralin vapor as a hydrogen donor in the same reactor arrangements. Kraft lignin was pyrolyzed in a molten $ZnCl_2$–KCl mixture with a molar ratio of 7/6. The temperature ranged from 400 to 700°C and the tetralin vapor was added in 0.4 and 4 mol% diluted with N_2. The gaseous products H_2, CH_4 and CO were analyzed by gas chromatography. The results did not show any significant effect of tetralin vapor addition on the H_2 yield, indicating that the hydrogen radical produced from tetralin was not consumed in the formation of H_2 but instead in the formation of phenolic compounds and light liquids. The yields of CH_4 and CO were on the other hand slightly increased with the addition of tetralin vapor. The yields of phenolic compounds such as *p*-, *m*- and *o*-cresols, phenol and 2,5- and 2,6-xylenols were all increased by tetralin vapor addition. At 600°C and 4 mol% tetralin vapor, the yields of cresols and total phenolic compounds were increased by 38 and 78%, respectively. The formation of the light liquids benzene, toluene and xylene were also enhanced by the tetralin vapor addition, most likely due to reactions between lignin tar and hydrogen radicals.

The arrangements for molten salt pyrolysis of lignin were further modified by Kudsy and Kumazawa [18] to allow investigation of the kinetics in the pyrolysis process. Kraft lignin was pyrolyzed in molten $ZnCl_2$ and KCl with a molar ratio of 7/6 at temperatures of 500, 550 and 600°C. The effect of the amount of salt was also examined by using three levels of salt-to-lignin ratios (SRs); SR = 1, 2 and 3. Nineteen kinds of phenolic compounds were identified and quantified by gas chromatography. Among these were monohydroxyphenols, guaiacols, catechols and syringols. The yields of both gaseous and liquid products were found to depend strongly on the amount of salt. SR = 1 gave the lowest value of gaseous products and the highest yield of phenolic compounds except for phenol. The latter attained highest yields at SR = 3. There was a maximum in the yields of all phenolic compounds at a reaction time of 15 min for SR = 1 and a temperature of 550°C. After the maximum, the yields of most phenolic compounds decreased, and the formation of gaseous products was observed. The study also examined the kinetics of the phenolic compounds' decomposition. It was found that the formation of cresols and guaiacols follow a first-order reaction sequence, while another model is required for catechol.

3.3 Hybridization with solar energy

Molten salt gasification has been proposed in hybridization with solar energy. The process was originally considered for the gasification of coal and active carbon [8, 20, 21], but the same principles may be applied for biomass [9, 22]. Conventional gasification depends on heat by partial combustion of the biomass feed within the reaction bed [4]. In solar gasification, a concentrating solar receiver could be used to heat and melt the salt. Biomass is introduced to the molten salt bath where the decomposition reactions occur. The molten salts may also be used as a thermal storage for solar energy. In this way, the gasification process is stable under the fluctuation of insolation [9].

Yoshida *et al.* [8] studied the gasification of active carbon and coal with CO_2 in a mixture of potassium carbonate (K_2CO_3) and sodium carbonate (Na_2CO_3) at 900°C. CO_2 was chosen as a gasifying agent instead of H_2O due to easier feeding to the reactor and the possibility to store more energy per mole of carbon. In addition, recycling of CO_2 helps reducing the amount of CO_2 emission in the environment. CO_2 was streamed along the molten salt surface, and the CO evolution rate was measured. The molten salt was found to enhance the gasification rate by 3.3 and 1.5 times for coal and active carbon, respectively, compared with the absence of the molten salt. However, the CO evolution rate decreased after 5 min due to sedimentation of the coke formed by coal pyrolysis. Matsunami *et al.* [20] modified the reactor to allow CO_2 bubbling through the molten salt. In the modified reactor, better contact between CO_2 and coke formed by coal pyrolysis was achieved. Due to the CO_2 gas bubbling, the coke particles were suspended in the molten salt thus preventing their sedimentation. This approach was found to be an effective method to maintain a high CO evolution rate.

Adinberg *et al.* [9] proposed a hybridization of solar and bioenergy using molten salts as a further development of the solar gasification of coal. In the experiments, a eutectic mixture of K_2CO_3 and Na_2CO_3 with a melting point of 710°C was used. Cellulose tablets were pyrolyzed at reaction temperatures of 800–915°C without any gasifying agent in order to study the first step in the gasification process. Experiments were also conducted without molten salt for investigation of the influence of molten salt on the process. The molten salt was found to increase the heating and reaction rates in the pyrolysis process and the total amount of gas produced. At 850°C, the reaction rate was increased by 20% and a total solid-to-gas conversion of 94 wt% was observed in the molten salt reaction medium, in contrast to 72 wt% in an inert atmosphere. The yield of H_2 was 26 and 21 vol% with and without salt, respectively. These observations were explained by enhanced heat transfer and the catalytic effect that carbonates have on the reaction between char and pyrolytic water.

A solar gasification study with independently explorations of pyrolysis and gasification reactions was reported by Hathaway *et al.* [22]. Pyrolysis of cellulose and steam gasification of activated wood charcoal were performed in a eutectic

mixture of lithium, potassium and sodium carbonates at temperatures ranging from 851 to 962°C. In the presence of molten salt, the pyrolysis rate was increased by 74% and the gasification rate by more than an order of magnitude. Catalysis was not observed in the pyrolysis because the reactions were too fast for sufficient contact between the melt and the cellulose. The increased pyrolysis rate was instead explained by enhanced heat transfer within the salt. However, the data supported a catalytic effect of salt during the steam gasification of carbon. For cellulose pyrolysis in molten salts, the yields of the primary products H_2 and CO were found to be increased by 29%, while the CO_2 yield decreased by 62% compared with pyrolysis in the absence of molten salts. The increase in H_2 and CO was explained by a combination of reduced CO_2 production and cracking of retained tars.

3.4 Thermal treatment of waste in molten salts

There have been several reports on using waste as feedstock in molten salt pyrolysis and/or gasification for the production of fuels. Experiments have been conducted with, for example, municipal refuse [16] and plastic waste [23–25]. More recent studies have focused on wastepaper and organic waste as feedstock [15, 26, 27].

Hammond and Mudge [16] reported a feasibility study of pyrolysis of municipal refuse in molten salts. A typical refuse mix was pyrolyzed in molten Na_2CO_3 at 870–1000°C. The off-gas initially contained ~50 mol% H_2, but pretreatment of the melt with steam gave up to 73 mol% H_2. The gas was essentially free of tars and oils, and as a consequence of this, minimal gas cleanup was required. To make the process autothermal, it was suggested to combust the char residue with air or oxygen. Molten salt pyrolysis of municipal refuse was found to be technically feasible, but economically impractical compared with other recovery methods. This was mainly due to the high cost of the materials needed for resisting the corrosivity of the molten salt. Also, the ash removal was found to be quite complicated. However, because noxious contaminants were retained in the melt, molten salt pyrolysis was recommended as a destruction method of hazardous wastes.

Menzel *et al.* [23] reported a study on using molten salt for recycling of plastics. Polyethylene, polystyrene and polyvinyl chloride (PVC) were pyrolyzed in a mixture of $MgCl_2$ and KCl at temperatures between 640 and 850°C. The main products from the pyrolysis of polyethylene were ethylene and methane. A small amount of propene was also detected, but the content decreased with increasing temperature. A large amount of styrene was found from the pyrolysis of polystyrene, but the yield decreased with increasing temperature in favor of benzene. Pyrolysis of PVC gave up to 58 wt% HCl, and only up to 29 wt% liquid hydrocarbons.

The work was followed up by Bertolini and Fontaine [24], who investigated the pyrolysis of plastic waste in molten salts in an eutectic salt consisting of NaOH and Na_2CO_3 at relatively low temperatures (420–480°C). The "pure" plastics polyethylene, polypropylene, polystyrene and polyvinyl chloride were used in the experimental studies. The studies showed that the pyrolysis of polyethylene and polypropylene gave usable paraffins and waxes, but they had to be separated from the pyrolysis oil. Chlorine containing plastics were almost completely dechlorinated by using basic salts, and no HCl acid was produced, in contrast to what Menzel *et al.* [23] reported. However, since salt was consumed in the process due to the formation of chlorides in the melt, Bertolini and Fontaine [24] primarily suggested molten salt pyrolysis as a method of productive elimination for mixed plastic waste.

Another study of the pyrolysis of polymer waste was reported by Chambers *et al.* [25]. They investigated the pyrolysis of the rubber-rich organic fraction from an automobile shredder in eight different eutectic mixtures of chlorides. The temperatures in the experiments were between 380 and 570°C. One of the aims of the research was to determine conditions maximizing both the amount of oil produced and the fraction of low-boiling components in the oil. Acidic melts such as $NaCl/AlCl_3$ gave the highest gas production, while the highest yields of oil were obtained in chloride melts containing copper at a temperature of 500°C. Oils with the largest fraction of low-boiling compounds were produced under conditions that gave methane as the largest hydrocarbon component in the gas. The light components of the oil were aromatic; primarily toluene, ethylbenzene, styrene and C_3 and C_4 alkylbenzenes. The results suggested that recycling of the higher boiling components through the melt would lead to further cracking. Hydrogen is a limiting factor in molten salt pyrolysis. Too low hydrogen content results in incomplete conversion of carbon to gaseous or liquid hydrocarbons and thus great amounts of carbon in the residue char. Chambers *et al.* found the most efficient conversion of H_2 in the KCl/LiCl melt with 10% CuCl.

More recent studies have focused on converting wastepaper and organic waste into valuable fuels by thermal processing in molten salts. The main content of wastepaper is cellulose, and it could be regarded as a kind of biomass. Iwaki *et al.* [15] studied wastepaper gasification with carbon dioxide and steam in molten carbonates at temperatures between 700 and 750°C. In the experiments, wastepaper was represented by tissue paper. Different mixtures of Li_2CO_3, Na_2CO_3 and K_2CO_3 were used. In CO_2 gasification, carbon conversion was most efficient when Li_2CO_3 was included in the melt. This was ascribed to the molecular size of the salts; smaller alkali metals ought to be more easily dipped into the wastepaper and thus have higher catalysis activity. A few experiments were also conducted with newspaper and copy paper. These also contain fillers like silicon dioxide, silicate, calcium carbonate and kaolin. The results implied that the process could be applied to all the materials, although copy paper had a somewhat lower reaction rate, most likely due to the calcium content which inhibits the contact efficiency between the paper and CO_2.

The work was followed up by Jin *et al.* [26] who focused on wastepaper gasification with CO_2 catalyzed by molten carbonate

melts at temperatures between 650 and 750°C. Experiments without salt were conducted for comparison. It was found that no CO was produced when the wastepaper was introduced in a gaseous environment without molten salts. Once Na_2CO_3 was present, a remarkably rise in the reaction rate was observed. This was explained by the shift of the interface between wastepaper and CO_2 in the reaction system from gas-solid to gas-liquid, allowing CO_2 to attack wastepaper effectively.

The maximum reaction rate increased by four times for the intermixture of Na_2CO_3 and K_2CO_3 and by five times when Li_2CO_3 was present. It was suggested that alkali metals catalyze the process of breaking β(1,4)-glycosidic bonds found between the glucose monomers that form the cellulose polymer.

Sugiura *et al.* [27] reported a study on the gasification of organic waste with CO_2 in a molten salt comprising Li_2CO_3 and K_2CO_3. Sludge from a sewage plant and rice were selected as representatives of organic waste, and experiments were conducted at temperatures from 500 to 750°C. The highest temperature was found to be best for gasification. Sulfur was assumed to be absorbed by the molten salt, but SO_x was found in the product gas. This was explained by too short contact time between sludge and molten salt.

4 CONCLUSIONS AND RECOMMENDATIONS FOR FUTURE WORK

Thermochemical conversion of biomass in molten salts is a relatively small research area compared with "traditional" methods. With increasing energy consumption and an increasing concern about the limitations and environmental problems associated with fossil fuels, the research area has gained renewed interest the last few years. However, only lab-scale experiments have been reported, and the processes are yet to be tested further in pilot and demonstration scales.

Molten salts have very good heat transfer characteristics and therefore provide an efficient heat transfer in the processes. Molten salts also have very high thermal stability and are capable of storing a great amount of heat over a long period of time. The fact that molten salt processing of biomass is proposed to be combined with solar energy makes the process even more interesting from a renewable point of view. Besides the role as a heat transfer medium, molten salts could work as a fluid reacting bed and as a catalyst in the conversion process.

Because noxious contaminants are retained in the melt, thermochemical conversion in molten salts might be a good way of destroying and converting hazardous waste into fuel or other valuable chemicals. Even chlorine containing plastics are completely dechlorinated, no HCl is produced in the pyrolysis process. However, the products have to be thoroughly examined so that no hazardous chemicals will be released during further processing.

The focus in most of the previous work on molten salt pyrolysis and gasification has been the yields of synthesis gas. Molten carbonate baths at relatively high temperatures have been used for this purpose, resulting in high yields of H_2 in the gaseous fraction. Some work has also been conducted with chlorides, but carbonates seem to give more desirable effect in these processes.

At lower temperatures, the liquid fraction is favored. Molten salts are found to give higher heating rates, which will promote the fast pyrolysis leading to a larger liquid fraction. The studies of production of bio-oil prescribe the liquid yield to the catalytic effect halides have on producing single-ring aromatic compounds. However, there seems to be no good explanation on why chlorides are chosen instead of other halides.

There has not been very much work on the characterization of the liquid fraction. The yield of phenolic compounds in the liquid fraction has been investigated, but further characterization needs to be conducted in order to explore the possible applications of the oil obtained from molten salt pyrolysis compared with oils from other pyrolysis processes.

REFERENCES

[1] *Key World Energy Statistics*. International Energy Agency, 2010. Available at http://www.iea.org/textbase/nppdf/free/2010/key_stats_2010.pdf.

[2] Basu P. *Biomass Gasification and Pyrolysis: Practical Design and Theory*. Elsevier Science and Technology, 2010.

[3] Venderbosch RH, Prins W. Fast pyrolysis technology development. *Biofuels Bioproducts and Biorefining* 2010;**4**:178–208.

[4] Bridgwater AV. Renewable fuels and chemicals by thermal processing of biomass. *Chem Eng J* 2003;**91**:87–102.

[5] Klass DL. *Biomass for Renewable Energy, Fuels, and Chemicals*. Academic Press, 1998.

[6] Bodig J, Jayne BA. *Mechanics of Wood and Wood Composites*. Van Nostrand Reinhold, 1982.

[7] Czernik S, Bridgwater AV. Overview of applications of biomass fast pyrolysis oil. *Energy Fuels* 2004;**18**:590–8.

[8] Yoshida S, Matsunami J, Hosokawa Y, *et al*. Coal/CO_2 gasification system using molten carbonate salt for solar/fossil energy hybridization. *Energy Fuels* 1999;**13**:961–4.

[9] Adinberg R, Epstein M, Karni J. Solar gasification of biomass: a Molten Salt Pyrolysis Study. *J Solar Energy Eng* 2004;**126**:850–7.

[10] Lovering DG. *Molten Salt Technology*. Plenum Press, 1982.

[11] Yasunishi A, Tada Y. Wood pyrolysis in molten-salt. *Kagaku Kogaku Ronbunshu* 1985;**11**:346–9.

[12] Sada E, Kumazawa H, Kudsy M. Pyrolysis of lignins in molten salt media. *Ind Eng Chem Res* 1992;**31**:612–6.

[13] Jiang H, Ai N, Wang M, *et al*. Experimental study on thermal pyrolysis of biomass in molten salt media. *Electrochemistry* 2009;**77**:730–5.

[14] Kudsy M, Kumazawa H, Sada E. Pyrolysis of kraft lignin in molten ZNCL2-KCL media with tetralin vapor addition. *Can J Chem Eng* 1995;**73**:411–5.

[15] Iwaki H, Ye S, Katagiri H, Kitagawa K. Wastepaper gasification with CO_2 or steam using catalysts of molten carbonates. *Appl Catal A Gen* 2004;**270**:237–43.

[16] Hammond VL, Mudge LK. Feasibility study of use of molten salt technology for pyrolysis of solid waste. *Final report*, Battelle Pacific Northwest Labs., Richland, Wash. 1975.

[17] Tada Y, Yasunishi A. Wood pyrolysis with molten-salt as heating medium. *Kagaku Kogaku Ronbunshu* 1987;**13**:376–9.

[18] Kudsy M, Kumazawa H. Pyrolysis of kraft lignin in the presence of molten $ZnCl_2$-KCl mixture. *Can J Chem Eng* 1999;**77**:1176–84.

[19] Scarrah WP. Molten salt hydrocracking of lignite. Screening of viscosity reducers and hydrogen sources. *Ind Eng Chem Prod Res Dev* 1980;**19**:442–6.

[20] Matsunami J, Yoshida S, Oku Y, *et al*. Coal gasification by CO_2 gas bubbling in molten salt for solar/fossil energy hybridization. *Solar Energy* 2000;**68**:257–61.

[21] Matsunami J, Yoshida S, Oku Y, *et al*. Coal gasification with CO_2 in molten salt for solar thermal/chemical energy conversion. *Energy* 2000;**25**:71–9.

[22] Hathaway BJ, Davidson JH, Kittelson DB. Solar gasification of biomass: kinetics of pyrolysis and steam gasification in molten salt. *J Solar Energy Eng* 2011;**133**:021011.

[23] Menzel J, Perkow H, Sinn H. Recycling plastics. *Chem Ind* 1973;**12**:570–3.

[24] Bertolini GE, Fontaine J. Value recovery from plastics waste by pyrolysis in molten salts. *Conserv Recycl* 1987;**10**:331–43.

[25] Chambers C, Larsen JW, Li W, Wiesen B. Polymer waste reclamation by pyrolysis in molten salts. *Ind Eng Chem Process Des Dev* 1984;**23**:648–54.

[26] Jin G, Iwaki H, Arai N, Kitagawa K. Study on the gasification of wastepaper/carbon dioxide catalyzed by molten carbonate salts. *Energy* 2005;**30**:1192–203.

[27] Sugiura K, Minami K, Yamauchi M, *et al*. Gasification characteristics of organic waste by molten salt. *J Power Sources* 2007;**171**:228–36.

Paper II

Westerhof, R. J. M.; **Nygård, Heidi S.**; Swaaij, W. P. M. van; Kersten, S. R. A.; Brilman, D. W. F.. Effect of Particle Geometry and Microstructure on Fast Pyrolysis of Beech Wood. *Energy & Fuels* 2012; 26 (4), 2274-2280.

energy&fuels

Article

pubs.acs.org/EF

Effect of Particle Geometry and Microstructure on Fast Pyrolysis of Beech Wood

R. J. M. Westerhof,*[,†] H. S. Nygård,[‡] W. P. M. van Swaaij,[†] S. R. A. Kersten,[†] and D. W. F. Brilman[†]

[†]Thermal Chemical Conversion of Biomass Group, Faculty of Science and Technology, University of Twente, P.O. Box 217, 7500 AE, Enschede, The Netherlands

[‡]Department of Mathematical Sciences and Technology, Norwegian University of Life Sciences, P.O. Box 5003, N-1432 Ås, Norway

ABSTRACT: The influence of particle geometry and microstructure in fast pyrolysis of beech wood has been investigated. Milled wood particles (<0.08−2.4 mm) and natural wood cylinders (2−14 mm) with different lengths (10−50 mm) and artificial wood cylinders (D_p = 0.5−14 mm) made of steel walls, filled with small milled wood particles (<0.08−0.140 mm), have been pyrolyzed in a fluidized bed at 500 °C. From the results of the experiments, the influence of particle geometry and microstructure on char, gas, and pyrolysis oil yield and pyrolysis oil composition has been derived. The product yields of large cylinders with diameters of 6−14 mm are primarily determined by the outer diameter and resulting heating rate. The microstructure of these cylinders, being either natural channels or randomly packed small milled wood particles, has turned out to be much less important. For the smaller milled wood particles, the microstructure does have a profound effect on the product yields. The smallest particles (<0.140 mm), which consist only out of cell wall material and have lost their typical wood channel structure, show a clearly higher oil yield and lower char yield. It is postulated that the high pyrolysis oil yield can be explained by larger mass transfer rates of pyrolysis products from these smallest particles, as compared to mass transfer from particles containing channels.

INTRODUCTION

Fast pyrolysis of biomass is a thermochemical conversion method to obtain a pyrolysis oil, along with a solid char and noncondensable gas, by fast heating of the biomass in the absence of oxygen. Pyrolysis oil is a complex mixture of many oxygenated compounds like sugars, acids, furans, phenols, aldehydes, ketones, and water insoluble lignin derived oligomers.[1−3] Water is one of the most abundant compounds in pyrolysis oil.[4] Water lowers the viscosity and the heating value of the oil, and at high concentrations, it causes the oil to phase separate.[5−8] Levoglucosan is an interesting monosugar that can be hydrolyzed to form glucose or can be directly fermented to produce ethanol.[9] The water-insoluble lignin derived oligomers present in pyrolysis oil have the potential to be used for the production of transportation fuels.[10]

In the last three decades, many pyrolysis reactors have been developed. Generally, these reactors can be classified as bubbling fluidized beds, circulated fluidized beds, ablative reactors, screw reactors, rotating cones, and vacuum reactors.[11−13] Design and optimization of these pyrolysis processes requires insight and understanding of the chemical reactions and physical processes involved during the conversion of the biomass particles. One area that still needs further research is the effect of the biomass particle shape and size on char, gas, and pyrolysis oil yield and composition. Wang et al.[14] have shown that variation of the diameter of wood cylinders between 0.7 and 14 mm ($L_p/D_p > 3$) has a minor effect on the total liquid yield. It was observed experimentally in their study that the water production increased as the diameter of the cylinder increased. Shen et al.[15] studied the effect of mallee wood particle size (18−5.6 mm) on the yield and composition of pyrolysis oil using a fluidized bed reactor operated at 500 °C. It was found that the bio-oil yield decreases as the particle size increased from 0.3 to 1.5 mm. Shen et al.[15] postulated that destruction of the wood particle structure by milling could be a reason for higher oil yields for smaller particles. In the particle size range of 1.5−5.6 mm, no further decrease of oil was found by these researches. Salehi et al.[16] pyrolyzed three fractions of milled wood particles, <0.59, 0.59−1, and 1−1.4 mm, in a fluidized bed operated at 500 °C and noticed that the oil yield decreased rapidly from 62 to 52 wt % as the sawdust size increased from <0.59 to 0.59−1 mm. For larger sawdust sizes, the decrease in oil yield leveled off.

Since the costs associated with biomass grinding increase with decreasing particle size,[17] there is need to identify the optimal particle size for which acceptable oil yields are obtained and if the oil still satisfies the specifications for further usage.

One of the important characteristics of the pyrolysis process is the heating rate of the biomass particle.[18−20] Heating rate and final pyrolysis temperature both have a large impact on the pyrolysis product yields and pyrolysis oil quality.[5,21,22] For particles larger than ∼1 mm, the external heat transfer and/or thermal diffusivity controls the conversion rate. For beech wood particles smaller than ∼1 mm, decomposition is said to take place very close to the reactor temperature and is more likely to be controlled by its kinetics.[18]

In addition to heat transfer and final pyrolysis temperature, the time needed for the (partial) depolymerized biomass, being in the liquid or solid state, to leave the reacting particle by vaporization/sublimation of vapors or physical entrainment of

Received: October 29, 2011
Revised: January 15, 2012
Published: January 25, 2012

dx.doi.org/10.1021/ef201688n | *Energy Fuels* 2012, 26, 2274−2280

aerosols is seen as an important issue determining the product distribution.[5,15,22,23] Haas et al.[23] performed real-time microscope analysis of poplar wood undergoing pyrolysis. The poplar wood was heated with 150 °C/min to 500 °C. It was clearly visualized that liquid droplets exist inside the decomposing wood structures and that some of the droplets were trapped inside the particle. This is a clear indication on limitations for newly formed liquid (partly depolymerized biomass) to leave the particle. Vapors/aerosols created inside the biomass particles find their way out mainly via channels inside the biomass structure (anisotropic vapor outflow).[23] When these compounds do not leave the hot biomass particle fast enough, they will cross-link and eventually form char.[22]

There are two main objectives in the present paper. The first objective concentrates on the effect of beech wood geometry (shape and size) on the char, gas, water, organics, water insolubles, and levoglucosan yield. Wood cylinders of 2−14 mm and milled particles of 0.25−2.5 mm were pyrolyzed in a fluidized bed at 500 °C. The second objective of this study is focused on the effect of wood microstructure and vapor/aerosol outflow patterns (anisotropic/isotropic) on the char yield. Artificial wood cylinders with solid walls (1, 6, 10, or 14 mm inner diameter) and wire-mesh end-caps at both sides, filled with milled particles (<0.08 mm), were used to study the effect of microstructure on pyrolysis. The results will be compared with those obtained with artificial cylinders completely made from wire mesh (6, 10, 14 mm), filled with milled particles of 0.140 mm to investigate the effect of isotropy/anisotropy in outflow of the produced vapors.

EXPERIMENTAL SECTION

Wood Particles. Beech wood (660 kg/m^3) was used as feedstock in the pyrolysis experiments. The ash content was determined to be between 0.5 and 0.6 wt % and elemental composition was as follows: N = 0.5 ± 0.1, C = 46 ± 1, H = 7 ± 0.5, and O = 46 ± 1 wt %. The biomass was dried for 24 h at 105 °C prior to the experiment. The residual moisture content is below 1 wt %. In this paper, we changed both the geometry (shape and size) and microstructure of the wood. Wood cylinders (D_p = 2−14 mm) and milled particles (L_s = <0.08−2.4 mm) were used. The length of the cylinders was always 50 mm resulting in an aspect ratio larger than 3, which made the particles one-dimensional (the diameter) with respect to internal heat transfer. Milled wood particles were obtained by extensive milling of the wood cylinders followed by sieving (using sieves of 0.08−2.4 mm) into several fractions. The size of the milled wood (L_s) is herein defined as the middle value of the upper and lower size limits of the sieve meshes. This definition of the particle size is about the same as that of Shen[15] used to allow for comparison. It must be noted that the smallest dimension of a particle in a certain sieve fraction, the one being most important for heat transfer, can be smaller than the size of the smallest sieve. The shape of the milled wood particles can vary a lot and is difficult to define. From microscope analysis, it became clear that most milled particles have rectangular or (almost) round shapes. The effects of the wood geometry on pyrolysis has been studied by comparing the pyrolysis product yields of wood cylinders and milled particles of varied sizes.

The effect of the microstructure of milled particles and wood cylinders on the char yield was also studied. The microstructures used in our work are schematically visualized in Figure 1. For wood cylinders, the microstructure consists of longitudinal channels (cells). The outflow of vapors, aerosols, and gases is anisotropic; these products leave the biomass mainly via the channels. Figure 2 shows that for the milled particles of 1 mm the wood still consist of channels. Milled particles of around 0.1 mm, however (shown in Figure 3), consist only of cell wall material. Microscope analysis of the sieve fractions showed the fractions of 0.14 mm and below only consisted of

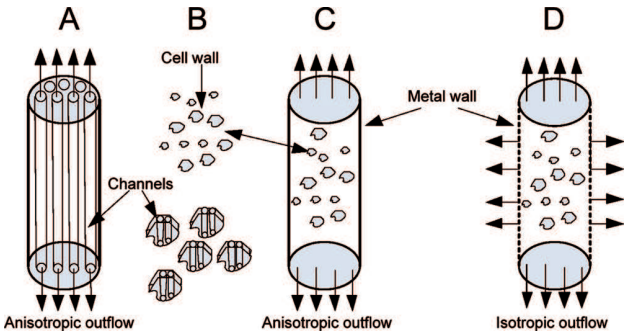

Figure 1. Particles used. (A) Wood cylinders having channels in longitudinal direction. (B) Milled particles containing channels or existing only out of cell wall material. (C) Milled particles inserted in metal cylinders with anisotropic outflow. (D) Milled particles in metal cylinders with isotropic outflow. Arrows out of the particles indicate the direction of the outflow of produced gases, vapors, and aerosols.

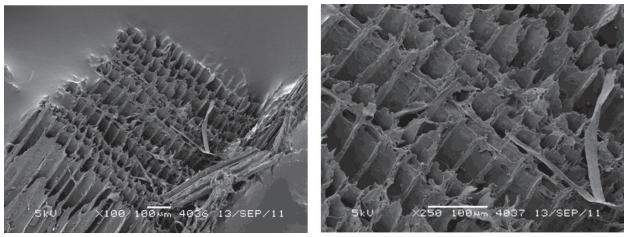

Figure 2. Scanning electron microscope (SEM) pictures of 1 mm beech wood particles.

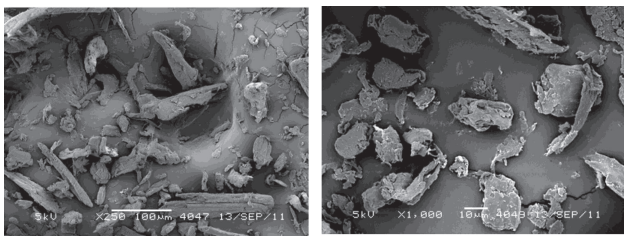

Figure 3. SEM pictures of beech wood particles smaller than 80 μm.

cell wall material. Hence, the microstructure of these particles is different compared to the cylinders and the larger milled particles.

The milled particles (<0.08 mm) are also inserted in metal (stainless steel) cylinders with a solid cylindrical wall (D_p = 0.5, 6, 10, 14 mm, internal diameter) and wire-meshes at the bottom and top. These cylinders are called further artificial solid wall (sw) cylinders. The microstructure of these artificial wood cylinders is very different compared to the natural wood cylinders: randomly packed particles versus highly structured longitudinal channels. By comparing the char yields of natural wood cylinders with those of artificial cylinders while varying the diameter, it can be evaluated whether cylinder diameter or internal microstructure is dominant with respect to the char yield.

Also artificial cylinders (filled with milled particles of 0.14 mm) completely made out of wire-mesh were used. Produced vapors, aerosols, and gases flow out of the particle in an isotropic manner. These cylinders are called further artificial wire-mesh (wm) cylinders. Comparison of the char yield of these cylinders with char yield of identical artificial cylinders with a solid cylindrical wall provides information on the importance of the outflow pattern.

Artificial wood cylinders of 0.5 mm ID and varied length (10−50 mm) were filled with small milled particles (<0.08 mm) consisting only of cell wall material. By comparing the char yields of the cylinders with different length, it is investigated if the contact time of produced vapors and aerosols with char has influence on the char yield.

dx.doi.org/10.1021/ef201688n | Energy Fuels 2012, 26, 2274−2280

Comparing the results of these artificial cylinders to natural particles of 0.5 mm gives information on the influence of the microstructure.

Preparation and Characteristics of the Metal Cylinders. Metal walled cylinders with varied diameter were prepared. The bottom and top of the solid wall cylinders were covered with wire-mesh to ensure the anisotropic outflow of vapors. The cylinders with a diameter (ID) of 6, 10, and 14 mm had a constant length of 50 mm. The length of the 0.5 mm artificial metal cylinder was varied between 50 and 10 mm. The solid cylindrical wall was made of a double layer of 0.025 mm thick metal foil and the 0.5 mm internal diameter cylinder was made of a 0.25 mm thick metal wall. The thermal resistance of the metal walls can be neglected ($\alpha > 10^4$ W/(m^2 K)) with respect to heating of the particle if the contact between the metal wall and the internal milled particles is sufficient. For the artificial cylinders of 6 mm and more, the mass of metal represents less than 0.1% of the total mass and can be also neglected. The mass of metal of the 0.5 mm artificial cylinders is >99% of the total mass leading to slower heating as compared to the 0.5 mm milled particle.

The overall density of the wood inside the artificial cylinders was set to 660 kg/m^3 (mass wood/internal volume artificial cylinder); identical to the natural wood cylinders.

Wood cylinders of 14 mm were inserted in the solid wall and wire-mesh steel cylinders with an internal diameter of 14 mm. After pyrolysis of the wood cylinder, both fed as wood cylinder and inside the metal cylinders, the char yield was determined. By comparing the char yields of the wood cylinders enclosed by the wire-mesh and solid wall cylinders with the separately pyrolyzed wood cylinders, possible heat transfer limitations and/or catalytic effects of the stainless steel cylinder walls became visible. The char yield of the wood cylinders and wood cylinders of the same size inserted in the artificial solid wall and wire-mesh cylinders was identical, 23.0, 23.1, and 23.0 wt %, respectively. Hence, no influence on the heating rate nor catalytic effects of the metal wall of the artificial wood cylinder was observed.

In another experiment, the heating rate of the 14 mm wood and artificial cylinder filled with milled particles in a fluidized bed at 500 °C was measured with a thermocouple inserted in the center of the cylinders. The initial heating rate (2.5 °C/s) and the time to reach 95% of the fluid bed temperature (210 s) of the wood and artificial cylinder filled with milled particles turned out to be nearly the same. It can be concluded that also the milled particles have sufficient contact with the wall of the artificial wood cylinder to experience an equal heating rate as the wood cylinder.

The mesh used for the artificial cylinders (wall in wire-mesh cylinder and bottom, top in both cylinders) was 9 μm. Because of the possible attrition of char inside the wire-mesh and solid cylindrical wall cylinders during the pyrolysis experiment, resulting char loss could be a problem. The char loss from the wire-mesh and solid cylindrical wall cylinders was determined experimentally, by fluidizing the cylinders filled with char for 2 h. The attrition loss of all artificial solid wall cylinders was found to be less than 0.4% of the initial char for the 140 and 300 particles. Due to too high char loss (1−3 wt %) for the artificial wire-mesh cylinders including milled particles of <80 μm, experiments with these smallest sizes (<80 μm) were only performed with solid wall cylinders. No sand entered the wire-mesh cylinders, as determined by measuring the ash content of the char before and after the 2 h experiments. No difference between the ash contents per unit weight char was found. Experiments with the artificial cylinders were always performed in triplicate to check the reproducibility.

Experimental setup. Fast pyrolysis experiments were performed in a fluidized bed reactor made of stainless steel and placed in an electric furnace. The setup used is shown in Figure 4. The reactor temperature was kept at 500 °C for all experiments. The incoming fluidization gas (nitrogen) was preheated to 500 °C.

As bed material 1 kg silica sand with a particle size of 212−300 μm was used. This size fraction was used in order to prevent entrainment of sand particles from the reaction section into the bio-oil recovery section of the setup, while minimizing the required volumetric flow of fluidization gas. The nitrogen flow was set to 12 normal L/min, resulting in a vapor/gas residence time of less than 2 s in the hot part of the setup.

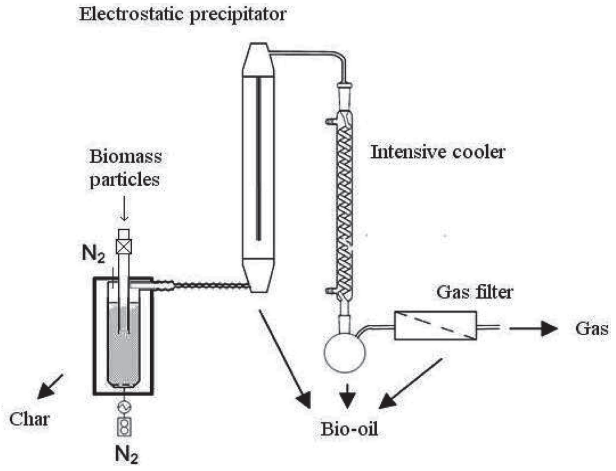

Figure 4. Fluidized bed fast pyrolysis setup: (1) feeding system, (2) reactor bed, (3) filter at the reactor outlet, (4) electrostatic precipitator, (5) intensive cooler, (6) gas filter, (7) gas analyzer .

One hundred grams of milled particles or wood cylinders was fed manually in batches of 4−8 g together with 2 g sand with a valve system into the fluidized bed reactor. The temperature drop of the reactor bed during feeding of the cold wood/sand mixtures never exceeded 10 °C.

A 5 μm filter at the reactor outlet was used to remove char/ash from the hot pyrolysis vapors. The pyrolysis liquid was collected by two sequential condensers. The first condenser was an electrostatic precipitator (ESP) operated at 17−21 kV and cooled externally with tap water at 20 °C. The remaining vapors, mostly lights, were further led to a glass wall intensive cooler (IC) operated at −5 °C. A tubular cotton gas filter (10 μm) was introduced to capture the remaining liquid. A dry gas meter was used to measure the gas flow before it was sent to the main ventilation system. A more detailed description of the setup can be found elsewhere.[24] The only modification in this study is the replacement of the continuous feeding system by a 2-valve, batchwise feeding system. The first valve (upper one) is opened to fill the tube above the second valve (lower one) with the feedstock. After filling, the first valve is closed and the second valve is opened to feed the feedstock to the reactor. No gas could escape to the environment in this closed system.

For experiments with sawdust and wood cylinders, the whole setup was used. An important feature of the setup is that it can facilitate enough biomass particle residence time, even for the 14 mm cylinders, to achieve full conversion. The total liquid yield was determined gravimetrically by weighing the condensers and the gas filter before and after the experiments. Gas samples were taken frequently (10 times) during the experiments, and the gas composition was determined. On the basis of the GC analysis and the known amount of nitrogen added, the produced noncondensable gases could be calculated. The char yield was measured as the difference between the bed and filter mass before and after experiments.

For the experiments with the artificial cylinders, only the char yield was determined as the small number of three cylinders fed to the reactor is insufficient for accurate oil and gas yield determination. The experiments with the artificial cylinders were performed in triplicate to ensure good reproducibility of the obtained char yields.

After the ESP, the remaining gases and vapors were sent to the main ventilation system. The operating conditions of the batch pyrolysis unit are summarized in Table 1.

Analysis. The water content of the oil is determined by Karl Fischer titration. Hydranal Composite 5 was used as titer. The elemental composition of the different wood cylinders and milled particles is determined by an elemental analyzer EA 1108 CHNS-O. The composition in terms of carbon, nitrogen, hydrogen, and oxygen (calculated) was obtained. Gas samples were analyzed in a gas chromatograph for H_2, CH_4, CO, CO_2, C_2H_4, C_2H_6, C_3H_6, C_3H_8

Table 1. Operating Conditions of the Batch Pyrolysis Unit

operating conditions pyrolysis unit	beech wood	dimension
experimental run time	30	min
mass sand	1.1	kg
diameter sand	212−300	μm
mass wood fed	100	g
total mass milled particles in artificial cylinders fed	0.07 − 16	g
bed height	0.20	m
U/U_{mf}	2−3	
residence time vapors	<2	s
temperature reactor bed	500	°C
temp gas out first condenser	20	°C
temp gas out intensive cooler	−5	°C

(Varian Micro GC CP-4900 with two analytical columns, 10 m mole sieve 5A and 10 m PPQ, using Helium as a carrier gas).

The water insolubles are determined by a cold water precipitation method described by Garcia-Perez.[25] The content of Solids[6] (char and traces of some possibly entrained sand) were determined by gravimetric analysis. The ash content of the biomass was determined by NPR-CEN/TS 15403-550 °C. The levoglucosan content in the pyrolysis oil was determined by HPLC (p.n. PL1170-6820 Agilent Technologies), Column PL Hi-PLex-Pb 9 μm, 7.7 × 300 mm. The eluent used was DDI water (0.6 mL/min). The injection volume was 10 μL, and the temperature of the column was 70 °C. The HPLC detectors used were the RID (55 °C) and VWD (210 nm).

RESULTS

Pyrolysis experiments were conducted on milled wood particles (d_p = 0.25−2.5 mm) and wood cylinders (d_c = 2−14 mm, l = 50 mm.). The obtained closure of the mass balances was always between 92% and 97%. Pyrolyzing very small particles of ≤0.3 mm in a fluidized bed reactor is difficult. Therefore, three identical experiments with these small particles were performed to check its reproducibility. The product yields were as follows: oil 71% ± 1%, gas 15% ± 1%, char 10% ± 1% showing that the experiments could be reproduced well. Only the pyrolysis of <0.08 mm particles led to major experimental difficulties. Therefore, the pyrolysis data of the <0.080 mm particles is excluded from this research. The terminal falling velocity (26 cm/s) of the 0.3 mm beech wood particles was always much higher than the applied fluidization velocity (8 cm/s). Because of the filter installed at the reactor outlet, the partly decomposed biomass will remain in the reactor anyway and decomposes further at 500 °C. Large particles >6 mm can float on the top of the bed, but if they do the heat transfer rate is still high enough to achieve fast pyrolysis because of the hot sand splashing at the top of the fluid bed. A detailed study on this phenomenon is described elsewhere.[14] The 9 μm solid filter positioned in the outlet of the reactor worked well. The amount of solids in the pyrolysis oil never exceeded the 0.05 wt % and there were no operational problems. The experiments with the artificial wood cylinders were always performed in triplicate. The standard deviation between the char yields of experiments of identical artificial cylinders was always smaller than 0.3%.

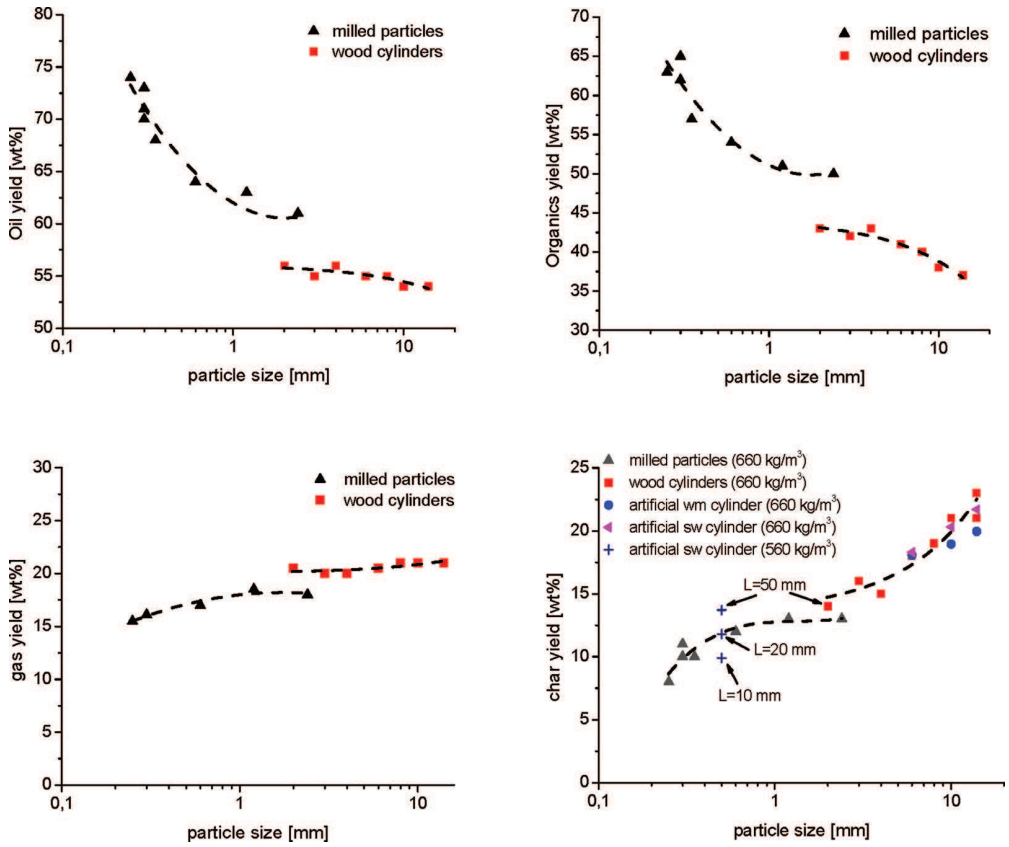

Figure 5. Pyrolysis oil, organics in pyrolysis oil, gas, and char yields are plotted as functions of the particle size. The char yield of the artificial solid wall (sw) and wire-mesh (wm) cylinders are plotted as a function of various sizes. The length of the artificial and wood cylinders was 50 mm. Only for the 0.5 mm cylinder was the length varied between 10 and 50 mm.

dx.doi.org/10.1021/ef201688n | Energy Fuels 2012, 26, 2274−2280

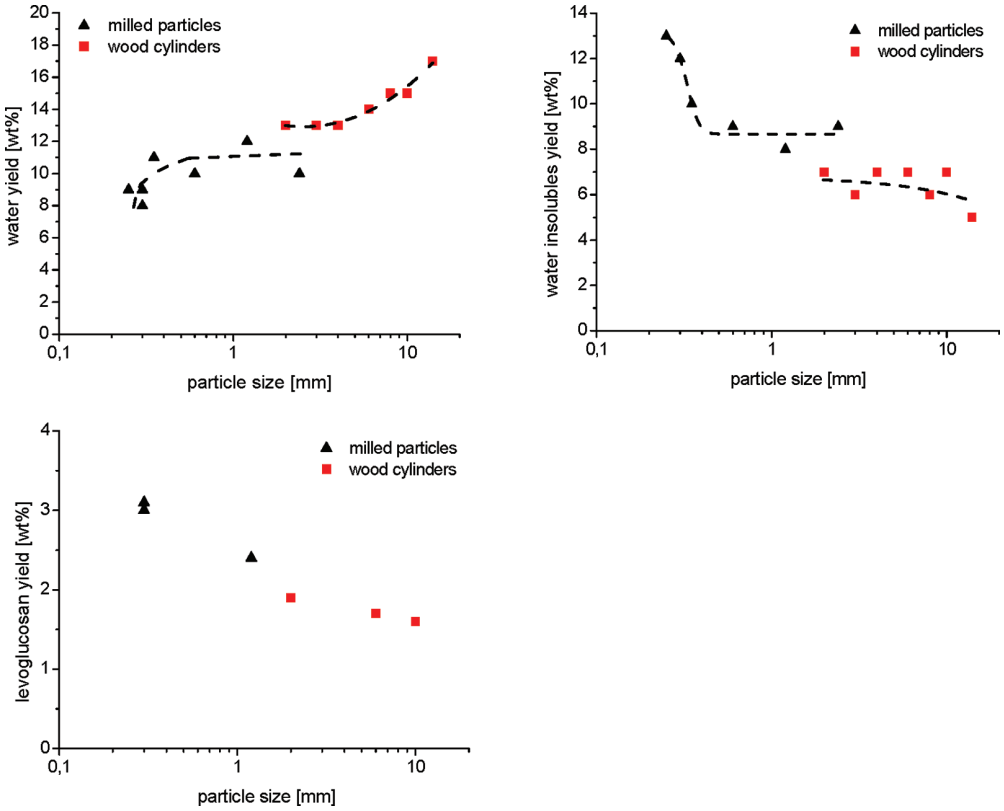

Figure 6. Yields of water, levoglucosan, and water insolubles as functions of the milled particle and wood cylinder size.

In Figure 5, the pyrolysis oil, organics in the pyrolysis oil, gas, and char yields are plotted versus the milled particle and wood cylinder size. In Figure 5, also the char yields of the artificial cylinders with solid and wire-mesh wall are included. Figure 6 shows the water, levoglucosan, and water insolubles yield as functions of the particle size.

According to Figures 5 and 6, for wood cylinders with a diameter between 2 and 14 mm, the yields of pyrolysis oil and gas is almost constant, while the yield of char and water increases as the particle size is increased. The organics yield remains almost constant between 2 and 5 mm and decreases as the wood cylinder diameter is further increased. These results are in line with the results obtained by Wang[14] for pine wood cylinders. The yields of levoglucosan and water insolubles only slightly decrease with the size of the wood cylinders between 2 and 14 mm.

A discontinuity between all the product yields obtained from wood cylinders and milled particles can be seen between 2 and 2.4 mm: the milled particles have higher oil and organics yields and lower char and gas yields. An explanation could be the shorter length of the milled particles compared to the wood cylinders. Another explanation is faster heating rates of the milled particles because of smaller aspect ratios and the presence of particles with smaller characteristic heat transfer lengths compared to the sieve size. A third explanation could be partial destruction of the particles by milling resulting in different microstructures compared to the wood cylinders[15] (see Figures 2 and 3).

For the milled particles, the pyrolysis oil, organics in the oil, levoglucosan, and water insolubles yields decrease rapidly as the particle size increases from 0.25 to 1 mm. The char yield increases drastically when the particle size is increased, while a less sharp increase in water and gas yield is observed. As the size of the milled particles is further increased from 1 to 2.4 mm, the decrease and increase of these aforementioned products tend to level off. It should be noted that similar results were obtained by Chen for milled particles of mallee wood.[15]

The sharp decrease in the yields of pyrolysis oil and organics in the pyrolysis oil as the milled particle size is increased from 0.25 to 1 mm could be caused by differences in microstructures. As can be seen from Figures 2 and 3, for very small particles only cell wall material is visible while the 1 mm particles still have the original structure of the wood cells containing wood channels.

During pyrolysis of only the cell wall material (Figure 3), resulting droplets can vaporize much faster than inside a channel of a large particle. Slower vaporization processes of droplets under high temperature pyrolysis conditions result in the formation of more char by cross-linking reactions instead of the outflow of produced vapors/aerosols from the reaction particle(s). This outcome is underpinned by a lower yield of high boiling point molecules like the water insolubles for the larger milled particles and an increasing yield of water, a component that is known to be formed as a side product of cross-linking and polycondensation reactions. This competition between the formation of char and the release of vapors/aerosols was clearly pointed out in our previous study on stepwise pyrolysis of pine wood.[22]

It is worthwhile to mention the observation that for the smallest milled particles with diameter <0.4 mm, the sand bed turned black, while only very little char particles were visually observed after the experiment This is not observed for pyrolysis of larger biomass particles that result in clearly identifiable char

dx.doi.org/10.1021/ef201688n | *Energy Fuels* 2012, 26, 2274–2280

particles and clean sand. This could mean that "explosions" or (complete) disruption of the wood structure takes place during pyrolysis so that these particles could not be found back. Another explanation could be that very large molecules leaving the small particle as aerosol or vapor adhere or recondensate on the sand particles. Our data show (see Figure 6) that indeed more heavies (water-insolubles) are produced from the smallest particles. A third explanation could be that liquid intermediates (droplets) attach to the sand by contact between the pyrolyzing biomass particle and the sand particles. From the observations made by Haas et al.,[23] it was found that these droplets originate from the middle lamella where most of the lignin fraction of the wood is situated.[26] If these droplets can find sand particles, they may adhere on these particles. A recent study on lignin pyrolysis clearly pointed out that lignin melts and adheres to the sand to eventually form lumps.[27]

Scott and Piskorz[21] reported oil yields as high as 75−80 wt % from pyrolysis of low ash Aspen-poplar and Maple. These values have been often used as reference in defining the maximal pyrolysis oil yield that can be obtained. However, these high oil yields are seldom, if at all, achieved by other researchers. In light of our results, an explanation for the high oil yields reported by Scott and Piskorz is the use of very small particles <105−250 μm, including considerable amounts of fines even smaller than 88 μm.

The gas yield decreases rapidly for particles <1 mm. For the smallest particles, pyrolysis does take place at the reactor temperature due to almost instantaneous heating. So practically the whole pyrolysis process takes place at the highest temperature. Still they have the lowest gas yields. This is rather surprising, given that most studies report that higher pyrolysis temperatures favor the production of gas.[5,17,22,28] A plausible explanation for the lower gas yield for the smallest particles is that gas is not only a product from vapor phase cracking but also a side product of cross-linking and polycondensation reactions inside the particles. For smaller particles cross-linking reactions proceed to a lesser extent indicated by a decrease in production of char and water.

Figure 5 includes the char yield data of the artificial wood cylinders as function of the cylinder diameter. First the experimental data of the artificial wood cylinders with a solid metal wall (called artificial sw cylinder in the further text and in the figure) with diameters between 6 and 14 mm are discussed and later the data of the artificial wood cylinders made completely from wire-mesh (called artificial wm cylinder in the further text and in the figure). It appears that the char yields of the artificial sw cylinder and the wood cylinders of equal diameter are comparable and could be considered equal, within the accuracy of the data. We have shown that the internal heating rate for a cylinder with a certain diameter is almost identical for the wood cylinders and the artificial sw cylinders (see the Preparation and Characteristics of the Metal Cylinders section). Hence, comparing the results for a fixed diameter should indicate the effect of the difference in microstructure. It can be concluded that the microstructure has no notable effect on the char yield of large cylinders (6−14 mm). The experimental results (see Figure 5) show that char yield of the wood and artificial wood cylinders is predominantly determined by the outer cylinder diameter; larger particles have a lower heating rate giving a lower average temperature at which the pyrolysis reactions run leading to more char.

Artificial wm cylinders with diameters of 6−14 mm, filled with 140 μm milled particles, were used to study the effect of outflow pattern by comparison with the artificial sw cylinders (isotropic vs anisotropic outflow). The hypotheses was that if vapors/aerosols can escape from the artificial cylinder in anisotropic manner, this results in overall less contact of the formed vapors/aerosols with char, because of the shorter outflow distances, and therefore less total char is produced due to less polycondensations of these vapors/aerosols on char. This is not contradicted by our data (the char yields of artificial wm cylinders of 10 and 14 mm lie below the yields of the artificial sw cylinders), but the observed effects are not very strong or may even not be real.

The length of the artificial sw cylinders with a diameter (ID) of 0.5 mm was varied between 10 and 50 mm. As can be seen from Figure 2, the milled particles of <0.08 mm inserted in the artificial cylinders only consist out of cell wall. The milled particles of 0.5 mm actually contain both particles with intact channels and some particles that consist only of cell wall material. For the 0.5 mm artificial sw cylinder with lengths of 50 and 20 mm, the char yield is higher compared to the 0.5 mm milled particles. This may be ascribed to the longer outflow distance of the vapors leading to more polymerization (char formation) on the internal milled particles, as compared with the milled particles used as such which had a length much shorter than 5 mm.

When the length of the 0.5 mm artificial sw cylinder is 10 mm, the char yield decreases further and is below the char yield of the 0.5 milled particles. This cannot be explained on basis of the outflow distance of vapors/aerosols. The length of the 10 mm (artificial sw cylinder) is much longer than the length of the 0.5 mm milled particles. If polymerization of vapors/aerosols in the pores (of the milled particles) or over the internal milled (char) particles of the artificial sw cylinder is dominant, this would lead to more char for the artificial sw cylinder. We observed the opposite experimentally. As mentioned before, the heating rate of tis artificial cylinder is considerably lower than the corresponding natural wood cylinder because of the high mass of the steel wall. Lower heating rates are typically reported to result in more char. Again, we observed the opposite. On the basis of these two observations, it is argued that, if polymerization of vapors/aerosols and heating rate are not dominating phenomena, the microstructure of the 0.5 mm artificial sw cylinder (filled with <0.08 mm milled particles) remains as an important factor controlling the char yield.

■ CONCLUSION

The effect of particle geometry and microstructure on the fast pyrolysis of beech wood was investigated in a fluidized bed reactor operated at 500 °C. When the particle size is decreased from 1 to 0.25, the pyrolysis oil yield and organic yield increases rapidly mostly due to the increase in production of levoglucosan and water insolubles. In contrast, the char and gas yield decreases rapidly. The wood microstructure is a major factor controlling the release of vapors/aerosols from the converting wood of 1−0.25 mm. For the very small particles, pure cell wall material is pyrolyzed resulting in less transport resistance of vapors/aerosols leaving the particle compared to particles that are intact and have their original cell structure which includes channels. For particles sizes between 1 and 5 mm, only little changes in all product yields were observed. When the particle size is further increased, the oil and organic yield decreases further while the char and gas yield increases. In this particle size regime, the release of the vapors is almost not

influenced by the microstructure and vapor outflow pattern, but mostly by internal heat transfer limitations.

AUTHOR INFORMATION

Corresponding Author

*E-mail: r.j.m.westerhof@utwente.nl.

Notes

The authors declare no competing financial interest.

ACKNOWLEDGMENTS

The authors wish to thank Dr. Espen Olsen of the Norwegian University of Life Sciences for the collaboration in this project. Ir. Stijn Oudenhoven and Ir. Mathijs Vos are acknowledged for their help in the experimental part of this study.

REFERENCES

(1) Oasmaa, A.; Meier, D. Norms and standards for fast pyrolysis liquids: 1. Round robin test. *J. Anal. Appl. Pyrolysis* **2005**, *73* (2), 323−334.

(2) Bridgwater, A. V., Ed. *Fast pyrolysis of biomass: A handbook*; CPL Press: UK, 2002; Vol. *2*.

(3) Westerhof, R. J. M.; Brilman, D. W. F.; Garcia-Perez, M.; Wang, Z.; Oudenhoven, S. R. G.; van Swaaij, W. P. M; Kersten, S. R. A. Fractional Condensation of Biomass Pyrolysis Vapors. *Energy Fuels* **2011**, *25* (4), 1817−1829.

(4) Westerhof, R. J. M.; Kuipers, N. J. M.; Kersten, S. R. A.; Swaaij van, W. P. M. Controlling the Water Content of Biomass Fast Pyrolysis Oil. *Ind. Eng. Chem. Res.* **2007**, *46* (26), 9238−9247.

(5) Westerhof, R. J. M.; Brilman, D. W. F.; van Swaaij, W. P. M; Kersten, S. R. A. Effect of Temperature in Fluidized Bed Fast Pyrolysis of Biomass: Oil Quality Assessment in Test Units. *Ind. Eng. Chem. Res.* **2009**, *49* (3), 1160−1168.

(6) Hoekstra, E.; Hogendoorn, K. J. A.; Wang, X.; Westerhof, R. J. M.; Kersten, S. R. A.; van Swaaij, W. P. M; Groeneveld, M. J. Fast Pyrolysis of Biomass in a Fluidized Bed Reactor: In Situ Filtering of the Vapors. *Ind. Eng. Chem. Res.* **2009**, *48* (10), 4744−4756.

(7) Oasmaa, A.; Czernik, S. Fuel Oil Quality of Biomass Pyrolysis Oils - State of the Art for the End Users. *Energy Fuels* **1999**, *13* (4), 914−921.

(8) Czernik, S.; Johnson, D. K.; Black, S. Stability of wood fast pyrolysis oil. *Biomass Bioenergy* **1994**, *7* (1−6), 187−192.

(9) Lian, J.; Chen, S.; Zhou, S.; Wang, Z.; O'Fallon, J.; Li, C.-Z.; Garcia-Perez, M. Separation, hydrolysis and fermentation of pyrolytic sugars to produce ethanol and lipids. *Bioresour. Technol.* **2010**, *101* (24), 9688−9699.

(10) de Miguel Mercader, F.; Groeneveld, M. J.; Kersten, S. R. A.; Geantet, C.; Toussaint, G.; Way, N. W. J.; Schaverien, C. J.; Hogendoorn, K. J. A. Hydrodeoxygenation of pyrolysis oil fractions: process understanding and quality assessment through co-processing in refinery units. *Energy Environ. Sci.* **2011**, *4* (3), 985−997.

(11) Mohan, D.; Pittman, C. U.; Steele, P. H. Pyrolysis of Wood/Biomass for Bio-oil: A Critical Review. *Energy Fuels* **2006**, *20* (3), 848−889.

(12) Bridgwater, A. V.; Meier, D.; Radlein, D. An overview of fast pyrolysis of biomass. *Org. Geochem.* **1999**, *30* (12), 1479−1493.

(13) Venderbosch, R. H.; Prins, W. . *Bioprod. Biorefin.* **2010**, *4*, 178−208.

(14) Wang, X.; Kersten, S. R. A.; Prins, W.; van Swaaij, W. P. M Biomass Pyrolysis in a Fluidized Bed Reactor. Part 2: Experimental Validation of Model Results. *Ind. Eng. Chem. Res.* **2005**, *44* (23), 8786−8795.

(15) Shen, J.; Wang, X.-S.; Garcia-Perez, M.; Mourant, D.; Rhodes, M. J.; Li, C.-Z. Effects of particle size on the fast pyrolysis of oil mallee woody biomass. *Fuel* **2009**, *88* (10), 1810−1817.

(16) Salehi, E.; Abedi, J.; Harding, T. Bio-oil from Sawdust: Effect of Operating Parameters on the Yield and Quality of Pyrolysis Products. *Energy Fuels* **2011**, *25* (9), 4145−4154.

(17) Scott, D. S.; Piskorz, J.; Bergougnou, M. A.; Graham, R.; Overend, R. P. The role of temperature in the fast pyrolysis of cellulose and wood. *Ind. Eng. Chem. Res.* **1988**, *27* (1), 8−15.

(18) Kersten, S. R. A.; Wang, X.; Prins, W.; van Swaaij, W. P. M. Biomass Pyrolysis in a Fluidized Bed Reactor. Part 1: Literature Review and Model Simulations. *Ind. Eng. Chem. Res.* **2005**, *44* (23), 8773−8785.

(19) Di Blasi, C.; Branca, C. Temperatures of Wood Particles in a Hot Sand Bed Fluidized by Nitrogen. *Energy Fuels* **2002**, *17* (1), 247−254.

(20) Chaiwat, W.; Hasegawa, I.; Tani, T.; Sunagawa, K.; Mae, K. Analysis of Cross-Linking Behavior during Pyrolysis of Cellulose for Elucidating Reaction Pathway. *Energy Fuels* **2009**, *23* (12), 5765−5772.

(21) Scott, D. S.; Piskorz, J. The flash pyrolysis of aspen-poplar wood. *Can. J. Chem. Eng.* **1982**, *60* (5), 666−674.

(22) Westerhof, R. J. M. Refining fast pyrolysis of biomass chapter 3: Step-wise pyrolysis of pine wood. Thesis, Univeristy of Twente, December 2011. ISBN: 978-94-6191-124-7.

(23) Haas, T. J.; Nimlos, M. R.; Donohoe, B. S. Real-Time and Post-reaction Microscopic Structural Analysis of Biomass Undergoing Pyrolysis. *Energy Fuels* **2009**, *23* (7), 3810−3817.

(24) Hoekstra, E.; Westerhof, R. J. M.; Windt, M.; Brilman, D. W. F.; van Swaaij, W. P. M.; Kersten, S. R. A.; Hogendoorn, K. J. A. Heterogeneous and homogeneous reactions of pyrolysis vapors from pine wood. *AIChE J* **2011**, DOI: 10.1002/aic.12799.

(25) Garcia-Perez, M.; Chaala, A.; Pakdel, H.; Kretschmer, D.; Roy, C. Characterization of bio-oils in chemical families. *Biomass Bioenergy* **2007**, *31* (4), 222−242.

(26) Hillis, W. E. Wood and biomass ultra-structure. In *Fundamentals of thermo-chemical biomass conversion*; Overend, R. P., Milne, T. A., Mudge, L. K., Eds.; 1982.

(27) Nowakowski, D. J.; Bridgwater, A. V.; Elliott, D. C.; Meier, D.; de Wild, P. Lignin fast pyrolysis: Results from an international collaboration. *J. Anal. Appl. Pyrolysis* **2010**, *88* (1), 53−72.

(28) Garcia-Perez, M.; Wang, X. S.; Shen, J.; Rhodes, M. J.; Tian, F.; Lee, W.-J.; Wu, H.; Li, C.-Z. Fast Pyrolysis of Oil Mallee Woody Biomass: Effect of Temperature on the Yield and Quality of Pyrolysis Products. *Ind. Eng. Chem. Res.* **2008**, *47* (6), 1846−1854.

Paper III

Nygård, Heidi S.; Danielsen, Filip; Olsen, Espen. Thermal History of Wood Particles in Molten Salt Pyrolysis. *Energy & Fuels* 2012, 26 (10), 6419-6425.

energy&fuels

Article

pubs.acs.org/EF

Thermal History of Wood Particles in Molten Salt Pyrolysis

Heidi S. Nygård,* Filip Danielsen, and Espen Olsen

Department of Mathematical Sciences and Technology, Norwegian University of Life Sciences, 1432 Ås, Norway

ABSTRACT: Molten salt pyrolysis is a thermochemical conversion process in which biomass is fed into and heated up by a molten salt bath. Molten salts have very high thermal stability, good heat transfer characteristics, and a catalytic effect in cracking and liquefaction of large molecules found in biomass. In this study, the heat transfer characteristics of molten salts are studied by recording the thermal history of wood particles in molten salt pyrolysis. Experiments have been carried out with cylindrical beech and pine wood particles with constant length (L = 30 mm) and varying diameter (d = 1−8 mm) in a FLiNaK melt with a temperature of 500 °C. The thermal history at the particle center has been used to evaluate the reaction temperatures, the heating rates, and the devolatilization times. Results have been compared with a similar study in a fluidized sand bed. It is found that FLiNaK gives significantly higher heating rates for cylinders with $d \leq 4$ mm. For larger cylinders, the process is dominated by heat transfer within the wood particle, and the heat transfer medium is of less importance. For the smallest cylinders (d = 1 mm), heating rates as high as 218 ± 6 and 186 ± 15 °C/s were observed for beech and pine wood, respectively. The average heating rate for wood cylinders until the main degradation takes place has been found to follow the empirical correlation $\beta = (k_{\text{eff}}/\rho)10^3(24 + 390\ e^{-0.49d})$, and the total devolatilization time has been found to follow the empirical correlation $t_{\text{dev}} = \rho(0.146\ e^{-k_{\text{eff}}} - 1.09)d^{1.05}$.

INTRODUCTION

With increasing energy consumption and greater environmental concerns, research on renewable energy has gained more attention in the last years. While renewable electricity has many alternatives, biomass is regarded as the main source of renewable liquid, gaseous and solid fuels.[1] Pyrolysis is a thermochemical conversion process in which biomass is heated in the absence of any oxidizing agent and is converted to a mixture of liquids (pyrolysis oil), noncondensable gases, and solid chars. In fast pyrolysis, the aim is to achieve high yields of liquids. The biomass should be heated so rapidly that it reaches the pyrolysis temperature (preferably around 500 °C) before it starts to decompose, and thus minimizes exposure to the lower temperatures that favor formation of char. A short vapor residence time of 2−3 s followed by rapid quenching of the pyrolysis vapors is also of importance.[2]

A number of laboratory reactor configurations for pyrolysis have been developed over the last 20 years, including bubbling fluid beds, circulating and transported beds, cyclonic reactors, ablative reactors, and vacuum moving beds. Several pilot plants have been constructed, in addition to a few demonstration installations.[1] A less studied approach is molten salt pyrolysis, in which the thermal decomposition of biomass is carried out in a molten salt bath. During the process, the molten salt is simultaneously used as a heat carrier, catalyst, and fluid reacting bed.[3] A review of thermal processing of biomass in molten salts has recently been published.[4] The research reviewed includes many investigations that have not so far progressed beyond the laboratory scale. It is a relatively small research area compared with traditional conversion methods, and there is clearly a need for more basic research on the subject.

Inorganic molten salts are found to have very good heat transfer characteristics, properties that make them suitable for rapid heat supply in thermal processing of biomass. They have large heat capacities and are very stable at high temperatures, and will give a stable reaction temperature throughout the process. Due to their low viscosity, the molten salts will enclose the biomass particles rapidly and also infiltrate the pores, leading to a larger particle area exposed to heating by the salt.[3]

Adinberg et al.[5] demonstrated that molten carbonates have a strong thermal impact upon pyrolysis reactions. Cellulose tablets were pyrolyzed in a eutectic mixture of K_2CO_3 and Na_2CO_3 and an increase of 20% in the reaction rates compared to in an inert gas atmosphere at 850 °C was observed. In their study, they also proposed hybridization of solar energy and bioenergy in which a concentrating solar receiver could be used to heat and melt the salt that was used in the pyrolysis process. In this way, the molten salts may provide thermal energy storage due to their high heat capacity. The process was originally considered for gasification of coal and active carbon,[6−8] but the same principles may be applied for biomass.[5]

Molten salts could also be used indirectly as a heat transfer medium in pyrolysis. In the Pyrocycling process,[9] the biomass is carried through horizontal plates and heated indirectly by a mixture of KNO_3, $NaNO_2$, and $NaNO_3$, and the produced vapors are instantly removed via a vacuum pump. The salt itself is heated by burning the noncondensable gases from the process.

Some molten salts have a catalytic effect in the decomposition of biomass, and this makes it possible to adjust the product yields and compound compositions of products by varying the composition[10] and amount of molten salts.[11] Zinc halides are found to catalyze production of single-ring aromatic compounds in thermal processing of hydrocarbons.[12] Sada et al.[10] investigated pyrolysis of lignin in a molten mixture of $ZnCl_2$ and KCl. They found that the yields of different phenolic

Received: July 5, 2012
Revised: September 4, 2012
Published: September 4, 2012

compounds depend on both the molar ratio of the two salts[10] and the salt-to-lignin ratio in the reactor.[11]

Another advantage in thermal processing of biomass in molten salts is that selected noxious contaminants are retained in the melt,[13] which makes it possible to apply the method on contaminated biomass and waste. Several studies have been reported on thermal treatment of municipal refuse,[13] plastic waste,[14−16] and organic waste.[17]

Molten salt pyrolysis has several technical challenges compared with more traditional methods. The corrosiveness of molten salts limits the choice of reactor materials.[13] An option is to use ceramic-lined vessels and pipes instead of metals. Another challenge is that the melts solidify at ambient temperatures, which complicates the startup and shutdown of the system. This could be solved by a form of storage and dump tank. When melted, however, molten salts may be easily circulated and pumped centrifugally or with gear pumps or by simple gas-lift pumps.[3]

A possible obstacle in molten salt pyrolysis is the separation of char and salt. Adinberg et al.[5] suggested in their continuous solar reactor concept that the char residue, together with some salt, could be drained out due to density differences. Hammond and Mudge[13] proposed that the char residue could be burned out of the salt and produce sufficient energy to make the process autothermal. Because of the very low vapor pressure and high boiling point, the salts will not decompose in the process. Another possibility is to add a gasifying agent and produce syngas in a separate reactor. The remaining ash in the salt may be removed electrolytically or as slag at higher temperatures.[3]

The heat transfer characteristics of molten salts have been investigated for applications other than thermal processing of biomass such as solar power towers and nuclear power plants. Among the salts studied are fluorides. Molten fluoride salts are characterized by high thermal conductivities, high specific heats, low viscosities, and high boiling points.[18] Williams[19] investigated the applicability of different fluorides, fluoroborates, and chlorides as a heat transfer fluid in nuclear plants. As a class of salts, fluorides showed to be the best heat-transfer fluids, and FLiNaK in particular showed the best heat-transfer performance. FLiNaK is a ternary eutectic alkaline metal fluoride salt mixture LiF−NaF−KF (46.5−11.5−42 mol %) with a melting point of 454 °C and a boiling point of 1570 °C.

The purpose of this study is to gain a better understanding of molten salts, particularly FLiNaK, as a heat transfer medium in the pyrolysis process. This is done by recording the thermal history undergone by wood particles. The thermal history is used to evaluate the heating rates, reaction temperatures, and devolatilization times. The results are compared with a similar study in a more "traditional" fluidized sand bed by Di Blasi and Branca.[20]

EXPERIMENTAL SECTION

Cylindrical beech and pine wood particles were used as feedstock in the pyrolysis experiments. These were chosen as representatives for hardwood and softwood, respectively. Because wood is an anisotropic material, the thermal properties vary with the direction of heat flow with respect to the fibers. The heat transfer takes place through a complex interaction between conduction of the cell wall substance and radiation and convection in the pore system. The term effective or equivalent conductivity (k_{eff}) is often introduced and is reported as either parallel (||) or perpendicular (⊥) relative to the fibers. The effective conductivity parallel is usually between 1.5 to 2.7 times higher than that perpendicular to the fibers. The effective thermal conductivities for the dry wood used in this study as reported by Grønli[21] are listed in Table 1, along with the chemical composition. The proximate and ultimate analysis are listed in Table 2.

Table 1. Properties and Chemical Composition of Dry Beech and Pine Wood[21]

	beech	pine
ρ (kg/m^3)	700	450
k_{eff} ||, (W/K·m)	3.490×10^{-1}	2.593×10^{-1}
k_{eff} ⊥, (W/K·m)	2.090×10^{-1}	9.769×10^{-2}
cellulose (%)	48	41
hemicellulose (%)	28	26
lignin (%)	22	28
extractives (%)	2	5

Table 2. Proximate and Ultimate Analysis of Dry Beech and Pine Wood

	beech[22]	pine[21]
volatile matter (wt %)	84.9	87.6
fixed carbon (wt %)	14.1	12.3
ash (wt %)	1.0	0.1
C (wt %)	42.2	46.9
H (wt %)	6.0	6.3
N (wt %)	0.2	0.1
O (wt %)	50.5	46.7

The cylinders were prepared from untreated wood sticks with the length parallel to the fibers. The cylinders with a diameter (d) of 2−8 mm had a constant length (L) of 30 mm. The length was chosen in order to always have an aspect ratio larger than 3, which makes the particles one-dimensional (1D) (the diameter) with respect to internal heat transfer.[23] This means that it is the heating perpendicular to the fibers that is measured in this study, and that k_{eff} (⊥) is of importance. The smallest cylinders (d = 1 mm) had a shorter length of L = 15 mm due to preparation difficulties, but the aspect ratio is still well within the limit for the one-dimensional requirement. The samples were dried at 105 °C for 24 h prior to the experiments.

A hole was drilled from top to the center of the cylinders where a type K thermocouple was placed for measuring the particle center temperature T. For the smallest cylinders ($d \leq 3$ mm) a 0.5 mm thermocouple was used, while for the larger particles ($d \geq 4$ mm) a 1 mm thermocouple was used. It was confirmed experimentally that the two thermocouples gave similar measurements for $d \geq 4$ mm, and the latter was chosen for practical reasons. The thermocouple was placed inside a steel tube for support.

Lithium fluoride (LiF), sodium fluoride (NaF), and potassium fluoride (KF) were purchased separately from Sigma-Aldrich, all in powder form and at least 98.5% purity (puriss). The salts were mixed mechanically to obtain the FLiNaK composition (LiF−NaF−KF: 46.5−11.5−42 mol %).

A schematic representation of the laboratory scale setup used in this study is shown in Figure 1.

The reactor was made of stainless steel and placed in an electrically resistance heated furnace for independent temperature control. The reactor temperature was kept at 500 °C for all experiments, controlled by a submerged type K thermocouple. The reactor height was 200 mm, and the inner diameter was 62 mm. 200 g of FLiNaK was placed in an inner vessel of nickel with an inner diameter of 52 mm, giving a bed height of 45 mm at 500 °C. Nickel was chosen because it is most compatible with FLiNaK with respect to corrosion.[18]

The incoming inert gas (Ar) was bubbled through the molten salt bath through a nickel tube. The Ar flow was set to 2 L/ min, giving a vapor/gas residence time of less than 3 s in the hot zone. The role of the inert gas was to ensure an inert atmosphere, remove the produced vapors from the hot reacting zone, as well as provide turbulent mixing

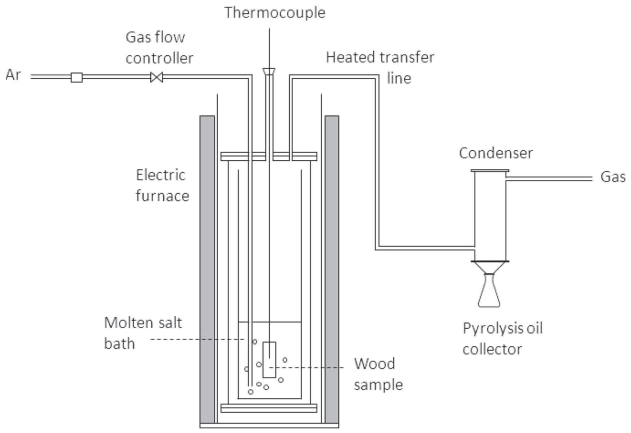

Figure 1. Schematic representation of the experimental setup for recording the thermal history of wood particles in molten salt pyrolysis.

of the salt. Turbulent mixing gives a homogeneous temperature in the reactor and enhances the heat transfer from the salt to the wood cylinders.

The samples were introduced to the molten salt reactor manually, and it was ensured that the wood particles were completely submerged in the molten salt bath during the experiments. The temperature was measured at a frequency of twice per second. Each experiment was performed at least three times to ensure reproducibility.

The produced pyrolysis vapors were led through a 4 mm heated transfer line (450 °C) and into a water cooled condenser where the pyrolysis oil could be collected. However, due to inadequate amounts, it was not possible to weigh and determine the pyrolysis oil yields in this study. After the condenser, the remaining gases and vapors were vented.

After the pyrolysis reactions were completed, the power was turned off, and the reactor and sample were left under Ar flow until the temperature was lowered to ambient temperature.

■ RESULTS AND DISCUSSION

Figure 2 shows a pine wood cylinder (d = 6 mm) before and after pyrolysis in FLiNaK at 500 °C. The shape remains the same after the pyrolysis process. The solid residues were very brittle, but they were, in most cases, still left on the thermocouple after the experiment was conducted. They were covered with salt, and it was also observed that the salt had infiltrated the samples. The charred particles could be burned to give heat to the process. The salts will remain unaffected due to the very low vapor pressure and high boiling point and could be recirculated.[13]

Figure 2. 6 mm pine wood cylinder before (left) and after (right) pyrolysis in FLiNaK at 500 °C. The solid residue is covered and infiltrated with salt.

Definitions. The temperature profile was recorded for all cylinders, and the heating rate was calculated using three point estimation. The graphical results for beech wood with d = 6 mm are shown as an example in Figure 3. We have chosen to follow the definitions of the characteristic points for the thermal behavior as given by Di Blasi and Branca[20] in order to compare the results. They studied pyrolysis of beech wood cylinders (L = 20 mm, d = 2−10 mm) in a hot sand bed (T = 534 °C) fluidized by nitrogen. The temperature was measured by a type K thermocouple (0.5 mm) in the center of the wood cylinders. Their results showed that the different pyrolysis stages have a strong influence on the heating rate at the particle center and that the pyrolysis in a fluidized bed is controlled by the rate of internal heat transfer under the studied conditions.

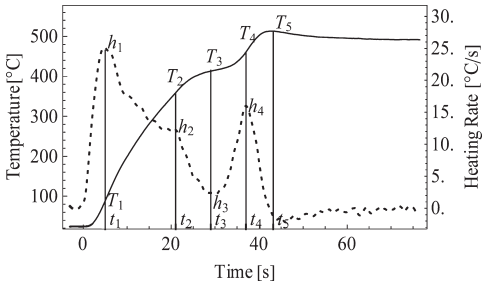

Figure 3. Temperature profile and calculated heating rate in the center of beech wood (d = 6 mm) at reactor temperature T = 500 °C as an example for the definitions of characteristic points in the thermal history of wood particles in molten salt pyrolysis.

The first characteristic point represents the maximum heating rate (h_1). This is the point where degradation starts in the outer part of the cylinder. The inward heat transfer is hindered, resulting in a decrease in the heating rate. The maximum heating rate is important because it is measured before any reactions occur, and it is therefore a way of measuring the heat transfer characteristics of the heat transfer medium.

The second characteristic point is a point of high variation in the heating rate (h_2). This represents the beginning of the endothermic degradation of cellulose and hemicellulose in the particle center.

The local minimum heating rate (h_3) represents the main degradation of cellulose and hemicellulose in the particle center. The corresponding reaction temperature T_3 is practically constant for a short while. According to Antal and Varhegyi,[24] the endothermic degradation of cellulose and hemicellulose is completed before the slower, high-temperature exothermic degradation of lignin starts. Since cellulose and hemicellulose contributes to up to 67 and 76% of the mass of pine and beech wood, respectively (Table 1), T_3 could be regarded as representative of the effective pyrolysis temperature.[25]

The main lignin degradation is represented by an increase in the heating rate. This reaction is slower, exothermic, and occurs over a wider temperature range.[24] Thus, it is not possible to define a clear reaction temperature such as for cellulose and

dx.doi.org/10.1021/ef301121j | Energy Fuels 2012, 26, 6419−6425

hemicellulose.[25] A local maximum of the heating rate is observed (h_4) when the lignin degradation slows down. For thick particles, this is the time when conversion is about 95%.[25] A maximum temperature (point 5) higher than the reactor temperature is attained due to the exothermic degradation of lignin. At this point, the conversion process is practically terminated, and t_5 is regarded as the total devolatilization time.

Temperature Profiles and Reaction Temperatures. The temperature profiles at the particle center for various cylinder diameters are shown in Figure 4. The beech and pine wood cylinders are represented by black and red lines, respectively, and one representative curve is chosen for each cylinder diameter. As expected, it can be clearly seen that, as the particle diameter increases, the time required reaching the characteristic points increases. The shape of the temperature profiles is qualitatively the same, with a plateau of nearly constant temperature where the main degradation of cellulose and hemicellulose occur. A higher maximum temperature than the reactor temperature is observed due to the exothermic degradation of lignin, and this is more evident for the thicker particles due to the higher mass of lignin and the longer time for the gases to escape from the particle. The higher thermal conductivity of beech wood (Table 1) is reflected as the beech wood cylinders reach the different stages faster than pine wood cylinders with the same dimensions.

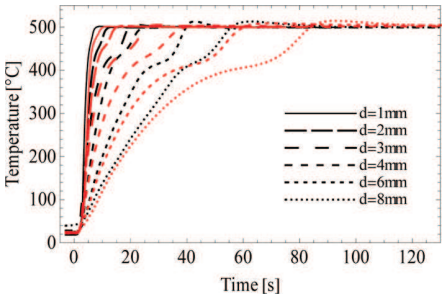

Figure 4. Temperature profiles at the particle center for beech (black) and pine (red) wood for various cylinder diameters in FLiNaK. The reactor temperature is 500 °C.

Figure 5 shows the characteristic temperatures for beech wood cylinders (black lines) and pine wood cylinders (red lines) as a function of cylinder diameter. A high scatter is observed for T_1 for small particles of both wood types. This could be due to the very high heating rates observed (Figure 6), making it difficult to evaluate the corresponding temperature accurately. Temperature measurements with higher sampling frequency would possibly have given less variance. The scatter could also be due to variations with respect to growth rings between such small samples. The values are, however, included in the results to show the trends.

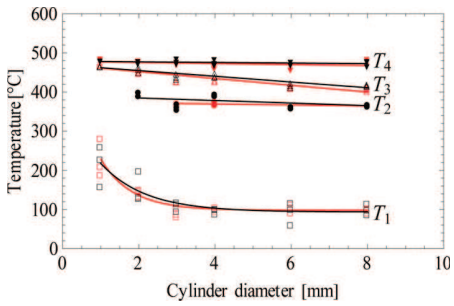

Figure 5. Characteristic temperatures at the particle center for beech (black) and pine (red) cylinders as functions of the cylinder diameter in FLiNaK at 500 °C.

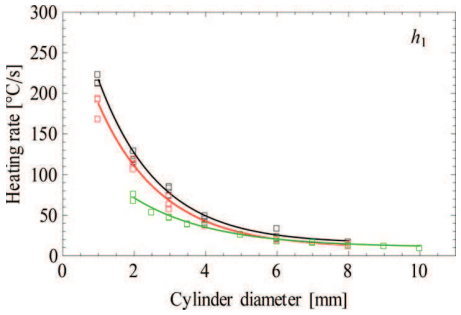

Figure 6. Maximum heating rate h_1 at the particle center for beech (black) and pine (red) cylinders in FLiNaK at 500 °C. Reference values (green) are estimated for beech wood cylinders in fluidized sand bed at 534 °C.[20]

Both T_2 and T_4 are practically independent of the cylinder diameter.

T_3 represents the effective pyrolysis temperature, where most of the cellulose and hemicellulose decompose.[25] The effective pyrolysis temperature affects the yields in pyrolysis. In fast pyrolysis, the goal is to reach a high temperature before the biomass starts to decompose in order to maximize the liquid fraction.[2]

The effective pyrolysis temperature in this study decreases as the particle size is increased, from 469 ± 4.5 °C for d = 1 mm to 412 ± 6.5 °C for d = 8 mm. This is in close agreement with the 1D model simulations for biomass pyrolysis in a fluidized bed reactor at 500 °C by Kersten et al.[23] The simulations also showed that the particle size only had a minor effect of the total liquid yield up to 20 mm (corresponding to an effective pyrolysis temperature down to 400 °C). This was also confirmed experimentally.[26] However, for particles larger than 3 mm, the water content of the produced pyrolysis oil increased substantially.

An interesting observation is that even though the two wood types reach the characteristic points at different times, the reaction temperatures are comparable. This means that the thermal properties of the wood particle play a less important role than the particle size for the reaction temperatures in the pyrolysis process.

Heating Rates. The characteristic heating rates (h_1–h_4) as a function of cylinder diameter are shown in Figures 6–9. Beech wood cylinders are represented by black lines and pine wood cylinders by red lines. Results for fluidized sand bed are estimated from Di Blasi and Branca[20] (green lines). h_2 could not be determined for d = 1 mm for beech wood and $d \leq 2$ mm for pine wood and is therefore not plotted in Figure 7. A general observation is that all of the characteristic heating rates at the particle center become slower as the particle size increases due to the increasing internal heat transfer resistance inside the wood cylinders. For molten salt pyrolysis, the values are always slightly higher for beech than pine wood for otherwise identical conditions. This is due to the higher conductivity of the former.

The maximum heating rate (h_1) decreases exponentially with the cylinder diameter for all types (Figure 6). For the smallest cylinders (d = 1 mm), heating rates as high as 218 ± 6 and 186

dx.doi.org/10.1021/ef301121j | Energy Fuels 2012, 26, 6419–6425

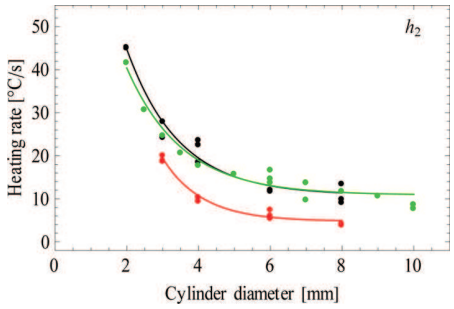

Figure 7. Point of high variation of the heating rate h_2 at the particle center for beech (black) and pine (red) cylinders in FLiNaK at 500 °C. Reference values (green) are estimated for beech wood cylinders in fluidized sand bed at 534 °C.[20]

± 15 °C/s were found for beech and pine wood, respectively. It is further observed that the maximum heating rates in molten salt pyrolysis are significantly higher than in fluidized sand bed for cylinders with $d \leq 4$ mm. For the smaller particles, the properties of the heat transfer medium dominate the process, while the properties of the wood limit the heat transfer for the larger particles.

The heating rates at the start of the degradation of cellulose and hemicellulose (h_2) are not significantly different for beech wood in molten salt and fluidized sand bed (Figure 7). The same could be said about the local minimum heating rate (h_3, Figure 8). This could be because cellulose and hemicellulose

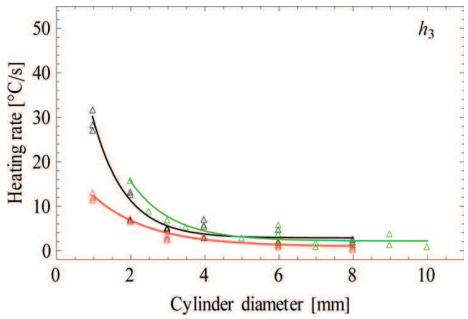

Figure 8. Local minimum heating rate h_3 at the particle center for beech (black) and pine (red) cylinders in FLiNaK at 500 °C. Reference values (green) are estimated for beech wood cylinders in fluidized sand bed at 534 °C.[20]

degrade over a very narrow range of temperatures,[27] and the process is less dependent on external factors such as the heat transfer medium and the reactor temperature. Both characteristic heating rates are, however, strongly dependent on internal factors such as the cylinder diameter and the wood type. Beech wood contains more cellulose and hemicellulose than pine wood (Table 1), and this will affect h_2 and h_3. Both h_2 and h_3 decrease exponentially with cylinder diameter, but not as prominently as h_1. The decrease is due to heat transfer limitations within the particle, but it could also be due to higher amounts of degrading cellulose and hemicellulose. The endothermic reactions will have a cooling effect on the sample.

The effects of external factors are more visible in the local maximum heating rates (h_4, Figure 9). Lignin decomposes over a wider range of temperatures[24] and is more dependent on external factors. This could also be the reason why more scatter is observed in h_4 for all types. The values for fluidized sand are

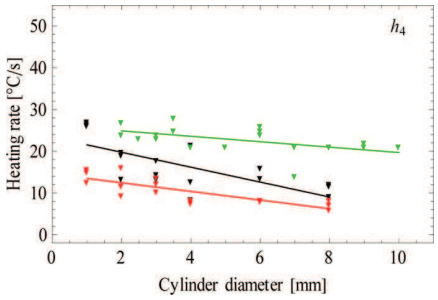

Figure 9. Local maximum heating rate h_4 at the particle center for beech (black) and pine (red) cylinders in FLiNaK at 500 °C. Reference values (green) are estimated for beech wood cylinders in fluidized sand bed at 534 °C.[20]

in this case higher than those for molten salt. This could be due to the higher bed temperature in the study by Di Blasi and Branca (534 vs 500 °C). h_4 shows a less dependence on the cylinder diameter, but a small decreasing trend is observed. The differences between the wood types are ascribed to the differences in the lignin content (Table 1).

Another approach to measure the heating rate in pyrolysis is the average heating rate until the main degradation of cellulose and hemicellulose occur:[25]

$$\beta = \frac{(T_3 - T_0)}{t_3} \quad (1)$$

where T_0 is the initial temperature.

For pyrolysis of wood cylinders in FLiNaK at 500 °C, it has been found that β may be correlated empirically to the initial diameter and the wood properties by

$$\beta = \frac{k_{\text{eff}}}{\rho} 10^3 (24 + 390\, e^{-0.49d}) \quad (2)$$

with the values for ρ and k_{eff} ($\perp$) as given in Table 1. The experimental data and the empirical correlations show a very good agreement (Figure 10).

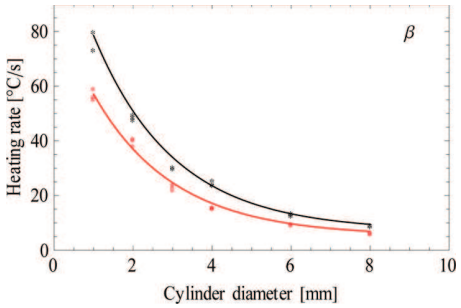

Figure 10. Average heating rate β at the particle center for beech (black) and pine (red) cylinders in FLiNaK at 500 °C. Symbols are for the experiments and solid lines for the empirical correlation given by eq 2.

Characteristic Times and Total Devolatilization Time. The characteristic heating times for beech wood cylinders (black lines) and pine wood cylinders (red lines) as a function of cylinder diameter are shown in Figure 11. The characteristic heating times follow a power law dependence on the cylinder diameter for both wood types. The times to reach the highest heating rate (t_1) are practically the same for beech and pine

dx.doi.org/10.1021/ef301121j | Energy Fuels 2012, 26, 6419−6425

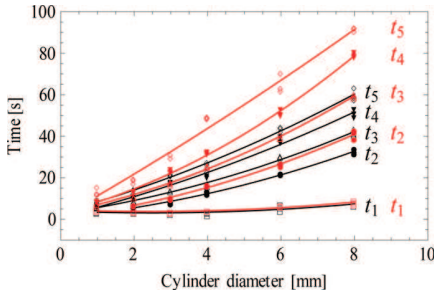

Figure 11. Characteristic heating times at the particle center for beech (black) and pine (red) cylinders as functions of the cylinder diameter in FLiNaK at 500 °C.

wood. As already discussed, the first characteristic point is measured before any reactions occur and depends mainly on the heat transfer characteristics of FLiNaK. For the remaining heating times, it is clear that beech wood conducts the heat to the particle center faster than pine wood.

Prediction of the total devolatization time (t_{dev}) in pyrolysis is important for reactor design. For coal particles, an empirical correlation for the effect of initial particle size is typically given by a power-law relation in the form of[28]

$$t_{dev} = Ad^n \tag{3}$$

where A and n are fitted to match the experimental data. Values for n typically range between 1 and 2. The variations reported in literature are believed to be caused by different experimental conditions and definitions of devolatilization time.[28] The same empirical correlation has been shown to be applicable for pyrolysis of wood particles in fluidized beds.[20,29,30]

The definition for the devolatilization time could be based on measuring gas evolution,[29] rate of weight loss,[31] or time history.[25] We have chosen to define the total devolatilization time as the time when the particle center attains the maximum temperature (t_5). This is the time when the reactions are practically terminated.[20] For pyrolysis of wood cylinders in FLiNaK, we found that the total devolatilization time follows the empirical correlation:

$$t_{dev} = \rho(0.146\ e^{-k_{eff}} - 1.09)d^{1.05} \tag{4}$$

with the values for ρ and k_{eff} ($\perp$) as given in Table 1.

Equation 4 gives A_{beech} = 6.625 and A_{pine} = 10.53. The experimental data and the empirical correlations are shown graphically in Figure 12.

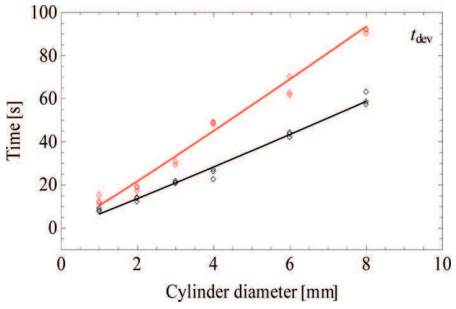

Figure 12. Total devolatilization times (t_{dev}) for beech (black) and pine (red) cylinders as functions of the cylinder diameter in FLiNaK at 500 °C. Symbols are for the experiments and solid lines for the empirical correlation given by eq 4.

We have found that the value of A depends on the properties of the wood for the particle sizes used in this study. The devolatilization time becomes longer as the density increases or the thermal conductivity decreases, with the effect of the density being more pronounced. Therefore, the devolatilization time for beech wood is larger than for pine wood, given the higher density and higher thermal conductivity (Table 1). These findings are in agreement with the model predictions performed by Di Blasi.[32] Di Blasi studied the effects of variable physical properties on the conversion time in biomass pyrolysis. It was found that the density was the most important factor, followed by the thermal conductivity. Only smaller effects were associated with other physical properties such as permeability and heat capacity. The linear increase in conversion time with the density is due to the successively slower particle heating rate, while the exponential reduction with conductivity is caused by the increased rate of heat transfer toward the interior of the particle.

The value n = 1.05 is well within the range of values reported previously for both biomass and coal devolatilization. According to Kanury,[33] the devolatilization times for combustible particles are proportional to either d or d^2, depending on external or internal heat- and mass-transfer control, respectively. A value between 1 and 2 indicates that the particle sizes used in this study cover both regimes.

CONCLUSIONS

The aim of this work was to study the heat transfer characteristics of FLiNaK in molten salt pyrolysis. The temperature history at the particle center of beech and pine wood cylinders of various sizes was recorded, and this was used to evaluate the reaction temperatures, heating rates, and devolatilization times.

Due to the higher thermal conductivity of beech wood, the characteristic heating rates (h_1–h_4) are slightly higher than for pine wood. The characteristic times (t_1–t_5) are larger for pine wood for the same reason. However, the reaction temperatures (T_1–T_4) for the two wood types are comparable. A decreasing trend in the effective pyrolysis temperature (T_3) is observed with larger particles, from 469 ± 4.5 °C for d = 1 mm to 412 ± 6.5 °C for d = 8 mm.

The maximum heating rate (h_1) for molten salt pyrolysis is significantly higher than for fluidized sand bed for smaller particles ($d \leq 4$ mm). Heating rates as high as 218 ± 6 and 186 ± 15 °C/s are observed for 1 mm beech and pine wood, respectively. For larger particles ($d > 4$ mm), the maximum heating rates are comparable.

The main degradation of cellulose and hemicellulose takes place at the effective pyrolysis temperature T_3. The average heating rate for wood cylinders until the main degradation takes place is found to follow the empirical correlation $\beta = (k_{eff}/\rho)10^3(24 + 390\ e^{-0.49d})$.

The total devolatilization time is found to follow the empirical correlation $t_{dev} = \rho(0.146\ e^{-k_{eff}} - 1.09)\ d^{1.05}$. The value of the exponent of d indicates that the particle sizes used in this study cover both external and internal heat transfer regimes.

The results show that FLiNaK is suitable as a heat transfer medium in fast pyrolysis, particularly for smaller particles where the properties of the heat transfer medium dominate the process. For larger particles the heat transfer process is limited by the wood properties, and the heat transfer medium is of less importance.

dx.doi.org/10.1021/ef301121j | Energy Fuels 2012, 26, 6419–6425

AUTHOR INFORMATION

Corresponding Author

*E-mail: heidi.nygard@umb.no.

Notes

The authors declare no competing financial interest.

REFERENCES

(1) Venderbosch, R. H.; Prins, W. Fast pyrolysis technology development. *Biofuels, Bioprod., Biorefin.* **2010**, *4* (2), 178−208.

(2) A.V, B. Review of fast pyrolysis of biomass and product upgrading. *Biomass Bioenergy* **2012**, *38* (0), 68−94.

(3) Lovering, D. G. *Molten Salt Technology*; Plenum Press: New York; London, 1982.

(4) Nygård, H. S.; Olsen, E. Review of thermal processing of biomass and waste in molten salts for production of renewable fuels and chemicals. *Int. J. Low-Carbon Technol.* **2012**, DOI: 10.1093/ijlct/ctr045.

(5) Adinberg, R.; Epstein, M.; Karni, J. Solar gasification of biomass: A molten salt pyrolysis study. *J. Sol. Energy Eng.* **2004**, *126* (3), 850−857.

(6) Yoshida, S.; Matsunami, J.; Hosokawa, Y.; Yokota, O.; Tamaura, Y.; Kitamura, M. Coal/CO_2 gasification system using molten carbonate salt for solar/fossil energy hybridization. *Energy Fuels* **1999**, *13* (5), 961−964.

(7) Matsunami, J.; Yoshida, S.; Oku, Y.; Yokota, O.; Tamaura, Y.; Kitamura, M. Coal gasification by CO_2 gas bubbling in molten salt for solar/fossil energy hybridization. *Sol. Energy* **2000**, *68* (3), 257−261.

(8) Matsunami, J.; Yoshida, S.; Oku, Y.; Yokota, O.; Tamaura, Y.; Kitamura, M. Coal gasification with CO_2 in molten salt for solar thermal/chemical energy conversion. *Energy* **2000**, *25* (1), 71−79.

(9) Roy, C.; Morin, D.; Dubé, F. The biomass Pyrocycling process. In *Biomass Gasification and Pyrolysis: State of the Art and Future Prospects*; Kaltschmidt, M., Bridgwater, A. V., Eds.; CPL Scientific Ltd: Newbury, Berkshire, U.K., 1997; pp 307−315.

(10) Sada, E.; Kumazawa, H.; Kudsy, M. Pyrolysis of lignins in molten salt media. *Ind. Eng. Chem. Res.* **1992**, *31* (2), 612−616.

(11) Kudsy, M.; Kumazawa, H. Pyrolysis of kraft lignin in the presence of molten $ZnCl_2$−KCl mixture. *Can. J. Chem. Eng.* **1999**, *77* (6), 1176−1184.

(12) Scarrah, W. P. Molten salt hydrocracking of lignite. Screening of viscosity reducers and hydrogen sources. *Ind. Eng. Chem. Prod. Res. Dev.* **1980**, *19* (3), 442−446.

(13) Hammond, V. L.; Mudge, L. K. *Feasibility Study of Use of Molten Salt Technology for Pyrolysis of Solid Waste*, Final Report; Battele Pacific Northwest Labs: Tichland, WA, 1975.

(14) Menzel, J.; Perkow, H.; Sinn, H. Recycling Plastics. *Chem. Ind.* **1973**, *12*, 570−573.

(15) Bertolini, G. E.; Fontaine, J. Value recovery from plastics waste by pyrolysis in molten salts. *Conserv. Recycl.* **1987**, *10* (4), 331−343.

(16) Chambers, C.; Larsen, J. W.; Li, W.; Wiesen, B. Polymer waste reclamation by pyrolysis in molten salts. *Ind. Eng. Chem. Process Des. Dev.* **1984**, *23* (4), 648−654.

(17) Sugiura, K.; Minami, K.; Yamauchi, M.; Morimitsu, S.; Tanimoto, K. Gasification characteristics of organic waste by molten salt. *J. Power Sources* **2007**, *171* (1), 228−236.

(18) Olson, L. C.; Ambrosek, J. W.; Sridharan, K.; Anderson, M. H.; Allen, T. R. Materials corrosion in molten LiF−NaF−KF salt. *J. Fluorine Chem.* **2009**, *130* (1), 67−73.

(19) Williams, D. F. *Assessment of Candidate Molten Salt Coolants for the NGNP/NHI Heat-Transfer Loop*; Oak Ridge National Laboratory: Oak Ridge, TN, 2006.

(20) Di Blasi, C.; Branca, C. Temperatures of wood particles in a hot sand bed fluidized by nitrogen. *Energy Fuels* **2003**, *17* (1), 247−254.

(21) Grønli, M. G. A theoretical and experimental study of the thermal degradation of biomass. Ph.D. Thesis, NTNU, Trondheim, Norway, 1996.

(22) Miccio, F.; Moersch, O.; Spliethoff, H.; Hein, K. R. G. Generation and conversion of carbonaceous fine particles during bubbling fluidized bed gasification of a biomass fuel. *Fuel* **1999**, *78* (12), 1473−1481.

(23) Kersten, S. R. A.; Wang, X.; Prins, W.; van Swaaij, W. P. M. Biomass pyrolysis in a fluidized bed reactor. Part 1: Literature review and model simulations. *Ind. Eng. Chem. Res.* **2005**, *44* (23), 8773−8785.

(24) Antal, M. J., Jr.; Varhegyi, G. Cellulose pyrolysis kinetics: The current state of knowledge. *Ind. Eng. Chem. Res.* **1995**, *34* (3), 703−717.

(25) Di Blasi, C.; Branca, C.; Santoro, A.; Gonzalez Hernandez, E. Pyrolytic behavior and products of some wood varieties. *Combust. Flame* **2001**, *124* (1−2), 165−177.

(26) Wang, X.; Kersten, S. R. A.; Prins, W.; van Swaaij, W. P. M. Biomass pyrolysis in a fluidized bed reactor. Part 2: Experimental validation of model results. *Ind. Eng. Chem. Res.* **2005**, *44* (23), 8786−8795.

(27) Di Blasi, C.; Branca, C. Kinetics of primary product formation from wood pyrolysis. *Ind. Eng. Chem. Res.* **2001**, *40* (23), 5547−5556.

(28) Ross, D. P.; Heidenreich, C. A.; Zhang, D. K. Devolatilization times of coal particles in a fluidized bed. *Fuel* **2000**, *79* (8), 873−883.

(29) de Diego, L. F.; García-Labiano, F.; Abad, A.; Gayán, P.; Adánez, J. Modeling of the devolatilization of nonspherical wet pine wood particles in fluidized beds. *Ind. Eng. Chem. Res.* **2002**, *41* (15), 3642−3650.

(30) Gaston, K. R.; Jarvis, M. W.; Pepiot, P.; Smith, K. M.; Frederick, W. J.; Nimlos, M. R. Biomass pyrolysis and gasification of varying particle sizes in a fluidized-bed reactor. *Energy Fuels* **2011**, *25* (8), 3747−3757.

(31) Di Blasi, C.; Hernandez, E. G.; Santoro, A. Radiative pyrolysis of single moist wood particles. *Ind. Eng. Chem. Res.* **2000**, *39* (4), 873−882.

(32) Di Blasi, C. Influences of physical properties on biomass devolatilization characteristics. *Fuel* **1997**, *76* (10), 957−964.

(33) Kanury, A. M. Combustion characteristics of biomass fuels. *Combust. Sci. Technol.* **1994**, *97* (4−6), 469−491.

Paper IV

Nygård, Heidi S.; Olsen, Espen. Effect of salt composition and temperature on the thermal behavior of beech wood particles in molten salt pyrolysis. *Energy Procedia* 2014, in press.

Available online at www.sciencedirect.com

ScienceDirect

Energy Procedia 00 (2014) 000–000

Energy Procedia

www.elsevier.com/locate/procedia

Renewable Energy Research Conference, RERC 2014

Effect of salt composition and temperature on the thermal behavior of beech wood in molten salt pyrolysis

Heidi S. Nygård*, Espen Olsen

Department of Mathematical Sciences and Technology, Norwegian University of Life Sciences, 1432 Ås, Norway

Abstract

The thermal behavior of wood particles in molten salt pyrolysis was investigated. Cylindrical beech wood particles (L = 30 mm, d = 3.5 mm) were pyrolyzed using different mixtures of molten salts (FLiNaK, $(LiNaK)_2CO_3$, $ZnCl_2$–KCl, KNO_3–$NaNO_3$) over the temperature range of 400–600 °C. The temperature at the particle center was measured during the process, and used to evaluate heating rates, reaction temperatures, and devolatilization times. A general observation was that beech wood is heated faster in fluoride and carbonate melts, but the differences diminish with increasing reactor temperatures. The highest heating rates at the particle center were observed in FLiNaK (46 – 56 °C/s). The effective pyrolysis temperature at which the main decomposition of cellulose and hemicellulose takes place showed a weak dependence on reactor temperature, but no significant difference between the heating media was discovered. The devolatilization time corresponding to conversion of 95% may be empirically correlated with the power law expression $t_{dev} = Ad_p^n$. Arrhenius plots were constructed to show the exponential dependence of temperature on the parameter A. The correspondingly low activation energies (13.3 – 27.4 kJ/mol) indicate heat transfer control during the decomposition process.

Peer-review under responsibility of the Scientific Committee of RERC 2014.
Keywords: Beech wood; Pyrolysis; Molten Salts; Heating rate

1. Introduction

In fast pyrolysis, biomass is heated rapidly in the absence of oxygen and converted to a mixture of liquids (pyrolysis oil), non–condensable gases and solid chars. Important process conditions for high pyrolysis oil yields are moderate reactor temperatures (~500 °C), high heating rates, short vapor residence time (2 – 3 s), and rapid quenching of the pyrolysis vapors. It is essential that the biomass particles reach optimum process temperatures before they start to decompose as exposure to lower temperatures would favor formation of charcoal.[1] This makes rapid heat transfer important in the process. There are several approaches to achieve rapid heat transfer in pyrolysis, including bubbling fluid beds, circulating and transported beds, cyclonic reactors, ablative reactors, and vacuum

* Corresponding author. Tel.: +47 64 96 54 63, *E–mail address: heidi.nygard@nmbu.no*

Peer-review under responsibility of the Scientific Committee of RERC 2014.

moving beds. A detailed description of these configurations may be found in the review of fast pyrolysis technology development by Venderbosch and Prins.[2]

A less studied approach is molten salt pyrolysis. The biomass is fed into a preheated molten salt bath where the decomposition takes place. Inorganic molten salts have very good heat transfer characteristics, large heat capacities, are very stable at high temperatures, and may be used over a wide range of temperatures, from around 120 °C to well above 1000 °C. Due to their low viscosity, they will cover the biomass particles rapidly and also infiltrate the pores, leading to a larger particle area exposed to heating by the salt.[3] A review of thermal processing of biomass in molten salts has recently been published.[4] The research reviewed includes many investigations that have not so far progressed beyond the laboratory scale. It is a relatively small research area compared with more traditional conversion methods, and there is clearly a need for more basic research on the subject.

The heat transfer characteristics of molten salts have been studied for various applications.[3] Several researchers have demonstrated an increase in reaction rates by molten carbonates in thermal processing of coal [5-7] and cellulose.[8, 9] $ZnCl_2$–KCl has been used in pyrolysis of lignin, and it is found that the yields of different phenolic compounds depend on both the molar ratio of the two salts [10] and the salt–to–lignin ratio in the reactor.[11] In the Pyrocycling process [12], a mixture of KNO_3, $NaNO_2$ and $NaNO_3$ was used as an indirect heat transfer medium in vacuum pyrolysis. Nitrates have also shown good heat transfer performance in storing thermal solar energy.[13] Molten fluoride salts have been studied as a heat transfer medium in solar power towers and nuclear power plants [14], and particularly FLiNaK has been found to have good heat transfer performance.[15]

The pyrolytic behavior of single particles is important for reactor design. The aim of this work is to study the behavior of beech wood particles in molten salt pyrolysis and gain a better understanding of molten salts as a heat transfer medium in the process. This is done by measuring particle temperatures, and use these to evaluate heating rates, reaction temperatures, and devolatilization times. In a previous study [16] we found that FLiNaK gives significantly higher heating rates compared with fluidized sand bed [17] for cylindrical beech wood particles with $d \leq 4$ mm at 500 °C. In the present work, we evaluate the effect of different salt mixtures (FLiNaK, $(LiNaK)_2CO_3$, $ZnCl_2$–KCl, KNO_3–$NaNO_3$) over a wider temperature range (400 – 600 °C).

2. Experimental section

Cylindrical beech wood particles with length (L) of 30 mm and diameter (d) of 3.5 mm were prepared from untreated wood sticks with the length parallel to the fibers. This gives an aspect ratio (L/d) well within the limit for one–dimensional (1D) internal heat transfer ($L/d > 3$) [18], and the heat transfer perpendicular to the fibers is measured. This is important because of the anisotropic nature of wood, with higher thermal conductivity parallel compared to perpendicular to the fibers.[19] The samples were dried at 105 °C for 24 h prior to the experiments in order to minimize the water content. A 1 mm type K thermocouple, placed inside a steel tube for support, was used to record the temperature T at the particle center at the frequency of 5 times per second. The salts were purchased separately in their simplest form from Sigma–Aldrich (> 98.5% purity) and mixed mechanically to obtain the 4 different compositions listed in Table 1. Differences in the experimental temperature ranges are due to the respective melting points. The nitrate mixture starts to decompose at 560 °C [13], and is only used up to 500 °C in this study.

Table 1. Composition and properties of salts used in the experiments.

Molten salts composition (wt %)	Experiment temperatures	Melting point	Reference for melting point
LiF–NaF–KF (29.2–11.7–59.1)	475 – 600°C	454 °C	[15]
Li_2CO_3–Na_2CO_3–K_2CO_3 (31.7–33.7–34.7)	450 – 600°C	397 °C	[9]
$ZnCl_2$–KCl (68.0–32.0)	400 – 600°C	181 °C	[20]
$NaNO_3$–KNO_3 (60.0–40.0)	400 – 500°C	220 °C	[13]

200 g of pre–dried salt mixture was filled in a nickel crucible (H = 190 mm, ID = 52 mm) placed inside a stainless steel reactor (H = 200 mm, ID = 62 mm) that was externally heated by an electric furnace (Figure 1).

Nickel was chosen for the inner crucible because it is more resistant to corrosion by molten salts.[14] When the heating was started, inert gas (Ar) was continuously flowed into the reactor through a nickel tube (4 mm) to ensure an oxygen–free atmosphere. The salt temperature was controlled by a submerged type K thermocouple. Once the salt was completely melted, the nickel tube was submerged in the melt to give turbulent mixing and a homogeneous temperature throughout the reactor. Turbulent mixing enhances the heat transfer from the salt to the wood particles in the pyrolysis process.

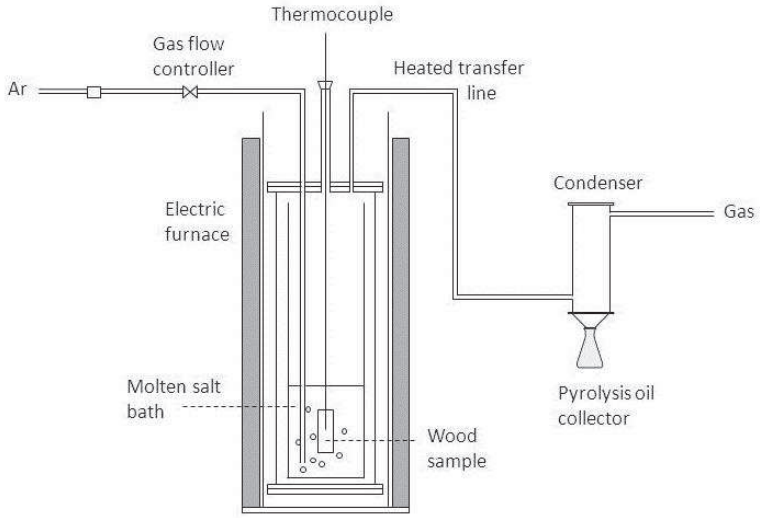

Figure 1. Experimental setup for recording the centre temperature of beech wood particles (d = 3.5 mm) in molten salt pyrolysis.

When the melt was stabilized at the desired temperature, the beech wood particles were introduced to the reactor manually through the top of the sealed reactor. It was ensured that the samples were completely immersed in the molten salt bath throughout the whole experiment. Each experiment was performed at least in triplicate, giving acceptable reproducibility. The flow rate of Ar was set to 2 L/min during the experiments to ensure removal of the produced pyrolysis vapors in less than 3 seconds. The vapors were led out of the reactor through a 4 mm heated transfer line (450 °C) made of stainless steel. The system was connected to a water cooled condenser, but the small samples in this study did not provide enough pyrolysis oil for accurate yield measurements. The non–condensable gases were vented off.

3. Results and discussions

3.1. Temperature profiles and definitions of characteristic points

The temperature measurements were used to construct temperature profiles and calculate heating rates. The temperature profiles at the particle center at reactor temperature T = 500 °C are shown in Figure 2a, where one representative curve is chosen for each salt mixture. Figure 2b shows the temperature profile and corresponding heating rate in FLiNaK at 475 °C, where several characteristic points stand out clearly.

It is clear that the salt mixtures have different effects on the thermal behavior of the wood samples. The temperature profile for the nitrate mixture is very different from the others; a sudden increase in temperature is observed with a maximum much higher than the reactor temperature. It is believed that the salt is reacting exothermically with the components in the wood sample. Carbon is one of the products from wood pyrolysis, and nitrates are reduced by this according to Eqs. (1) and (2) (simulations performed in HSC Chemistry software [21]).

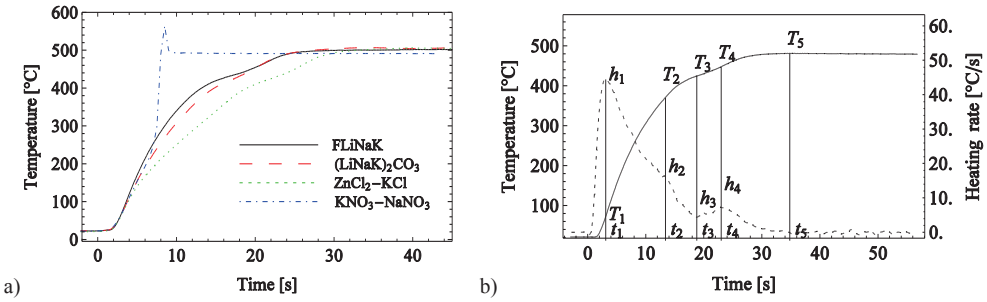

Figure 2.(a) Temperature profiles at the center of beech wood particles (d = 3.5 mm) at reactor temperature T = 500 °C in FLiNaK (black), $(LiNaK)_2CO_3$ (red), $ZnCl_2$–KCl (green), and KNO_3–$NaNO_3$ (blue); (b) Temperature profile and calculated heating rate at the center of beech wood (d = 3.5 mm) in FLiNaK pyrolysis at reactor temperature T = 475 °C.

$$2KNO_3(l) + C \leftrightarrow CO_2(g) + 2KNO_2(l), \qquad \Delta G_{500°C} = -311.86\ kJ/mol \tag{1}$$

$$2NaNO_3(l) + C \leftrightarrow CO_2(g) + 2NaNO_2(l), \qquad \Delta G_{500°C} = -562.09\ kJ/mol \tag{2}$$

A similar pattern is observed for the other reactor temperatures, and the results for this salt are excluded from further analyses since the characteristic pyrolysis points are not clear. For the remaining salts, the shape of both the temperature profiles and heating rates are qualitatively the same for all the investigated reactor temperatures.

The characteristic points shown in Figure 2b are briefly described in Table 2. We have used the same definitions as in our previous study, where we have also included more thorough descriptions.[16] The characteristic points were originally proposed by Di Blasi and Branca in their study of pyrolysis of cylindrical beech wood particles (L = 20 mm, d = 2 – 10 mm) in a hot sand bed (T = 534 °C) fluidized by nitrogen.[17]

Table 2. Description of characteristic points during pyrolysis of beech wood particles.

Characteristic points	Description
h_1 / t_1 /T_1	Maximum heating rate. This is measured right before any reactions occur. After this point, degradation starts in the outer part of the particle and inward heat transfer is hindered.
h_2 / t_2 /T_2	Point of high variation. This indicates the beginning of the endothermic degradation of cellulose and hemicellulose at the particle center.
h_3 / t_3 / T_3	Local minimum of heating rate. This point represents the main occurrence of degradation of cellulose and hemicellulose, and T_3 may be regarded as the effective pyrolysis temperature.
h_4 / t_4 / T_4	Local maximum of heating rate. The exothermic degradation of lignin – which happens over a wider temperature range than cellulose and hemicellulose – starts to slow down. At this point, the conversion is about 95%.
t_5 / T_5	Maximum temperature. The conversion process is practically terminated, and t_5 may be regarded as the total devolatilization time.

3.2. Reaction temperatures and heating rates

The effect of reactor temperature (400 – 600 °C) on the characteristic temperatures in molten salt pyrolysis is shown in Figure 3. For T_1 there is a relatively high scatter in the observations. The high heating rates at this point (Figure 4) makes it difficult to evaluate precise corresponding temperatures. Since the variation within one salt is greater than the variation between the salts, it is not possible to say if there are differences between the salt mixtures. The other characteristic temperatures are more consistent. They are slightly, but not significantly, lower for $ZnCl_2$–KCl. The values are comparable to a corresponding study in fluidized sand bed by Di Blasi and Branca [17], indicating that the heat transfer medium is of less importance to the reaction temperatures. For T_2 and T_3 there is only a weak dependence on reactor temperature, with values in the range 352 – 386 and 404 – 438 °C, respectively.

These temperatures are associated with the beginning and the main occurrence of cellulose and hemicellulose degradation. The reactions are known to occur at a narrow temperature range [22], and depend more on particle size [16] than heat transfer medium. T_4 is related to the degradation of lignin. This happens over a wider temperature range [23], and is more dependent on the reactor temperature than the other characteristic temperatures. An increase in T_4 from 435 to 522 °C is observed as the reactor temperature is increased from 450 to 600 °C.

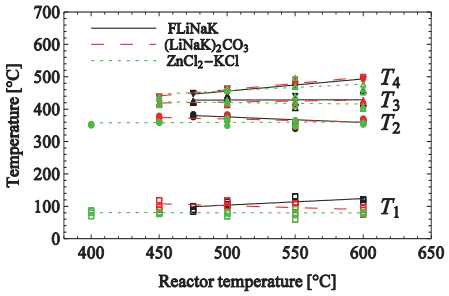

Figure 3. Characteristic temperatures at the center of beech wood particles (d = 3.5 mm) as functions of the reactor temperature in FLiNaK (black), $(LiNaK)_2CO_3$ (red), and $ZnCl_2$–KCl (green).

The characteristic heating rates (h_1 – h_4) as a function of reactor temperature are shown in Figure 4. All the heating rates show an increasing trend with increasing reactor temperature. The maximum heating rate (h_1) is of special interest because it is measured before any reactions occur, and this is where variations between heat transfer media are shown. Although there is some scatter in the observations, it is clear that FLiNaK generally has higher values (46 – 56 °C/s), followed by $(LiNaK)_2CO_3$ (38 – 52 °C/s) and then $ZnCl_2$–KCl (35 – 43 °C/s). The other characteristic heating rates show a strong dependence on reactor temperature; h_2 increases from 8 to 31 °C/s, h_3 from 1 to 20 °C/s, and h_4 from 4 to 43 °C/s. Variations between the salts are, however, negligible.

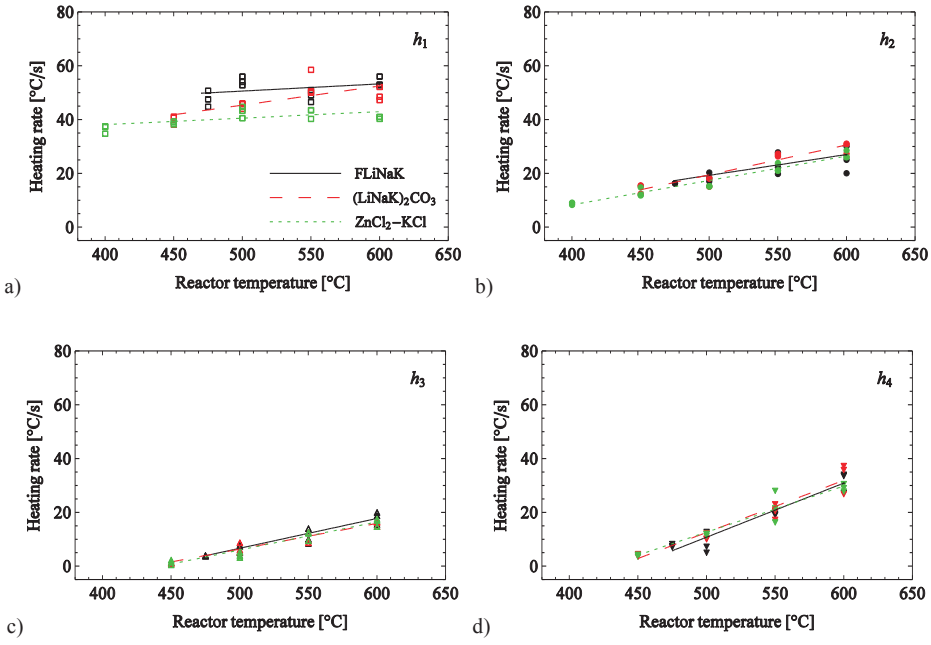

Figure 4. Characteristic heating rates at the center of beech wood particles (d = 3.5 mm) as functions of the reactor temperature in FLiNaK (black), $(LiNaK)_2CO_3$ (red), and $ZnCl_2$–KCl (green).

3.3. Devolatilization times

Prediction of the total devolatilization time in pyrolysis is important for reactor design. Several definitions are used in literature; measurements of gas evolution [24], rate of weight loss [25], or temperature history [26]. Based on the definitions previously introduced (Figure 2b), t_5 could be regarded as the total devolatilization time. However, precise evaluation of t_5 is difficult in this study, because the maximum temperature T_5 cannot be distinguished from small temperature oscillations associated with structural changes or measurement errors for such small particles. We have instead chosen to use t_4 for the evaluation of the devolatilization time to allow for comparison between salt mixtures and reactor temperatures. This corresponds to the second local maximum in the heating rate at the particle center, and the conversion is about 95%.[26]

Figure 5a shows t_4 as a function of the reactor temperature. Values for FLiNaK and $(LiNaK)_2CO_3$ are comparable for all reactor temperatures, while the pyrolysis process takes longer time in $ZnCl_2$–KCl. However, the differences diminish as the bed temperature is increased, and for reactor temperature T = 600 °C there are no significant differences. A common empirical correlation for the devolatilization time is the power–law relation $t_{dev} = Ad^n$, where A and n are fitted to match the experimental data. This was originally proposed for coal particles [27], but has also been shown to be applicable for pyrolysis of wood particles.[17, 24, 28] Values for n typically range between 1 and 2, depending on external or internal heat– and mass–transfer control.[29] Factors such as bed temperature, sample varieties, oxygen concentration, etc., are usually incorporated in the parameter A.[27] In our previous study [16] we found n = 1.05 for cylindrical beech wood particles with diameters between 1 and 8 mm in FLiNaK at 500 °C. We continue to use this value for n, and focus on the parameter A in the following. We have constructed an Arrhenius plot of ln(A) as function of $1000/T_{reactor}$ for each salt mixture (Figure 5b), and found that A depends exponentially on reactor temperature with the relations given in Table 3. This is in agreement with the results reported by other researchers for both coal [27] and wood.[17, 28]

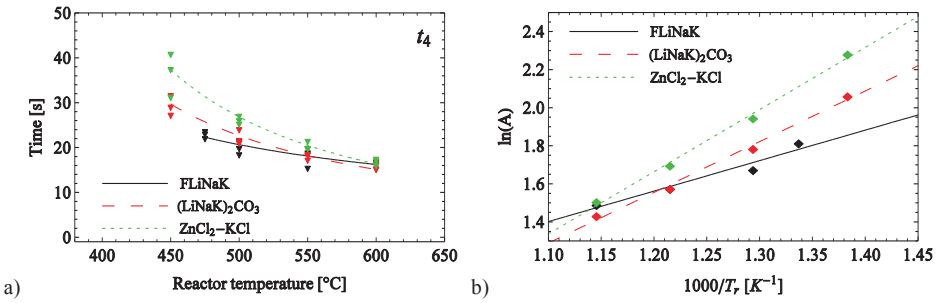

Figure 5. (a) Characteristic heating times for beech wood particles (d = 3.5 mm) as functions of the reactor temperature in FLiNaK (black), $(LiNaK)_2CO_3$ (red), and $ZnCl_2$–KCl (green). (b) Effect of reactor temperature on the correlation parameter A for the devolatilization time for pyrolysis of beech wood particles (d = 3.5 mm) in FLiNaK (black), $(LiNaK)_2CO_3$ (red), and $ZnCl_2$–KCl (green).

The R^2 values for the regression analysis are very good (Table 3), especially for $(LiNaK)_2CO_3$ and $ZnCl_2$–KCl. We have calculated the corresponding activation energies (Table 3), and these are in the same range as found by other researchers.[17, 27] The values are quite low on chemical kinetic scales, indicating heat transfer being the controlling mechanism in the process.[30]

Table 3. Correlation parameter A and corresponding values for the activation energy of beech wood particles in molten salt pyrolysis.

Molten salt	A	R^2	Corresponding activation energy
FLiNaK	$0.698e^{1600/T}$	95.98	13.3 kJ/mol
$(LiNaK)_2CO_3$	$0.194e^{2662/T}$	99.28	22.1 kJ/mol
$ZnCl_2$–KCl	$0.105e^{3264/T}$	99.51	27.4 kJ/mol

4. Conclusions

The pyrolytic behavior of cylindrical beech wood particles (L = 30 mm, d = 3.5 mm) in FLiNaK, $(LiNaK)_2CO_3$, $ZnCl_2$–KCl, and KNO_3–$NaNO_3$ at temperatures between 400 to 600 °C was investigated. Temperature profiles were made based on temperature measurements at the particle center during pyrolysis reactions, and these were used to evaluate the reaction temperatures, heating rates, and devolatilization times.

The nitrate mixture was not suitable for pyrolysis. The temperature profiles differed greatly from the others with a sudden increase in temperature and a maximum much higher than the reactor temperature. This indicates that the salts react exothermic with the carbon formed in the process, also supported by large negative Gibbs free energies for simulated reactions in HSC Chemistry software. Although nitrates have previously shown good heat transfer performance in storage of solar energy [13] and in vacuum pyrolysis [12], these studies do not involve direct contact with carbon containing material.

The characteristic reaction temperatures are slightly, but not significantly, lower for $ZnCl_2$–KCl. The main degradation of cellulose and hemicellulose (T_3) show a weak dependence on reactor temperature (404 – 438 °C), but a stronger dependence is observed for T_4 (435 – 522 °C), which is associated with the degradation of lignin. The highest heating rate (h_1) is measured before any reactions start. Some scatter exists in the observations, but it is still clear that FLiNaK generally has higher values (46 – 56 °C/s), followed by $(LiNaK)_2CO_3$ (38 – 52 °C/s) and then $ZnCl_2$–KCl (35 – 43 °C/s). The other characteristic heating rates are comparable for the salts, but they all depend strongly upon reactor temperature. The devolatilization time t_4 (corresponding to conversion of about 95%) is found to follow the empirical power–law relation $t_{dev} = Ad_p^n$. Arrhenius plots were constructed for each salt mixture to show that A depends exponentially upon temperature. The plots were in good agreement with experimental results, with R^2 values above 96%. Corresponding activation energies were calculated to be in the range from 13.3 to 27.4 kJ/mol, indicating heat transfer control rather than kinetic control in the decomposition process.

The results show that all though the highest heating rate and devolatilization times are affected by the external heating, the heat transfer media is of less importance to reaction temperatures and the remaining heating rates.

References

[1] Bridgwater AV. Review of fast pyrolysis of biomass and product upgrading. *Biomass & Bioenergy* 2012; 38(0): 68-94.

[2] Venderbosch RH, Prins W. Fast pyrolysis technology development. *Biofuels, Bioproducts & Biorefining* 2010; 4(2): 178-208.

[3] Lovering DG. *Molten salt technology*. Plenum Press;1982.

[4] Nygård HS, Olsen E. Review of thermal processing of biomass and waste in molten salts for production of renewable fuels and chemicals. *International Journal of Low-Carbon Technologies* 2012; 7(4): 318-324.

[5] Yoshida S, Matsunami J, Hosokawa Y., Yokota O., Tamaura Y. Coal/CO2 gasification system using molten carbonate salt for solar/fossil energy hybridization. *Energy & fuels* 1999; 13(5): 961-964.

[6] Matsunami J, Yoshida S, Oku Y, Yokota O, Tamaura Y, Kitamura M. Coal gasification by CO2 gas bubbling in molten salt for solar/fossil energy hybridization. *Solar Energy* 2000; 68(3): 257-261.

[7] Matsunami J, Yoshida S, Oku Y, Yokota O, Tamaura Y, Kitamura M. Coal gasification with CO2 in molten salt for solar thermal/chemical energy conversion. *Energy* 2000; 25(1): 71-79.

[8] Adinberg R, Epstein M, Karni J. Solar Gasification of Biomass: A Molten Salt Pyrolysis Study. *Journal of Solar Energy Engineering* 2004; 126(3): 850-857.

[9] Hathaway BJ, Davidson JH, Kittelson DB. Solar Gasification of Biomass: Kinetics of Pyrolysis and Steam Gasification in Molten Salt. *Journal of Solar Energy Engineering* 2011; 133(2): 021011-1 – 021011-9.

[10] Sada E, Kumazawa H, Kudsy M. Pyrolysis of lignins in molten salt media. *Industrial & Engineering Chemistry Research* 1992; 31(2): 612-616.

[11] Kudsy M, Kumazawa H. Pyrolysis of kraft lignin in the presence of molten ZnCl2-KCl mixture. *The Canadian Journal of Chemical Engineering* 1999; 77(6): 1176-1184.

[12] Roy C, Morin D, Dubé F. The biomass PyrolycyclingTM process. In: Kaltschmidt M, Bridgwater AV, editors. *Biomass Gasification and Pyrolysis: State of the Art and Future Prospects*, UK: CPL Press; 1997, p. 307-315.

[13] Mao A, Park JH, Han GY, Seo T, Kang Y. Heat transfer characteristics of high temperature molten salt for storage of thermal energy. *Korean Journal of Chemical Engineering* 2010; 27(5): 1452-1457.

[14] Olson LC, Ambrosek JW, Sridharan K, Anderson MH, Allen TR. Materials corrosion in molten LiF–NaF–KF salt. *Journal of Fluorine Chemistry* 2009; 130(1): 67-73.

[15] Williams D. Assessment of candidate molten salt coolants for the NGNP/NHI Heat-Transfer Loop. ORNL/TM-2006/69, *Oak Ridge National Laboratory*, Oak Ridge, Tennessee, 2006.
[16] Nygård HS, Danielsen F, Olsen E. Thermal History of Wood Particles in Molten Salt Pyrolysis. *Energy & Fuels* 2012; 26(10): 6419-6425.
[17] Di Blasi C, Branca C. Temperatures of Wood Particles in a Hot Sand Bed Fluidized by Nitrogen. *Energy & Fuels* 2003; 17(1): 247-254.
[18] Kersten SRA, Wang X, Prins W, van Swaaij WPM. Biomass Pyrolysis in a Fluidized Bed Reactor. Part 1: Literature Review and Model Simulations. *Industrial & Engineering Chemistry Research* 2005; 44(23): 8773-8785.
[19] Grønli MG. A Theoretical and Experimental Study of the Thermal Degradation of Biomass. PhD thesis, *Norwegian University of Science and Technology* 1996.
[20] Jiang H, Ai N, Wang M, Ji D, Ji J. Experimental Study on Thermal Pyrolysis of Biomass in Molten Salt Media. *Electrochemistry* 2009; 77(8): 730-735.
[21] HSC Chemistry software, version 6.1.
[22] Di Blasi C, Branca C. Kinetics of Primary Product Formation from Wood Pyrolysis. *Industrial & Engineering Chemistry Research* 2001; 40(23): 5547-5556.
[23] Antal MJ Jr, Varhegyi G. Cellulose Pyrolysis Kinetics: The Current State of Knowledge. *Industrial & Engineering Chemistry Research* 1995; 34(3): 703-717.
[24] de Diego LF, García-Labiano F, Abad A, Gayán P, Adánez J. Modeling of the Devolatilization of Nonspherical Wet Pine Wood Particles in Fluidized Beds. *Industrial & Engineering Chemistry Research* 2002; 41(15): 3642-3650.
[25] Di Blasi C, Hernandez EG, Santoro A. Radiative Pyrolysis of Single Moist Wood Particles. *Industrial & Engineering Chemistry Research* 2000; 39(4): 873-882.
[26] Di Blasi C, Branca C, Santoro A, Hernandez EG. Pyrolytic behavior and products of some wood varieties. *Combustion and Flame* 2001; 124(1–2): 165-177.
[27] Ross DP, Heidenreich CA, Zhang DK. Devolatilisation times of coal particles in a fluidised-bed. *Fuel* 2000; 79(8): 873-883.
[28] Gaston KR, Jarvis MW, Pepiot P, Smith KM, Frederick WJ, Nimlos MR. Biomass Pyrolysis and Gasification of Varying Particle Sizes in a Fluidized-Bed Reactor. Energy & Fuels 2011; 25(8): 3747-3757.
[29] Kanury AM. Combustion Characteristics of Biomass Fuels. *Combustion Science and Technology* 1994; 97(4-6): 469-491.
[30] Jia L, Becker HA, Code RK. Devolatilization and char burning of coal particles in a fluidized bed combustor. *The Canadian Journal of Chemical Engineering* 1993; 71(1): 10-19.

Paper V

Nygård, Heidi S.; Olsen, Espen. Use of electrostatic precipitator (ESP) for oil collection in molten salt pyrolysis of milled beech wood. Submitted to *Energy & Fuels*.

Use of electrostatic precipitator (ESP) for oil collection in molten salt pyrolysis of milled beech wood

Heidi S. Nygård[*]*, Espen Olsen*

Department of Mathematical Sciences and Technology, Norwegian University of Life Sciences, 1432 Ås, Norway

Keywords: Beech wood – Pyrolysis – Molten Salts – Electrostatic precipitator

Abstract. A tubular electrostatic precipitator (ESP) was designed and tested for collection of pyrolysis oil in molten salt pyrolysis of milled beech wood (0.5 – 2 mm). The voltage-current (V-I) characteristics were studied, showing most stable performance of the ESP when N_2 was utilized as inert gas. The pyrolysis experiments were carried out in FLiNaK and $(LiNaK)_2CO_3$ over the temperature range of 450 – 600 °C. The highest yields of pyrolysis oil were achieved in FLiNaK, with a maximum of 34.2 wt % at 500 °C, followed by a decrease with increasing reactor temperature. The temperature had nearly no effect on the oil yield for pyrolysis in $(LiNaK)_2CO_3$ (19.0 - 22.5 wt %). Possible hydration reactions and

[*] heidi.nygard@nmbu.no

formation of HF gas during FLiNaK pyrolysis were investigated by simulations (HSC Chemistry software) and measurements of the outlet gas (FTIR), but no significant amounts of HF were detected.

Introduction

Pyrolysis is a thermochemical conversion process in which biomass is heated in the absence of oxygen. The products are pyrolysis oil, non-condensable gases and solid char, with respective yields depending on various process parameters such as heating rate, reaction temperature, and residence time in the hot zone of the reactor system.[1] In fast pyrolysis, the biomass particles should be heated rapidly to temperatures around 500 °C, followed by quenching of the produced vapors. In this way secondary reactions are kept to a minimum and the oil yield is maximized.[2]

Inorganic molten salts are potential candidates for rapid heat transfer in fast pyrolysis due to their good heat transfer characteristics, thermal stability and large heat capacities.[3] However, there are limited reported results with focus on the yield of pyrolysis oil in molten salt pyrolysis. Jiang et al.[4] performed an experimental study on pyrolysis of biomass in molten chlorides, and claimed that both the oil yield and water content of pyrolysis oil can be adjusted by varying the composition of molten salts. The highest yield of pyrolysis oil (35.0 wt %) was obtained from cellulose pyrolysis in $ZnCl_2$ at 450 °C, while the use of other chlorides mixtures ($ZnCl_2$-KCl, KCl-CuCl, $ZnCl_2$-KCl-CuCl, ZnCl-KCl-$FeCl_2$) only gave yields up to 15.0 wt %. Other researchers have concentrated on gasification of cellulose in carbonates[5,6] or production of specific phenolic compounds from lignin in chlorides.[7,8] The use of molten salts have also been reported for thermal treatment of municipal refuse,[9] wastepaper,[10,11] and recycling of plastics.[12-14] Other applications of molten salts as heat transfer media include solar power towers and nuclear power plants.[15]

In most pyrolysis reactor configurations, a large volume of inert gas is needed for fluidization and/or transportation of the produced vapors out of the reactor.[2] This means that the vapors, which are mostly in the form of aerosols, are present at relatively low concentrations in an inert gas (< 5 vol %), and the

separation is a difficult task.[16,17] Quenching by direct contact with product pyrolysis oil or in an immiscible hydrocarbon solvent has been widely practiced,[1] but careful design and temperature control are needed to avoid blockages in the system due to broad condensation temperature range of the organic volatiles.[17] Solvent methods have relatively high collection efficiencies, but the need for subsequent separation of the pyrolysis oil from the solvent adds cost to the process.[18] The currently preferred method is electrostatic precipitation (ESP),[1] a method that has been found to be more effective than solvent and cooling methods.[18] In an ESP, the vapors are charged by a corona discharge and separated from the inert gas by an electric field. The charged droplets are attracted to a grounded wall where they are neutralized and collected.[19]

There are two main objectives in the present paper. The first objective is the design of a tubular ESP for collection of pyrolysis oil. The voltage-current (V-I) characteristics are investigated with pure inert gases (N_2 and Ar) and with pyrolysis vapors included in the gas streams. The second objective is to use the ESP for collection of pyrolysis oil in molten salt pyrolysis of milled beech wood (0.5 – 2 mm). In a previous study[20] we found that FLiNaK gives significantly higher heating rates compared with fluidized sand bed[21] for beech wood cylinders with d ≤ 4 mm. In a subsequent study[22] $(LiNaK)_2CO_3$ also showed good heat transfer characteristics. In this study we focus on the yield of pyrolysis oil in molten salt pyrolysis. Experiments are performed in FLiNaK and $(LiNaK)_2CO_3$ in the temperature range 450 – 600 °C. The effects of salt mixture and reactor temperature on the yields of pyrolysis oil and char are investigated, and the oil is analyzed with respect to water content.

Design characteristics of electrostatic precipitator

A schematic of the constructed ESP is shown in Figure 1, with the design adopted from Bedmutha et al.[19] The inner cylinder was made of stainless steel and was electrically grounded. It was 50 mm in diameter and 150 mm long. A stainless steel wire (1 mm) co-axial with the inner cylinder was connected to a high voltage source and used as discharge electrode (positive potential). The outer cylinder was

made of polyoxymethylene (POM), an isolating material with a low coefficient of friction, good dielectric properties and good resistance to oils, greases, and solvents.[23] The ESP was cooled externally with tap water (~20 °C).

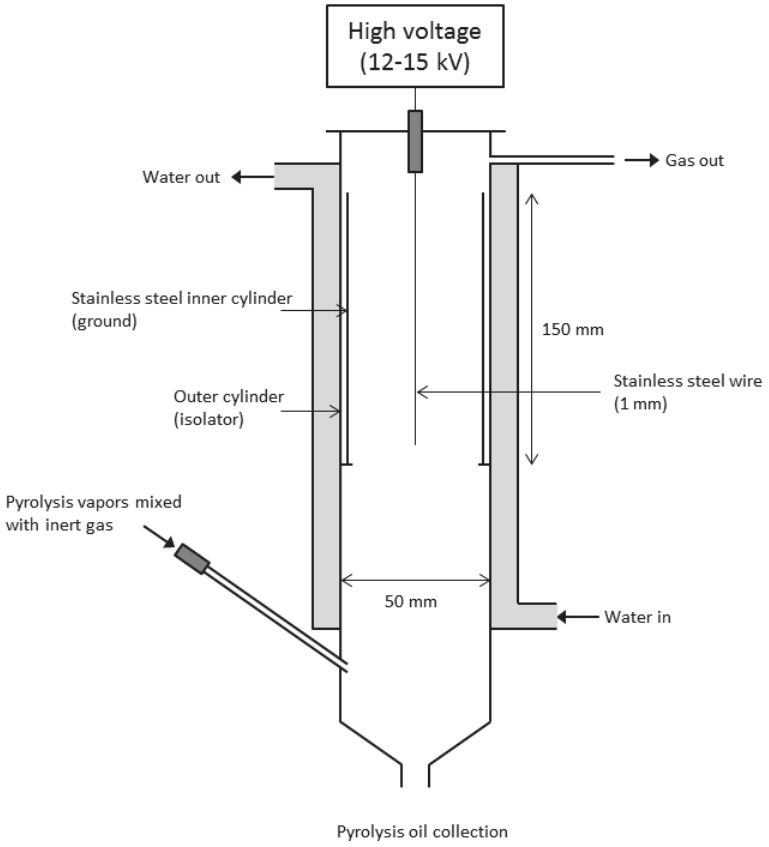

Figure 1. Schematic of the electrostatic precipitator (ESP).

For the initial testing, a bubble flask with water was attached at the exhaust of the ESP. It could be easily observed if the outlet gas contained any uncondensed pyrolysis vapors as these would fill the empty part of the flask with white "smoke". Argon (Ar, purity 99.99%, $H_2O \leq 20$ ppm, $O_2 \leq 20$ ppm) and nitrogen (N_2, purity 99.999%, $H_2O \leq 3$ ppm, $O_2 \leq 3$ ppm) purchased from AGA were used as inert gases.

The ESP was operated by setting the central electrode at a positive potential ranging from 0 to 20 kV, and the V-I characteristics (Figure 2) were determined with pure inert gases and during pyrolysis experiments with milled beech wood particles in FLiNaK at 500 °C. The voltage was increased slowly

until spark-over occurred, and the values of the output voltage and current were read directly from the power supply. The procedure was performed several times to assure reproducibility.

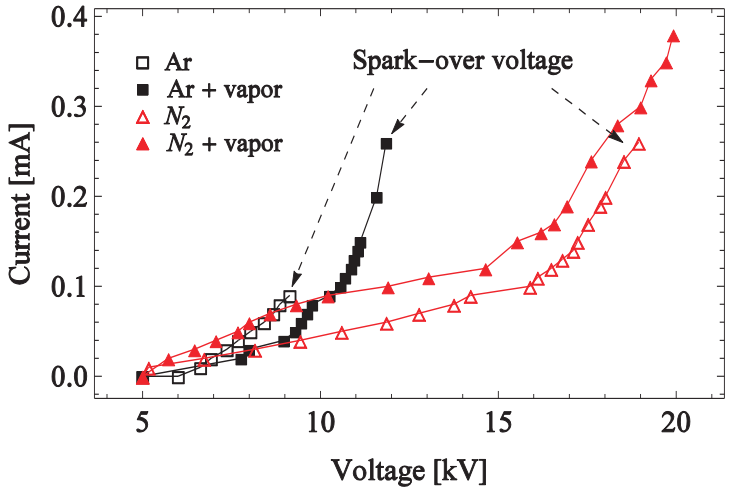

Figure 2. Current vs voltage characteristics for the electrostatic precipitator.

The two employed gases showed very different influence on the V-I characteristics, with the point for spark-over being the most prominent. Sparking is a phenomenon occurring when a conducting path is formed between the electrodes and electrons reach the grounded wall without being captured by molecules or particles. This can happen when the voltage is too high or the inert gas breaks down.[24] With pure inert gas streams, the spark-over occurred at 9.1 kV for Ar and 18.9 kV for N_2. Argon and molecular nitrogen have similar ionization energies (1520.6 and 1503.0 kJ/mol, respectively[25]), but the break down voltages are generally observed to be lower for argon.[26] The different V-I behaviors could be caused by differences of impurities as well, an observation also reported by Bedmutha et al.[19] In the presence of pyrolysis vapors, the spark-over voltage for Ar was increased to 11.9 kV, while no spark-over was observed for N_2 within the voltage range of the power supply. This could be explained by the pyrolysis vapors absorbing the electrons formed at the cathode and thus reducing the possibility for sparking.

It was visually observed that a minimum of 12 kV was required for separation of pyrolysis vapors and the remaining gas stream. Since these conditions were not possible without experiencing spark-overs using Ar, N_2 was chosen for the rest of the experiments in this study. Also, with N_2 as an inert gas, the increase in current with applied voltage is slower (Figure 2). This indicates poor conductivity of the gas, giving a more stable operation of the ESP.

Experimental procedure for pyrolysis of beech wood

Beech wood was used as feedstock in all the pyrolysis experiments. Beech wood is a hardwood consisting of 48% cellulose, 28% hemicellulose, 22% lignin and 2% extractives.[27] Untreated beech wood logs were milled and sieved, and a fraction of particle diameter of 0.5 – 2 mm was used. The samples were dried at 105 °C for 24 h prior to the experiments in order to minimize the water content.

The salts were purchased separately in their simplest form from Sigma-Aldrich (> 98.5% purity). The salts were mixed mechanically to obtain the different compositions listed in Table 1. The mixtures were pre-melted at 500 °C and kept in a drying oven (> 200 °C) for at least 24 h.

Table 1. Composition and properties of salts used in the experiments.

Molten salts composition (wt %)	Melting point	Experiment temperatures
LiF-NaF-KF (29.2-11.7-59.1)	454 °C[15]	475-600 °C
Li_2CO_3-Na_2CO_3-K_2CO_3 (31.7-33.7-34.7)	397 °C[28]	450-600 °C

300 g of dried salt mixture was filled in a nickel crucible (H = 190 mm, ID = 52 mm) placed inside a stainless steel reactor (H = 200 mm, ID = 62 mm) that was heated externally by an electric furnace (Figure 3). Nickel was chosen because it is more resistant to corrosion by molten salts.[29] The height of the melt varied between 60 and 70 mm, depending on the type of salt mixture and reactor temperature.

A 9 µm wire mesh filter was placed at the exit of the reactor to remove char and ash from the hot pyrolysis vapors. This type of in situ vapor filtration prior to condensation has been shown to give yields comparable to those obtained when cyclones are used, but with less solids, alkali metals, and ash in the pyrolysis oil.[30] The filter also ensures that possibly unreacted wood particles remain in the hot reactor.

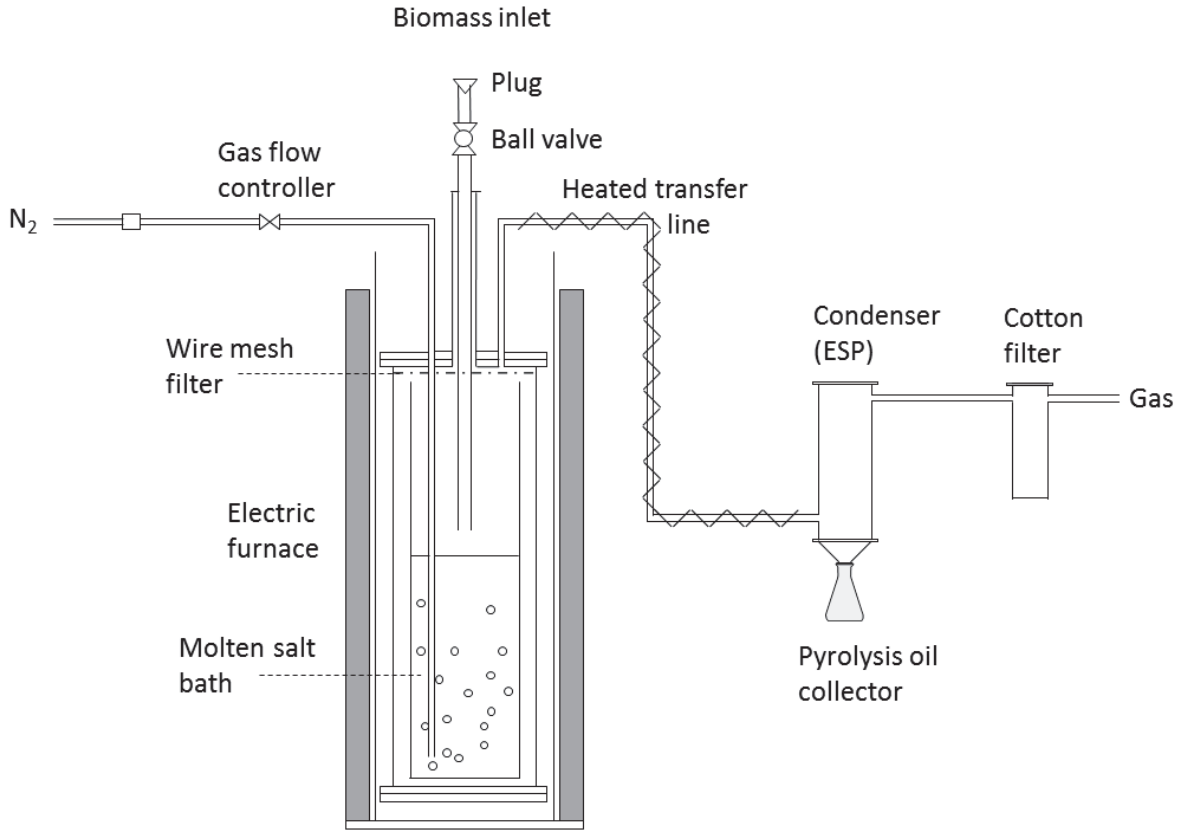

Figure 3. Schematic representation of the experimental setup for pyrolysis of biomass in molten salts.

When the heating was started, inert gas (N_2) was continuously flowed into the reactor through a nickel tube (4 mm) to ensure an oxygen-free atmosphere. The salt temperature was controlled by a submerged type K thermocouple. Once the salt was completely melted, the nickel tube was submerged in the melt to give turbulent mixing and a homogeneous temperature throughout the reactor. Turbulent mixing enhances the heat transfer from the salt to the wood samples in the pyrolysis process. The

heating was continued until the desired reactor temperature was reached. The temperature ranges used in the experiments for the two salt compositions are listed in Table 1.

The samples were introduced to the reactor manually through a ball valve based feeding system. The small particles were filled in a tube above the ball valve. The tube was then closed with a plug, and the valve was opened to feed the wood to the reactor. No gas could escape to the environment in this closed system. Due to problems with clogging of the feeding tube, the tube was kept 1 – 2 cm above the molten salt bath and the particles were fed to the top of the melt with the aid of a push rod. A total of ca 20 – 25 grams was added in small batches of 0.3 – 0.5 gram every minute. In preliminary experiments, the mixing of wood particles with a fluid bed (water-sugar solution to obtain similar characteristics as molten salts) was studied visually in a cold-flow glass model. At room temperature, the particles were mixed well in the fluid due to the turbulent bubbling of inert gas.

The flow rate of N_2 was set to 0.6 L/min during the experiments. This was a tradeoff between relatively short vapor residence time in the order of a few seconds and to avoid extensive splashing of the salt which could possibly clog the wire mesh filter at the top of the reactor. The vapors were led out of the reactor through a 4 mm heated transfer line (450 °C) made of stainless steel. The system was connected to the previously described ESP for collection of pyrolysis oil. The ESP was operated at 12 – 15 kV and cooled externally with tap water at 20 °C. A tubular cotton gas filter (filtration level 10 µm) was attached to the exhaust of the ESP for capturing the remaining vapors, and the non-condensable gases were vented off. After the experiments were completed, the power was turned off, and the system was left under inert atmosphere until ambient temperature to prevent corrosion.

The char yield was measured as difference between the reactor mass before and after experiment. The total pyrolysis oil yield was determined by weighing the ESP condenser and the cotton filter before and after the experiment. The water content of the oil was determined by Karl Fischer titration, using Hydranal Composite 5 as titer.

Results and discussions

Three identical experiments with beech wood in FLiNaK at 500 °C were conducted to assure reproducibility of the experimental method. The remaining experiments were performed once, except for a few cases where clogging of the feeding tube or failing of the electrostatic precipitator occurred. These experiments were repeated, and the results from the failed experiments were disregarded. For the successful experiments, no uncondensed pyrolysis vapors were observed at the outlet of the ESP.

The ESP contained between 92 and 97 % of the produced pyrolysis oil, with the remaining amount found in the cotton filter. Only the fraction condensed in the ESP was analyzed further with respect to water content. The collected oil was in one phase in the case of FLiNaK at 475 and 500 °C, while a two-phase oil was recovered for the rest of the experiments. The two-phase samples were heated slowly until good mixing was achieved before the water content was determined.

Effect of salt mixture and temperature on product yields

The yields of pyrolysis oil and solid char as a function of reactor temperature are plotted in Figure 4. Figure 5 shows the influence of reactor temperature and salt composition on the water content of the pyrolysis oil.

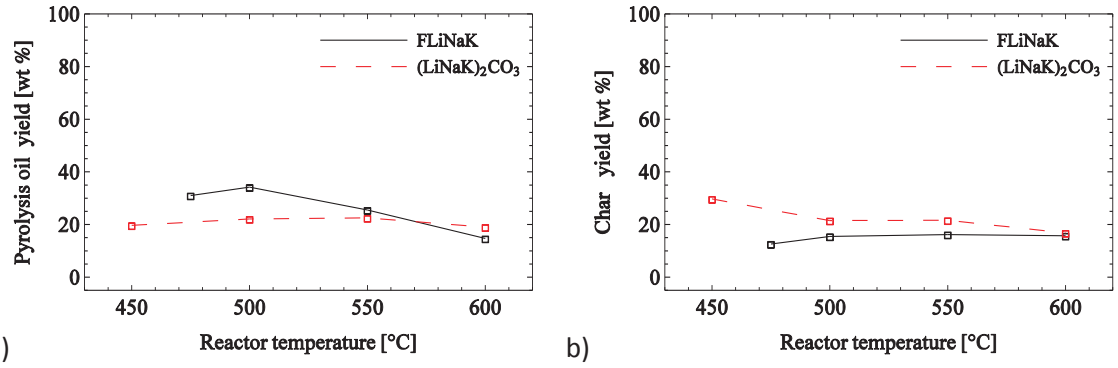

Figure 4. Yields of pyrolysis oil (a) and solid char (b) as function of the reactor temperature in FLiNaK (black) and $(LiNaK)_2CO_3$ (red).

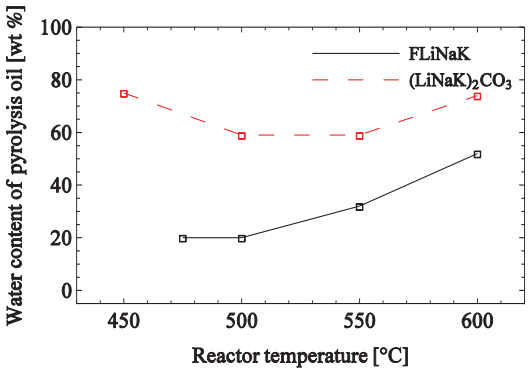

Figure 5. Water content of pyrolysis oil (collected from the ESP) as a function of reactor temperature for pyrolysis of beech wood in FLiNaK (black) and $(LiNaK)_2CO_3$ (red).

The reactor temperature showed a strong effect on the pyrolysis oil yield in FLiNaK, with a maximum of 34.2 wt % at 500 °C, followed by a decrease with increasing reactor temperature. The yield of pyrolysis oil in $(LiNaK)_2CO_3$ was nearly constant with temperature, with values between 19.0 and 22.5 wt %. For the char yield, only a minor temperature dependence was observed in both salt mixtures for reactor temperatures above 500 °C. The water content varied greatly between pyrolysis in FLiNaK and $(LiNaK)_2CO_3$, but the same trend with lower water content for higher oil yields are observed.

The pyrolysis oil yields are for the most part higher than those reported in molten chloride pyrolysis by Jiang et al.[4], where cold trap condensers were utilized for oil collection. But the oil yields are generally lower and the char yields higher compared to typical values reported for other fast pyrolysis technologies.[2] These results, in addition to the high water contents of the pyrolysis oils (Figure 5), indicate that secondary reactions are occurring. Even though the inert gas should bring the vapors out of the reactor within a few seconds, the vapors could experience mass transfer resistance in the melt leading to longer vapor residence time at elevated temperatures. However, several researchers have stated that the oil yield is much less dependent on vapor residence times than originally assumed. Wang et al.[31] did not observe any effect on the product yields for vapor residence times between 1 and 6 seconds, while Scott et al.[32] found no significant influence up to 10 seconds. Hoekstra et al.[33] stated that

pyrolysis vapors can be exposed to elevated temperatures for a long time, given that these are poor in mineral content, since minerals containing alkali elements such as Na and K promote the formation of gaseous species and char on the expense of pyrolysis oil. Taking this into account, it is likely that the presence of minerals in the molten salts play a role in the pyrolysis process, and that the lower yields of pyrolysis oil are caused by a combination of longer vapor residence times and prolonged contact between the salts and the formed vapors.

Another possible explanation is insufficient mixing of wood and salt leading to slower heating than assumed based on our previous work where single particles were studied,[20,34] and thus dehydration and carbonization reactions could take place at lower temperatures on the expense of depolymerization to condensable gases. However, turbulent bubbling and splashing of the molten salt should ensure the same contact between the hot melt and the wood particles giving heating rates typical for fast pyrolysis.

Formation of HF in FLiNaK pyrolysis

Hydration of metal halides can result in formation of HX, where X represents a halide ion. Given the hygroscopic nature of FLiNaK, formation of HF gas (Eqs. 1 – 6) is a possible concern when this salt is utilized in pyrolysis where water is one of the species formed in the process. The HF gas could contaminate the pyrolysis products and also lead to extensive corrosion of metal elements found in process equipment.[35]

$$2LiF(l) + H_2O(g) \leftrightarrow Li_2O(l) + 2HF(g) \quad (1)$$

$$2NaF(l) + H_2O(g) \leftrightarrow Na_2O(l) + 2HF(g) \quad (2)$$

$$2KF(l) + H_2O(g) \leftrightarrow K_2O(l) + 2HF(g) \quad (3)$$

$$LiF(l) + H_2O(g) \leftrightarrow LiOH(l) + HF(g) \quad (4)$$

$$NaF(l) + H_2O(g) \leftrightarrow NaOH(l) + HF(g) \quad (5)$$

$$KF(l) + H_2O(g) \leftrightarrow KOH(l) + HF(g) \quad (6)$$

The hydration reactions were simulated in HSC Chemistry software[7], with the results plotted in Figure 6. According to the simulations, hydration will not occur in the experimental temperature ranges of this study. It should be noted that the Gibbs free energies are well above zero for temperatures relevant for gasification processes as well.

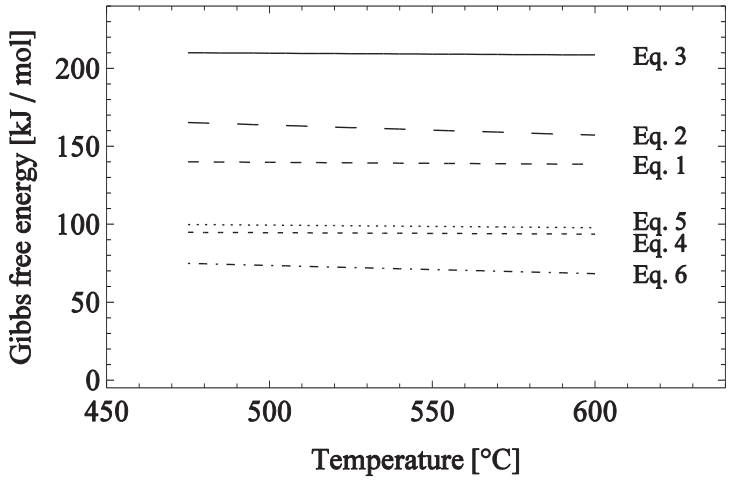

Figure 6. Gibbs free energy versus temperature for possible hydration reactions in FLiNaK.

The concentration of HF in the outlet gas was also examined during FLiNaK pyrolysis at 600 °C by means of a FTIR gas analyzer (Thermo Scientific, Nicolet 6700), but no significant amounts were detected.

Conclusions

The aim of this work was to investigate molten salt pyrolysis with the focus on pyrolysis oil production. A tubular electrostatic precipitator (ESP) was designed and tested for collection of pyrolysis oil in the process. The voltage-current (V-I) characteristics of the ESP were studied with the inert gases N_2 and Ar, and N_2 was found to give the most stable operation. This was attributed to higher break down voltages, and lower concentrations of impurities, and lower conductivity of the inert gas. The minimum voltage required for separation of pyrolysis vapors from the remaining gas stream was found to be 12 kV.

Beech wood particles (0.5 – 2 mm) were pyrolyzed in FLiNaK and $(LiNaK)_2CO_3$ at temperatures between 450 and 600 °C. The ESP worked well, and no uncondensed vapors were observed at the gas outlet. The pyrolysis oil yields were generally higher than those reported in chloride pyrolysis by Jiang et al.[4], with a maximum of 34.2 wt % for FLiNaK at 500 °C. The pyrolysis oil yields were lower and the char yields higher compared to other fast pyrolysis technologies. The oils were also high in water content. These results were somewhat unexpected, since the employed molten salts have been found to give very high heating rates for beech wood particles in our previous work.[20,22] One possible explanation to this is transport resistance of vapors leaving the melt leading to longer vapor residence times and secondary reactions into char, non-condensable gases and water. Another reason could be contact between the formed vapors and alkali elements (Na/K) in the melt leading to the formation of gaseous species and char on the expense of pyrolysis oil.

A possible concern when using FLiNaK as a reaction medium in thermochemical conversion of biomass is the reaction between the salt and produced water to form HF gas. According to both simulations and FTIR measurements of the outlet gas, no significant amounts of HF are produced during beech wood pyrolysis in FLiNaK.

References

(1) A.V, B.: Review of fast pyrolysis of biomass and product upgrading. *Biomass and Bioenergy* **2012**, *38*, 68-94.

(2) Venderbosch, R. H.; Prins, W.: Fast pyrolysis technology development. *Biofuels, Bioproducts and Biorefining* **2010**, *4*, 178-208.

(3) Lovering, D. G.: *Molten salt technology*; Plenum Press, 1982.

(4) Jiang, H.; Ai, N.; Wang, M.; Ji, D.; Ji, J.: Experimental Study on Thermal Pyrolysis of Biomass in Molten Salt Media. *Electrochemistry* **2009**, *77*, 730-735.

(5) Adinberg, R.; Epstein, M.; Karni, J.: Solar Gasification of Biomass: A Molten Salt Pyrolysis Study. *Journal of Solar Energy Engineering* **2004**, *126*, 850-857.

(6) Hathaway, B. J.; Davidson, J. H.; Kittelson, D. B.: Solar Gasification of Biomass: Kinetics of Pyrolysis and Steam Gasification in Molten Salt. *Journal of Solar Energy Engineering* **2011**, *133*, 021011.

(7) Sada, E.; Kumazawa, H.; Kudsy, M.: Pyrolysis of lignins in molten salt media. *Industrial & Engineering Chemistry Research* **1992**, *31*, 612-616.

(8) Kudsy, M.; Kumazawa, H.; Sada, E.: Pyrolysis of kraft lignin in molten ZNCL2-KCL media with tetralin vapor addition. *The Canadian Journal of Chemical Engineering* **1995**, *73*, 411-415.

(9) Hammond, V. L.; Mudge, L. K. "Feasibility study of use of molten salt technology for pyrolysis of solid waste. Final report," 1975.

(10) Iwaki, H.; Ye, S.; Katagiri, H.; Kitagawa, K.: Wastepaper gasification with CO2 or steam using catalysts of molten carbonates. *Applied Catalysis A: General* **2004**, *270*, 237-243.

(11) Jin, G.; Iwaki, H.; Arai, N.; Kitagawa, K.: Study on the gasification of wastepaper/carbon dioxide catalyzed by molten carbonate salts. *Energy* **2005**, *30*, 1192-1203.

(12) Menzel, J.; Perkow, H.; Sinn, H.: RECYCLING PLASTICS. *Chemistry & Industry* **1973**, 570-573.

(13) Bertolini, G. E.; Fontaine, J.: Value recovery from plastics waste by pyrolysis in molten salts. *Conservation & Recycling* **1987**, *10*, 331-343.

(14) Chambers, C.; Larsen, J. W.; Li, W.; Wiesen, B.: Polymer waste reclamation by pyrolysis in molten salts. *Industrial & Engineering Chemistry Process Design and Development* **1984**, *23*, 648-654.

(15) Williams, D.: Assessment of candidate molten salt coolants for the NGNP/NHI Heat-Transfer Loop. *ORNL/TM-2006/69, Oak Ridge National Laboratory, Oak Ridge, Tennessee* **2006**.

(16) Bridgwater, A. V.; Peacocke, G. V. C.: Fast pyrolysis processes for biomass. *Renewable and Sustainable Energy Reviews* **2000**, *4*, 1-73.

(17) Oasmaa, A.; Peacocke, C.: Properties and fuel use of biomass-derived fast pyrolysis liquids. *VTT PUBLICATIONS 731* **2010**.

(18) Mochizuki, T.; Toba, M.; Yoshimura, Y.: Effect of Electrostatic Precipitator on COllection Efficiency of Bio-oil in Fast Pyrolysis of Biomass. *Journal of the Japan Petroleum Institute* **2013**, *56*, 401-405.

(19) Bedmutha, R. J.; Ferrante, L.; Briens, C.; Berruti, F.; Inculet, I.: Single and two-stage electrostatic demisters for biomass pyrolysis application. *Chemical Engineering and Processing: Process Intensification* **2009**, *48*, 1112-1120.

(20) Nygård, H. S.; Danielsen, F.; Olsen, E.: Thermal History of Wood Particles in Molten Salt Pyrolysis. *Energy & Fuels* **2012**, *26*, 6419-6425.

(21) Di Blasi, C.; Branca, C.: Temperatures of Wood Particles in a Hot Sand Bed Fluidized by Nitrogen. *Energy & Fuels* **2003**, *17*, 247-254.

(22) Nygård, H. S.; Olsen, E.: Effect of salt composition and temperature on the thermal behavior of beech wood particles in molten salt pyrolysis. *Energy Procedia* **2014**, *(in press)*.

(23) Lüftl, S.; M, V. P.; Chandran, S.: *Polyoxymethylene Handbook: Structure, Properties, Applications and their Nanocomposites*; Wiley, 2014.

(24) Lucas, J. R.: High voltage engineering. *Colombo, Open University of Sri. Lanka* **2001**, 64-89.

(25) Huheey, J. E.: *Inorganic chemistry: principles of structure and reactivity*; Harper & Row, 1983.

(26) Klas, M.; Radmilović-Radjenović, M.; Radjenović, B.; Stano, M.; Matejčik, Š.: Transport parameters and breakdown voltage characteristics of the dry air and its constituents. *Nuclear Instruments and Methods in Physics Research Section B: Beam Interactions with Materials and Atoms* **2012**, *279*, 96-99.

(27) Grønli, M. G.: A Theoretical and Experimental Study of the Thermal Degradation of Biomass. Norwegian University of Science and Technology, 1996.

(28) Hathaway, B. J.; Davidson, J. H.; Kittelson, D. B.: Solar Gasification of Biomass: Kinetics of Pyrolysis and Steam Gasification in Molten Salt. *Journal of Solar Energy Engineering* **2011**, *133*, 021011-021011.

(29) Olson, L. C.; Ambrosek, J. W.; Sridharan, K.; Anderson, M. H.; Allen, T. R.: Materials corrosion in molten LiF–NaF–KF salt. *Journal of Fluorine Chemistry* **2009**, *130*, 67-73.

(30) Hoekstra, E.; Hogendoorn, K. J.; Wang, X.; Westerhof, R. J.; Kersten, S. R.; van Swaaij, W. P.; Groeneveld, M. J.: Fast pyrolysis of biomass in a fluidized bed reactor: in situ filtering of the vapors. *Industrial & Engineering Chemistry Research* **2009**, *48*, 4744-4756.

(31) Wang, X.; Kersten, S. R. A.; Prins, W.; van Swaaij, W. P. M.: Biomass Pyrolysis in a Fluidized Bed Reactor. Part 2: Experimental Validation of Model Results. *Industrial & Engineering Chemistry Research* **2005**, *44*, 8786-8795.

(32) Scott, D. S.; Majerski, P.; Piskorz, J.; Radlein, D.: A second look at fast pyrolysis of biomass—the RTI process. *Journal of Analytical and Applied Pyrolysis* **1999**, *51*, 23-37.

(33) Hoekstra, E.; Westerhof, R. J. M.; Brilman, W.; Van Swaaij, W. P. M.; Kersten, S. R. A.; Hogendoorn, K. J. A.; Windt, M.: Heterogeneous and homogeneous reactions of pyrolysis vapors from pine wood. *AIChE Journal* **2012**, *58*, 2830-2842.

(34) Nygård, H. S.; Olsen, E.: Effect of Salt Composition and Temperature on the Thermal Behavior of Beech Wood Particles in Molten Salt Pyrolysis. *Submitted to Energy Procedia* **2014**.

(35) Ouyang, F.-Y.; Chang, C.-H.; Kai, J.-J.: Long-term corrosion behaviors of Hastelloy-N and Hastelloy-B3 in moisture-containing molten FLiNaK salt environments. *Journal of Nuclear Materials* **2014**, *446*, 81-89.